II. Medizinische Klinik
Klinikum rechts der Isar
der Technischen Universität München
(Direktor: Univ.-Prof. Dr. R. M. Schmid)

Characterization of Pancreas-Specific Conditional *Notch1* Knockout Mice

Marcel Lee

Vollständiger Abdruck der von der Fakultät für Medizin der Technischen Universität München zur Erlangung des akademischen Grades eines

Doktors der Medizin

genehmigten Dissertation.

Vorsitzender: Univ.-Prof. Dr. D. Neumeier

Prüfer der Dissertation:

1. Priv.-Doz. Dr. J. Th. Siveke

2. Univ.-Prof. Dr. R. M. Schmid

Die Dissertation wurde am 12.05.2010 bei der Technischen Universität München eingereicht und durch die Fakultät für Medizin am 22.09.2010 angenommen

Table of Contents

Abbreviations

°C	Degree Celsius
ADAM	A disintegrin and metalloproteinase
ANK	Ankyrin repeats
APP	β-amyloid precursor protein
bHLH	Basic helix-loop-helix
bp	Base pairs
BrdU	5-bromo-2-deoxyuridine
BW	Body weight
CBF1	C-promoter binding factor
CCK	Cholecystokinin
CK19	Cytokeratin 19
CPA	Carboxypeptidase A
Cre	Causes recombination
CSL	CBF1, Su(H), LAG-1
DBA	Dolichus biflorus agglutinin
DBZ	Dibenzazepine
Dll	Delta like
DNA	Deoxyribonucleic acid
DSL	Delta, Serrate and Lag-2
EBD	EGF-motif binding domain
EC	Extracellular
EGF	Epidermal-growth-factor
ELR	EGF-like repeats
H&E	Hematoxylin & eosin staining
HERP	Hes-related repressor protein
Hes	Hairy/Enhancer of Split
i.p.	Intraperitoneal
IC	Intracellular
kDa	Kilodalton
LNG	Lin12/Notch/Glp-1

loxP	Locus of crossing over of P1
M	Molar
mA	Milliampere
ml	Milliliter
mRNA	Messenger RNA
N1KO	*Notch1* knockout
Ngn3	Neurogenin 3
NIC	Notch intracellular domain
NT domain	N-terminal extracellular domain
PCR	Polymerase chain reaction
PDX1	Pancreatic-duodenal homeobox gene-1
PFA	Paraformaldehyde
PP	Pancreatic polypeptide
PTF1	Pancreas specific transcription factor 1
PTF1a	Pancreas specific transcription factor 1a
RBP	Recombination signal binding protein
RNA	Ribonucleic acid
rpm	Rotations per minute
SDS	Sodium dodecyl sulfate
SEM	Standard error of the mean
SS	Somatostatin
Su(H)	Suppressor of hairless
TACE	Tumor necrosis factor-α converting enzyme
TAD	Transactivation domain
Taq	Thermus aquaticus
TM	Transmembrane domain
V	Volt
wt	Wildtype
X-gal	5-bromo-4-chloro-3-indolyl-β-D-galactosidase
µm	Micrometer

1 Introduction

1.1 The Pancreas

1.1.1 Anatomy

The adult pancreas in mammals is a gland comprising two distinct compartments that have specific roles in food digestion, nutrition uptake and homeostasis. It is located adjacent to and encircled by the duodenal loop and extends to the pyloric region of the stomach and the left lateral flank towards the spleen (Fig. 1-1 A).

1.1.2 Exocrine Function

The majority of the pancreas consists of exocrine tissue, which is composed of secretory cell clusters called acini, and the ductal epithelium. Acini produce and secrete digestive enzymes that are drained into the duodenum via the elaborate pancreatic ductal system. Additionally, the ductal epithelium secretes bicarbonate ions into the lumen (Fig. 1-1 B, C) (Junqueira 1996).

1.1.3 Endocrine Function

The endocrine compartment makes up 2-3% of the entire pancreas. It is organized in small cell clusters called islets of Langerhans, scattered within the exocrine tissue. The islets are composed of five different cell types, each producing one specific peptide hormone

- α-cells: Glucagon
- β-cells: Insulin
- δ-cells: Somatostatin (SS)
- PP-cells: Pancreatic polypeptide (PP)
- ε-cells: Ghrelin

β-cells make up 70-80% of the islets and form a core that is surrounded by the other cell types. α-cells make up 15-20%, δ-cells 5-10%, PP-cells <2% and ε-cells even less (Fig. 1-1 D).

Insulin and glucagon are involved in glucose homeostasis as well as protein and lipid metabolism, somatostatin inhibits the secretion of insulin and glucagon in a paracrine way, and the pancreatic polypeptide inhibits exocrine secretion and gastrointestinal

motility (Junqueira 1996). Expression of ghrelin in islet cells has only been discovered recently, and its function remains to be clarified (Wierup 2002; Prado 2004).

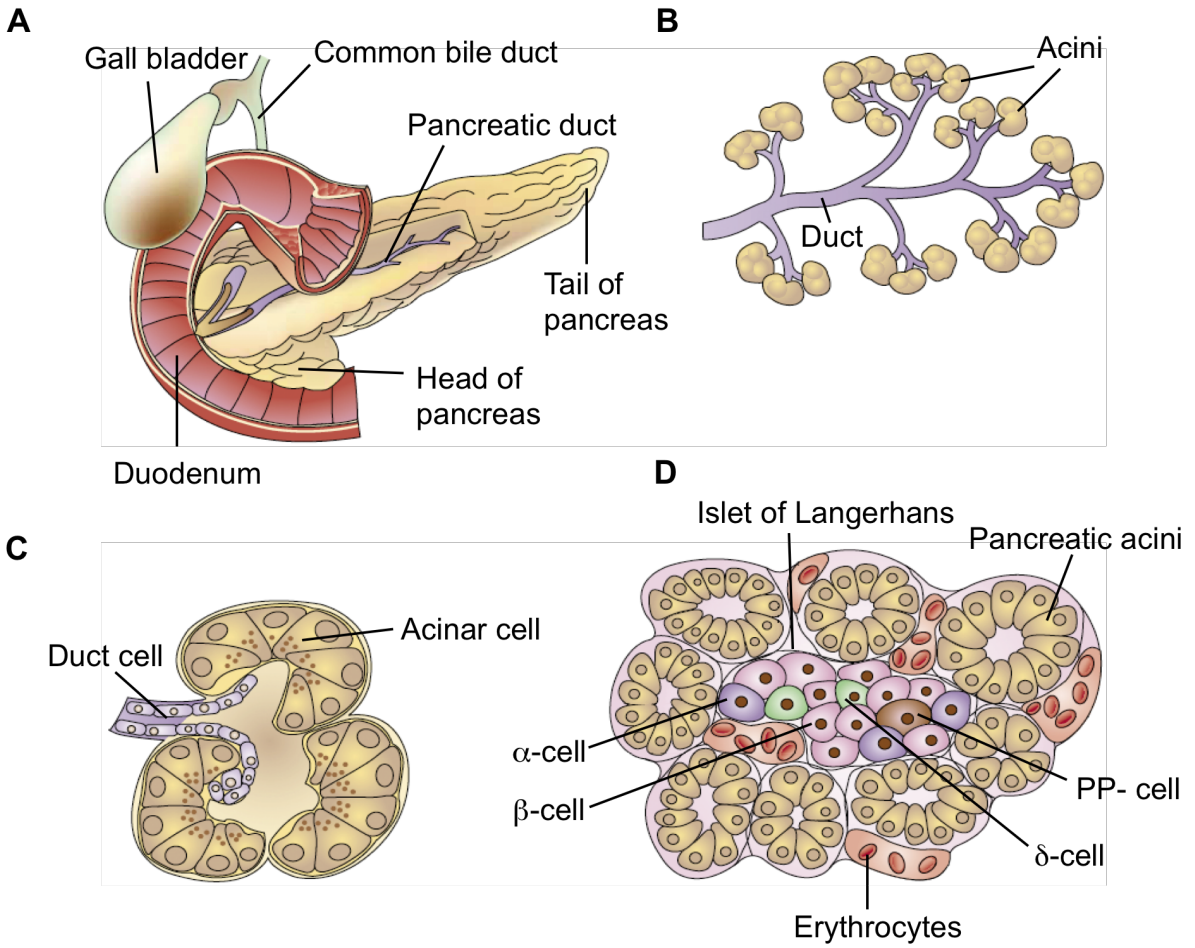

Fig. 1-1: Anatomy of the pancreas

A) Adult human pancreas and its in-situ location adjacent to the duodenum.
B) Schematic representation of the exocrine pancreas with acini and the branched ductal tree.
C) Histology of a pancreatic acinus with an adjacent duct.
D) Schematic representation of an islet of Langerhans with typical distribution of endocrine cells.
Modified from Bardeesy (2002)

1.1.4 Embryonic Development of the Murine Pancreas

The pancreas originates from specialized, prepatterned endodermal foregut-epithelium committed to a pancreatic fate. Pancreatic determination of this region occurs between the 8 to 10 somite stage in murine embryos (embryonic day 8 [E8]), 24 hours prior to the appearance of the dorsal bud (Wessells 1967; Slack 1995;

Habener 2004; Spagnoli 2007). First visible signs of pancreatic morphogenesis are recognizable in 20-25 somite embryos (E9.5) with the evagination of endodermal cells in the dorsal and ventral region of the foregut. (Wessells 1967; Spooner 1970; Pictet 1972). This stage of beginning pancreatogenesis with alterations in shape of the pancreatic foregut is referred to as the first transition (Fig. 1-2 A, B). Evagination of the anlagen into the surrounding mesenchyme continues, and on E10.5, branching morphogenesis of the partially differentiated epithelium commences, leading to a highly branched ductal tree, which retains continuity with the duodenum (Habener 2004; Jensen 2005; Murtaugh 2007). By E12.5, two primordial pancreatic organs are visible, consisting mainly of undifferentiated epithelium (Fig. 1-2 C). As a result of gut rotation from E12.5 on, the dorsal pancreas is translocated to the ventral side where the primordia fuse. Between E13.5 and E15.5, epithelial expansion leads to massive differentiation of exocrine pancreas from the ductal epithelium and the appearance of zymogen granules (second developmental transition). Exocrine cells, organized as acini, and ducts become clearly discernible as histologically distinct structures (Fig. 1-2 D) (Slack 1995; Habener 2004; Cano 2007). During this developmental period, the mRNA concentration and specific activities of exocrine products increases by three orders of magnitude (Sanders 1974; Han 1986). The differentiation and proliferation processes during the second transition result in an entirely functional organ just prior to birth. During the first weeks post partum, further proliferation of acinar tissue leads to growth of the organ and an increase in exocrine tissue mass that condenses to form compact acini (Fig. 1-2 E) (Slack 1995; Jensen 2003; Cano 2007; Murtaugh 2007).

From the endocrine compartment, cells expressing glucagon and members of the PP fold family of hormones, peptide YY, PP, and neuropeptide Y, are detectable on E9.5 (Habener 2004; Murtaugh 2007). Mature β-cells expressing Insulin alone start appearing on E13.5, and Somatostatin expressing cells emerge on around E14.5, concomitant with the second transition (Fig. 1-2 C). Beginning on E13.5, endocrine progenitor cells delaminate from the epithelium, migrate into the surrounding mesenchyme and from E16 start aggregating into islet-like cell cluster (Fig. 1-2 D). They ultimately condense into islets of Langerhans shortly before birth on E18-E19. The islets go through further maturation for 2-3 weeks post partum (third developmental transition) (Fig. 1-2 E) (Schwitzgebel 2001; Habener 2004; Cano 2007; Murtaugh 2007).

1.1.5 Transcription Factors Involved in Pancreatogenesis

Several transcription factors can be identified in the course of organogenesis before pancreas-specific differentiation markers can be detected. Two pivotal transcription factors in early pancreatic organogenesis are PDX1 (pancreatic-duodenal homeobox gene-1), and the basic helix-loop-helix (bHLH) transcription factor PTF1a (pancreatic specific transcription factor 1a), also known as p48 (Murtaugh 2007).

1.1.5.1 PDX1

Pdx1 was the first gene shown to be required in a cell autonomous fashion for the development of the pancreas. It is generally recognized as the earliest pancreas-specific transcription factor detected, marking the developing pre-pancreatic endoderm, with expression starting in the pancreatic progenitor cells at E8.5 (Fig. 1-2 A), prior to morphogenesis and expression of glucagon and insulin (Guz 1995; Offield 1996). Lineage tracing demonstrated that PDX1 expressing cells represent pancreatic progenitor cells that contribute to the development of endocrine, exocrine and ductal cells (Gu 2002). On E9.5, PDX1 is expressed homogeneously in the pancreatic epithelium of the dorsal and ventral buds (Fig. 1-2 B). Additionally, PDX1 is expressed in the adjacent endoderm of the presumptive duodenum, the antral stomach, cystic duct and common bile duct (Guz 1995; Offield 1996). During the second developmental transition, PDX1 is essential for initiation of the acinar lineage and terminal differentiation of acinar cells (Hale 2005). From E16.5, expression of PDX1 is downregulated in differentiating exocrine cells and ductal cells (Guz 1995; Offield 1996). In the adult pancreas, PDX1 expression persists at high levels in insulin secreting β-cells where it is involved in transcriptional regulation of the insulin gene and maintenance of mature β-cell function (Fig. 1-2 E) (Ohlsson 1993; Guz 1995; Ahlgren 1998; Holland 2002; Kaneto 2007).

1.1.5.2 PTF1a

Ptf1a was initially recognized as an acinar gene activator and encodes the exocrine pancreas-specific subunit of the transcription factor PTF1 (Pancreas specific transcription factor 1) (Krapp 1996). PTF1 is a hetero-oligomeric protein complex comprising three distinct subunits: PTF1a, RBP-J or RBP-L and a class A bHLH transcription factor (Beres 2006). It binds to sequence elements of promoters located in the 5' region of genes specifically expressed in the exocrine pancreas

(Cockell 1989; Roux 1989). PTF1a expression can be detected as early as E9.5 (Fig. 1-2 B), shortly after the formation of the pancreatic anlagen and prior to the onset of exocrine specification (Obata 2001; Fujikura 2007). Its expression is essential for development of all acinar cells and correct spatial organization of endocrine cells (Krapp 1998). Lineage tracing analysis revealed that exocrine, endocrine and ductal cells are derived from progenitor cells expressing PTF1a, and that PTF1a is essential for instructing uncommitted pancreatic precursors in the foregut endoderm to adopt the pancreatic differentiation program (Kawaguchi 2002). Thus, Ptf1a function goes beyond mere exocrine fate specification but is a key regulator in early pancreatogenesis. Its expression is inactivated in mature endocrine cells and becomes restricted to the acinar compartment from E13.5 onward where it controls the selective transcription of acinar specific genes (Fig. 1-2 D) (Krapp 1996; Rose 2001; Kawaguchi 2002; Murtaugh 2007).

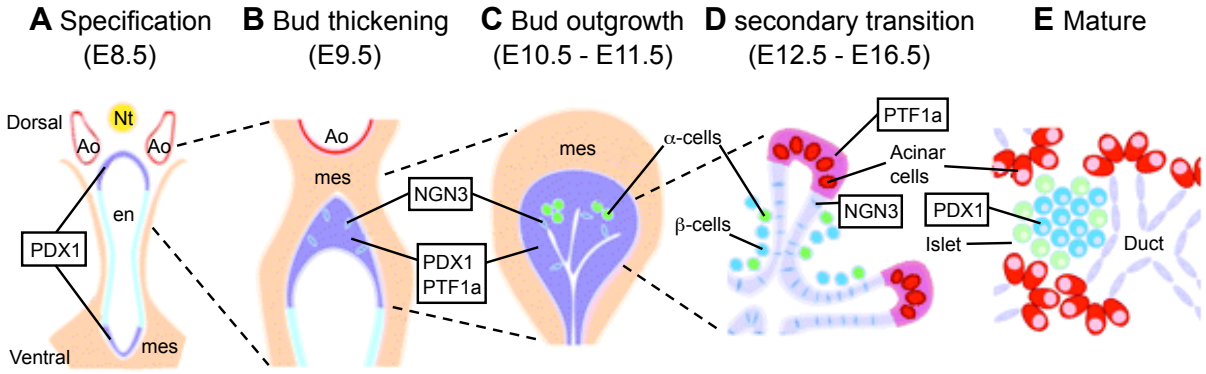

Fig. 1-2: Embryonic development of the pancreas

Schematic representation of different stages of pancreatic development.
A) Specification of the organ occurs simultaneously with expression of PDX1 in two discrete regions of the foregut endoderm (en). Ao: Aorta, Nt: Notochord
B) Bud thickening as first visible evidence of pancreatic development. Expression of PTF1a commences. Appearance of first $NGN3^+$ endocrine precursor cells.
C) Outgrowth of epithelial buds with differentiation of early α-cells.
D) Further growth and branching leads to the secondary transition characterized by a massive differentiation of β-cells and acinar cells and differentiation of δ- and PP-cells. Expression of PDX1 and PTF1a becomes restricted to β-cells and acinar cells, respectively.
E) Mature organ with endocrine islets of Langerhans interspersed between exocrine acini and duct cells.
Modified from Murtaugh (2007)

1.1.6 Notch Signaling During Pancreatic Development

Notch signaling has been shown to crucially affect pancreatic organogenesis. The next chapter will first recapitulate the most important aspects of this conserved signaling pathway before describing its involvement in pancreatic homeostasis.

1.2 Notch Signaling

1.2.1 History

Effects of partial loss of function (haploinsuffiency) of the Notch receptor were first observed in Drosophila melanogaster (Morgan 1917; Mohr 1919). The name derives from the phenotype of mutant female fruit flies heterozygous for a genetic defect in a gene, then designated Notch8 (Poulson 1937, 1940). These flies develop notches at the wing margins (Fig. 1-3). Moreover, since in D. melanogaster the *Notch* gene is located on the X-chromosome, male flies lacking a normal copy of the X chromosome, and thus lacking a functional Notch protein, showed a lethal phenotype with severe developmental defects leading to almost complete transformation of surface ectoderm into cells of the nervous system, referred to as the “neurogenic” phenotype (Poulson 1937).

The *Notch* gene from D. melanogaster was cloned in the mid-1980s and found to encode a transmembrane receptor. (Artavanis-Tsakonas 1983; Wharton 1985)

In the 1990s, four mammalian homologues of the Drosophila *Notch* gene, *Notch1-4*, were identified (Ellisen 1991; Weinmaster 1992; del Amo 1993; Lardelli 1994; Uyttendaele 1996).

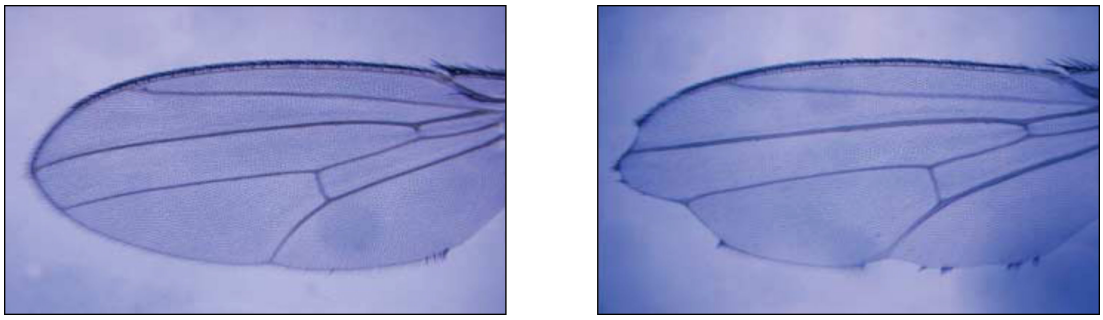

Fig. 1-3: Notched wing

Normal wing of a wildtype Drosophila melanogaster (left), and a wing with notches at the border of the wing margins of a mutant fly with partial loss of the *Notch* gene (right).
From Radtke (2003)

1.2.2 Elements Involved in the Mammalian Notch Core Pathway

1.2.2.1 Receptors

Notch proteins are single pass heterodimeric transmembrane receptors (Type-I integral membrane proteins). They are synthesized in the endoplasmatic reticulum as 300 kDa single-chain precursor proteins. On their way through the secretory pathway, the extracellular domain of Notch precursors is subject to constitutive cleavage in the trans-Golgi network by a furin-like convertase (site 1 or S1 cleavage) (Jarriault 1998; Logeat 1998). As a result, the active, ligand accessible form of the receptors is presented on the cell surface as a single pass transmembrane heterodimer, consisting of two components: One part constituting the majority of the extracellular (EC) domain, the other comprising a short extracellular stump, the transmembrane domain (TM) and the intracellular domain (NIC). The cleaved EC domain is non-covalently tethered to the TM domain (Fig. 1-4 A) (Blaumueller 1997).

The extracellular part contains tandemly arranged epidermal-growth-factor (EGF)-like repeats (ELR) followed by three cysteine rich family specific Lin12/Notch/Glp-1 (LNG) domains (Wharton 1985). EGF 11 and 12 are essential for ligand binding (Rebay 1991), whereas the LNG repeats prevent ligand-independent signaling (Fig. 1-4 A) (Radtke 2003).

The intracellular region consists of five distinct regions: the RAM domain, six highly conserved ankyrin repeats (ANK or CDC10 repeats) surrounded by nuclear localization sequences (NLS), a transactivation domain (TAD), a PEST (proline-, glutamate-, serine-, threonine-rich) sequence, and an ED domain (Oswald 2001). The RAM domain physically interacts with the CSL transcription factor, the mammalian RBP-J (Tamura 1995). The ANK repeats associate with CSL and in concert with the RAM domain play a critical role in transactivation (detailed explanation at 1.2.3) (Kato 1997; Kurooka 1998; Beatus 2001; Tani 2001).

There are several variations between the four receptors in the extracellular and intracellular regions (Fig. 1-4 A). Notch1 and Notch2 contain 36 ELR (Ellisen 1991; Weinmaster 1992) in the ectodomain, whereas Notch3 possesses 34 (Lardelli 1994) and Notch4 29 (Uyttendaele 1996). In the intracellular domain, Notch1 contains a strong TAD, and Notch2 a weaker TAD. No TAD has been identified in Notch3 and Notch4 (Radtke 2003). However, all four types of Notch receptors associate with the ubiquitous RBP-J transcription factor (Kato 1996).

1.2.2.2 Ligands

In mammals, five Notch ligands taking part in receptor-ligand interaction have been identified: Jagged 1 and 2, and Delta like (Dll) 1, 3, and 4 (Fig. 1-4 B) (Bettenhausen 1995; Lindsell 1995; Wilson 2006). Similar to Notch receptors, the ligands are synthesized as single precursor proteins, posttranscriptionally cleaved and presented on the cell surface as single-pass heterodimers.

The ligands are composed of an extracellular (EC) part, a transmembrane (TM) domain and an intracellular (IC) region (Fleming 1997; 1999). The EC domain comprises a signal peptide, followed by an N-terminal extracellular domain (NT domain). Next to the NT domain is the DSL motif, named after its identification in the Notch ligands Delta, Serrate and Lag-2 (from C. elegans) (DSL ligands). This motif is unique to this protein family and essential for interactions with the Notch receptor (Bray 2006). It is followed by multiple EGF-like repeats (ELR). The NT domain, together with the adjacent DSL segment, forms the EGF-motif binding domain (EBD), which as a unity is required for receptor-ligand binding (Muskavitch 1994; Fleming 1997; 1999).

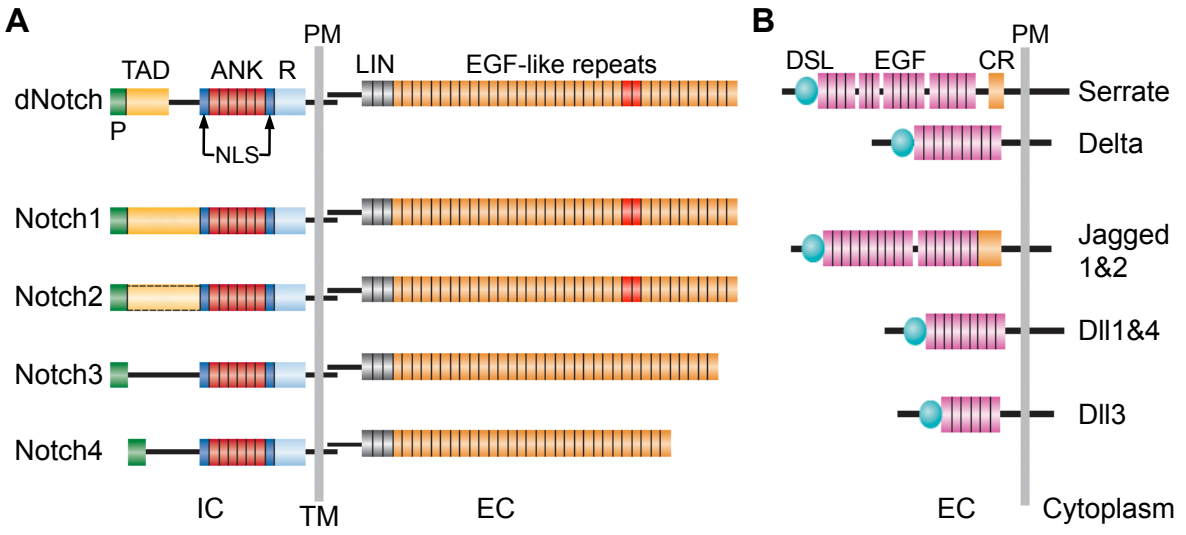

Fig. 1-4: Notch receptors and ligands

A) Drosophila possesses one Notch receptor (dNotch) and two ligands (Delta and Serrate). Mammalians have four Notch receptors (Notch1-4) and five ligands (Jagged 1&2 homologous to Serrate, and Delta-like [Dll] 1, 3 and 4 homologous to Delta).
Notch receptors are heterodimeric proteins expressed on the cell surface. The extracellular domain (EC) consists of 29 - 36 EGF-like repeats and 3 cysteine rich LIN repeats. EGF 11 and 12 are essential for ligand binding (red). The intracellular domain (IC) contains the RAM domain (R), 6 ankyrin repeats (ANK) flanked by 2 nuclear localization-signals (NLS), a transactivation domain (TAD) and a PEST sequence (P).

B) Notch ligands are also transmembrane proteins. They contain an amino-terminal DSL domain that is followed by varying numbers of EGF-like repeats. Serrate, Jaggged1 and 2 have a cysteine rich (CR) domain downstream of the EGF-like repeats.
TM: Transmembrane domain, PM: Plasma membrane
Modified from Radtke (2005)

1.2.3 The Notch Core Pathway

Signaling is initiated upon ligand-receptor interaction between neighboring cells. This leads to a second proteolytic cleavage of the receptor (S2 cleavage) within the EC domain close to the TM domain. This cleavage is mediated by members of the ADAM (A Disintegrin And Metalloproteinase) family. In mammals, TACE (Tumor necrosis factor-α converting enzyme, also known as ADAM17) and ADAM10 (also known as Kuzbanian) have been identified to participate in this process (Fig. 1-5) (Brou 2000; Mumm 2000; Jarriault 2005). The targeted sequence of S2 cleavage is located proximate to the extracellular part of the TM domain, leaving a short stump of the Notch receptor on the surface of the cell membrane. The liberated EC domain remains bound to the ligand, and both are subject to endocytosis of the ligand-expressing cell (Brou 2000; Mumm 2000).

A third and final cleavage (S3) – prompted by S2 cleavage – occurs within the TM domain of Notch, and leads to the release of the NIC domain into the cytoplasm (Fig. 1-5) (Schroeter 1998; De Strooper 1999). This cleavage is mediated by a multi protein complex named γ-secretase that has also been shown to be responsible for cleavage of the β-amyloid precursor protein (APP), a step crucial in the pathophysiology of Alzheimer's disease. (Haass 1999)

NIC is the functionally active form of the receptor and conveys the signal through translocation into the nucleus where it forms a trimeric complex with the DNA-binding transcription factor CSL (acronym of CBF1 [C-promoter binding factor] in human/RBP-J [recombination signal binding protein] in mammals; Su(H) [Suppressor of hairless] in Drosophila melanogaster; LAG-1 in Caenorhabditis elegans), primarily through interaction with the RAM23 domain (Tamura 1995; Kovall 2004; Miele 2006). In the absence of active Notch signaling (and thus NIC), CSL acts as a constitutive repressor of transcription through interaction with corepressors like SMRT (silencing mediator of retinoid and thyroid receptors)/NCor (nuclear receptor corepressor), SHARP, CtBP, CIR (CBF1 interacting corepressor), and the nuclear factor SKIP to form a histone deacetylase corepressor complex (Beatus 2001; Bray 2006)

Binding of NIC to CSL leads to the acquisition of the co-activators MAML1 (Wu 2000), the histone acetyltransferase p300 (Oswald 2001), and other factors, leading to the disruption of the transcriptional repressor complex, thereby initiating the expression of target genes. CSL recognizes and specifically binds to the conserved consensus sequence CGTGGGAA (Matsunami 1989; Tun 1994).

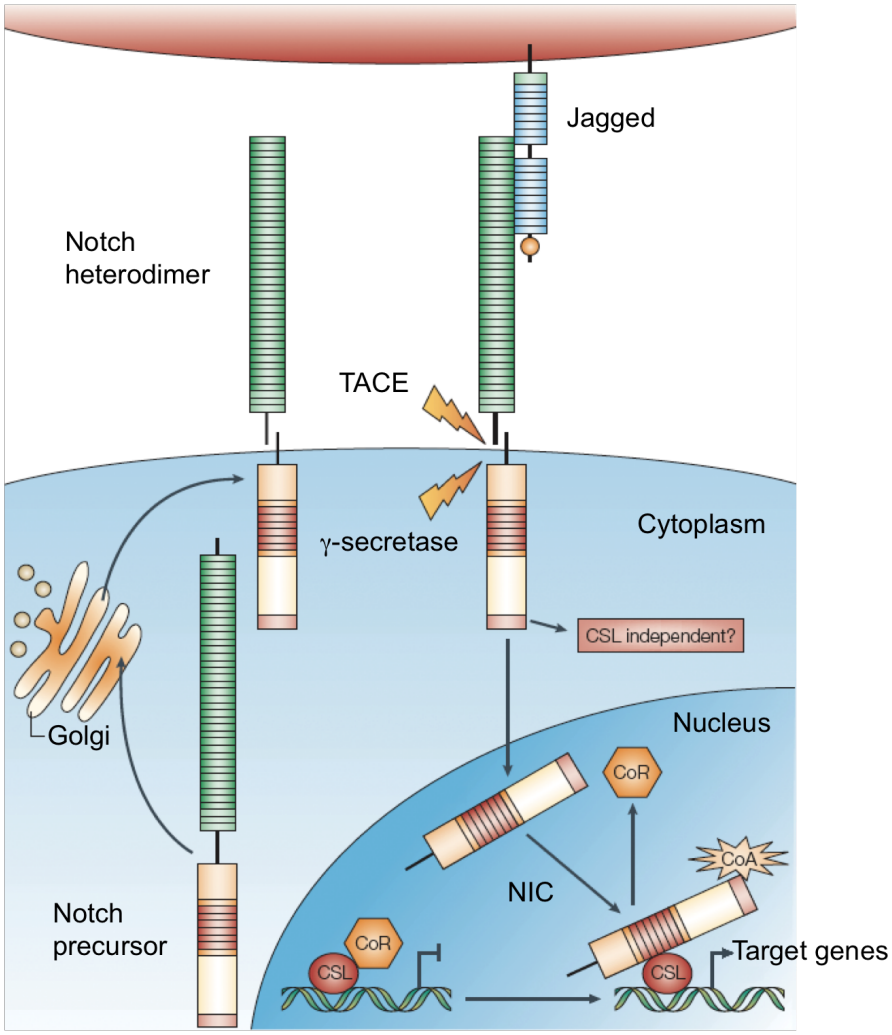

Fig. 1-5: Notch core pathway

Notch receptors are synthesized in the endoplasmatic reticulum as single-chain precursor proteins. They are cleaved in the Golgi by the furin-like convertase (S1) and transported to the cell surface where they are presented as heterodimers. Interaction of one of the ligands with a Notch receptor initiates the signaling cascade, leading to two consecutive proteolytic cleavage events. The first cleavage (S2) occurs in the EC domain mediated by TACE. The second cleavage (S3) occurs within the TM domain and is mediated by the γ-secretase. This leads to the release of the intracellular domain of Notch (NIC). NIC translocates into the nucleus where it interacts with the transcription factor CSL, which leads to the displacement of corepressors (CoR) and recruitment of coactivators (CoA). As a result, transcription of target genes commences.
Modified from Radtke (2003)

1.2.3.1 Notch Target Genes

The best-known target genes of Notch activation in mammals are the bHLH (basic-helix-loop-helix) transcription factors of the *Hairy/Enhancer of Split* (*Hes*) class. Of the seven genes identified (*Hes1-7*), *Hes1*, *Hes5* and *Hes7* can be induced by Notch signaling (Jarriault 1995; 1998; Kuroda 1999; Bessho 2001; Iso 2003). They belong to the bHLH class C proteins (Fisher 1998) and function as transcriptional repressors, suppressing the expression of other bHLH genes.

HERP (Hes-related repressor protein), also known as HEY transcription factors constitute another target-gene family. They are also bHLH class C proteins and act as transcriptional repressors. All three *Hey* genes (*Hey1, 2, L*) are target genes of Notch signaling (Leimeister 1999; Steidl 2000; Iso 2002; 2003).

Other Notch effectors have been described, albeit their direct link remains to be clarified. These include cell cycle regulator CDKN1a (also known as $p21^{Cip/Waf}$), Cyclin D1, Cyclin A (Miele 2006) and transcription factors of the nuclear factor-κB (NF-κB) family (Oswald 1998) among others.

1.2.4 Regulation of the Pathway

The core Notch signaling pathway outlined above is far more complex as there are numerous factors that influence and regulate the processes involved in signal transduction. Receptors and ligands are subject to various potential posttranscriptional alterations, e.g. glycosylation and cross interaction, leading to a broad spectrum of differential activity and signaling patterns (Hansson 2004; Bray 2006).

1.3 Notch Signaling During Pancreatic Organogenesis

1.3.1 Expression Pattern

Expression studies have demonstrated that all four Notch receptors are involved in pancreatic organogenesis, with varying spatial and temporal expression patterns (Apelqvist 1999; Jensen 2000a; 2000b; Lammert 2000; Del Monte 2007). Notch1 and Notch2 are detectable on E9.5 in epithelial cells of the pancreas, and expression of HES1 indicates active Notch signaling (Apelqvist 1999; Lammert 2000; Hald 2003). The initial partial overlap of Notch1 and Notch2 expression diverges from E11.5 on after the onset of branching morphogenesis (Lammert 2000). Whereas Notch1

expression remains high in nascent acini until E14.5, Notch2 expression becomes restricted to ductal structures (Lammert 2000; Hart 2003). During early pancreatic development (E10.5), Notch3 and Notch4 expression is confined to the mesenchyme, with Notch3 being more dispersed and Notch4 expression being limited to endothelial cells (Jensen 2000b; Lammert 2000). During later stages of development (E15.5), Notch3 and Notch4 are expressed in endothelial cells (Lammert 2000). The Notch ligand Dll1 can be detected on E9.5 in the dorsal pancreatic epithelium. During later stages it is predominantly expressed in duct epithelium in a scattered fashion (Apelqvist 1999; Beckers 1999; Lammert 2000). On E13.5, Jagged1 can also be detected in the pancreatic epithelium (Apelqvist 1999). The ligands Jagged1 and Jagged2 are primarily expressed in endothelial cells (Apelqvist 1999; Lammert 2000; Norgaard 2003).

1.3.2 Functional Analysis

Loss-of-function as well as gain-of-function studies have demonstrated Notch signaling to be crucial in regulation of cell differentiation as well as cell fate specification of endocrine and exocrine lineages in the developing pancreas.

Analysis of mice deficient in *Dll1* or its downstream target *Rbpj* – impairing Notch signaling at the ligand and intracellular level respectively – showed accelerated differentiation of $PDX1^+$ progenitor cells in the pancreatic bud into endocrine cells. First signs of altered gene expressions could be detected as early as E9.5 through a reduction in HES1 expression and an increase in $NGN3^+$ cells. On E10.5, *Dll1* mutant pancreata displayed small pancreatic buds and a precocious appearance of differentiated endocrine cells. Examination of the development of β-cells and exocrine tissue was precluded due to early embryonic lethality (Apelqvist 1999). Studies on mice deficient for *Hes1* – impairing Notch signaling on the target-gene level – demonstrated increased numbers in $glucagon^+$ cells, upregulation of NGN3 expression, and pancreatic hypoplasia (Jensen 2000b). Both studies found no alteration in apoptotic rate at early stages of development, implying that Notch signaling is not significantly involved in regulation of apoptosis during pancreatic development, and that pancreatic hypoplasia results from the depletion of a pancreatic precursor cell pool rather than elevated apoptosis.

Overexpression of Notch ligands Delta1 and Serrate1 in developing chicken pancreas, leading to cell autonomous inhibition of Notch signal reception through a

dominant negative effect, recapitulated the findings of increased and precocious endocrine differentiation as well as pancreatic hypoplasia, suggesting a conserved function of Notch signaling in pancreatic endocrine development between mice and chicken (Ahnfelt-Rønne 2007).

Conditional overexpression of NIC in pancreatic precursor cells leads to pancreatic hypoplasia with an almost complete absence of NGN3 expression on E12.5 and subsequent lack of endocrine differentiation, with pancreatic progenitor cells remaining in an undifferentiated state (Hald 2003; Murtaugh 2003). Furthermore, Notch signaling inhibits differentiation of $PDX1^+$ progenitor cells at multiple stages of pancreatogenesis, even after the pancreas has been specified (Murtaugh 2003).

Overexpression of NIC in developing chicken pancreas prevented endocrine differentiation via inhibition of NGN3 and NeuroD expression and function (Ahnfelt-Rønne 2007). These studies confirm the repressive function of Notch signaling on NGN3 expression and function, as well as endocrine differentiation.

In addition to alterations in endocrine lineage, mice with constitutive Notch activity in pancreatic precursor cells display completely abolished exocrine development, implicating Notch signaling in the regulation of exocrine specification during pancreatic development (Hald 2003; Murtaugh 2003). In vitro analysis of forced Notch pathway activation on explant cultures of mouse E10.5 dorsal pancreatic buds demonstrated that whereas early commitment to the exocrine lineage persisted – as evidenced by sustained PTF1a expression – terminal acinar differentiation was prevented, as evidenced by a lack of amylase expressing cells (Esni 2004). In vivo analysis of Notch signaling on exocrine differentiation in developing zebrafish pancreas revealed delayed exocrine development after forced expression of Notch and, conversely, accelerated exocrine differentiation in the absence of Notch signaling, defining an inhibitory role of Notch on exocrine differentiation. Subsequent in-vitro studies demonstrated that transcriptional activation of PTF1 is impaired by NIC and Notch target genes. These data imply that the mechanism by which Notch regulates exocrine development is through inhibition of PTF1 activity rather than through suppression of PTF1a expression (Esni 2004; Beres 2006).

A recent study on *Hes1* knockout mice combined with lineage tracing marking the pancreatic progenitor cells and their progeny revealed ectopic formation of pancreatic tissue through misexpression of PTF1a at an early developmental stage. The spatial distribution of ectopic pancreas development was limited to the PDX1-expressing

endoderm. Thus, HES1 mediated Notch signaling is not only crucial for cell differentiation and maintenance of a progenitor pool, but also required for region-appropriate specification of the pancreas in the developing foregut endoderm through regulation of PTF1a expression (Fukuda 2006). This is in accordance with a study showing that Notch target genes interact with and inhibit the PTF1 transcriptional complex (Esni 2004).

The above studies demonstrate that during the earliest stages of pancreatogenesis

a) Notch signaling prevents endocrine differentiation through repression of NGN3 expression and through inhibition of NGN3 function (Skipper 2000; Lee 2001; Ahnfelt-Rønne 2007),
b) absence of Notch signaling leads to premature endocrine differentiation at the expense of undifferentiated pancreatic progenitor cells, resulting in depletion of these cells,
c) Notch signaling is decisive in maintenance of a pool of undifferentiated precursors,
d) Notch regulates exocrine development through interaction with PTF1,
e) Notch signaling controls regional specification of pancreas in the developing endoderm.

The regenerative program of acini during acute pancreatitis has been found to resemble stages and gene expression profiles of embryonic development, including expression of Notch signaling members. Therefore, the cerulein-induced pancreatitis model has been used to investigate the role of Notch signaling during that process.

1.4 Notch Signaling in Adult Pancreatic Homeostasis

In the adult pancreas, Notch signaling is downregulated (Miyamoto 2003). However, studies have shown upregulation of Notch signaling elements in the regenerative process after cerulein induced acute pancreatitis (Gomez 2004; Jensen 2005) Comparison of regenerating cells to cells of the embryonic pancreas revealed that regenerating cells exhibit gene expression patterns characteristic for cells during embryonic development of the pancreas, indicating a change in differentiation status of pancreatic cells during regeneration (Jensen 2005). These studies suggest that Notch signaling is involved in restoring the physiological homeostasis of the adult pancreas through regulation of regeneration processes of acinar tissue during acute pancreatitis.

1.5 Cerulein-Induced Pancreatitis

It has been shown that experimental models using the application of cholecystokinin (CCK) lead to the induction of pancreatic injury (Adler 1983; Gorelick 1993). Doses that maintain continued maximal stimulation of the pancreas are accompanied by increase in protein synthesis and secretion, although the rate of secretion eventually surpasses the increase in synthesis, leading to a depletion of enzyme granules. Application of doses orders of magnitude higher than levels sufficient for maintaining maximal stimulation are referred to as supramaximal stimulation or hyperstimulation. (Gorelick 1993) Cerulein, an amphibian peptide isolated from the Australian frog Hyla caerulea has the same biological activity as CCK and can be used to induce pancreatitis in mice through repeated intraperitoneal injections of supramaximal doses in a highly reproducible, time-dependent way (Gorelick 1993; Reid 1999). The half life of cerulein is 3 – 5 minutes (De Caro 1972).

In the course of this treatment, pancreatic damage can be observed, including edema, increased serum levels of pancreatic enzymes, invasion of inflammatory cells, formation of metaplastic ductal lesions (e.g. tubular complexes), apoptosis and necrosis (Gorelick 1993; Bockman 1997; Reid 1999). However, in contrast to other pancreatitis models, the cerulein-induced pancreatitis never leads to hemorrhagic pancreatitis or death, resembling a mild form of pancreatitis. Complete pancreatic regeneration occurs within 7 to 10 days, resulting in the restitution of normal weight and morphology. This form of pancreatitis resembles the mild form of pancreatitis seen in humans in many ways, e.g. morphologic changes such as edema, loss of cellular polarity, invasion of inflammatory cells and acinar cell necrosis/apoptosis, as well as changes in biochemical parameters such as increase in serum levels of pancreatic enzymes. Therefore, this procedure provides a feasible experimental model for studying the pathobiology of acute experimental pancreatitis and serves as a valid animal model of the human disease (Gorelick 1993).

1.6 Notch Signaling During Pancreatic Organogenesis and Acute Pancreatitis

The involvement of Notch signaling during embryonic pancreatogenesis has been shown, and its impact on differentiation, cell fate specification, proliferation and apoptosis has been demonstrated through loss-of-function and gain-of-function

studies. These and other studies revealed that an intricate interplay of Notch signaling elements, transcription factors expressed during embryonic development of the pancreas and other signal transduction pathways is required for an accurate spatial and temporal pancreatic morphogenesis during embryogenesis (see 1.3.2).
Furthermore, it was shown that induction of acute pancreatitis leads to temporary upregulation of Notch signaling elements during the regenerative process, and that the gene expression profile of regenerating cells resembles that of pancreatic precursor cells during embryonic pancreatogenesis. These results suggest a role for Notch signaling during putative dedifferentiation processes and subsequent regeneration after pancreatic injury and imply similarities between the developmental program and regeneration.
The individual role of each of the four Notch receptors on pancreatic organogenesis, proliferation, differentiation, cell fate specification, dedifferentiation and subsequent regeneration during embryogenesis and after acute pancreatitis has so far not been established due to embryonic lethality of *Notch1* knockout mice on around E9.5, precluding further investigation of pancreatic development (Swiatek 1994; Conlon 1995). Targeted conditional disruption of one of the receptors specifically in the pancreas e.g. through utilization of Cre/loxP constructs could circumvent that problem, but have not yet been reported.

1.7 Site-Specific DNA Recombination: The Cre/loxP System

The site-specific Cre/loxP recombination system was discovered in the bacteriophage P1 and consists of two components: The Cre (*c*auses *re*combination) recombinase and a loxP (locus of crossing over of P1) site (Sternberg 1981; Hoess 1982; Abremski 1984; Hamilton 1984). The Cre recombinase is a 38 kDa protein belonging to the integrase family of site-specific recombinases and promotes site-specific, conservative recombination of DNA between loxP sites. The Cre recombinase protein can bind to DNA and perform recombination regardless of the conformation of the DNA containing the loxP sites. Furthermore, it functions autonomously, precluding the need for high-energy cofactors or accessory proteins for this recombination system to function efficiently. Cre can carry out intermolecular as well as intramolecular recombination between two loxP sites. Recombination products are dependent on relative orientation and location of loxP sites.

For intramolecular recombination, if the loxP sites are oriented in the same direction, the DNA that is flanked by loxP sites (floxed) is excised, leaving one loxP site behind (Fig. 1-6 A). If the loxP sites are oriented in opposite direction, the floxed DNA is inverted. Recombination of loxP sites that are located on separate DNA molecules (intermolecular recombination) results either in DNA integration or translocation. Intramolecular recombination is more efficient than intermolecular recombination (Abremski 1984; Metzger 1999).

The loxP site is a 34 bp DNA consensus sequence that is specifically recognized by the Cre recombinase (Fig. 1-6 B). It comprises two 13 bp inverted repeats whose axis of dyad symmetry is located within an 8 bp nonpalindromic core that defines the orientation of the overall sequence of the recognition site (Hoess 1982; Kwan 2002). Since the random occurrence of one specific 34 bp sequence requires a 10^{18} bp length of DNA, and the entire mammalian genome is only approximately $3x10^{9}$ bp, accidental recombination through incidental endogenous loxP sites is extremely unlikely, rendering this system highly specific (Nagy 2000).

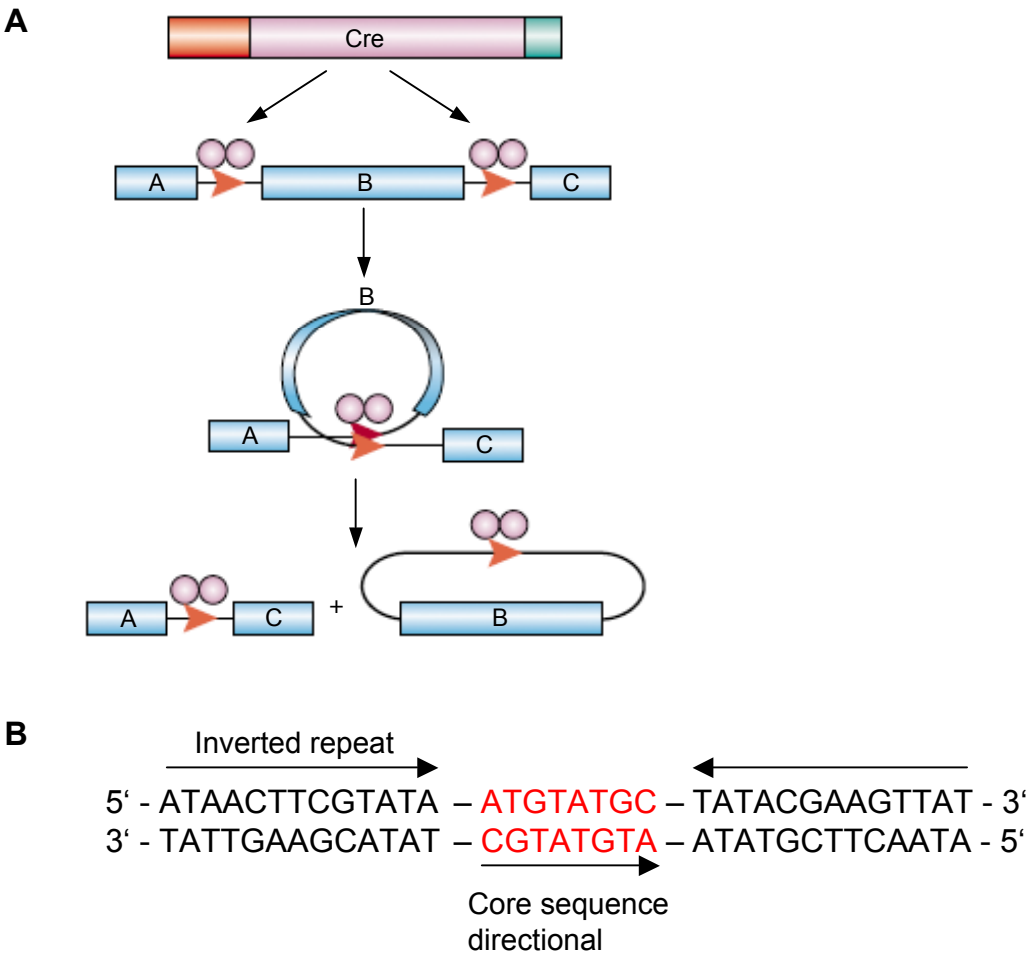

Fig. 1-6: Schematic representation of Cre/loxP mediated recombination

A) Dimers of Cre catalyze the recombination between loxP sites (red arrows). Region B is excised leading to juxtaposition of region A and C. If region B is an essential region of a gene, recombination renders the gene inactive.
B) The 34 bp sequence of the loxP site comprises two 13 bp inverse repeats flanking an 8 bp asymmetric core sequence (red) which defines the orientation of the loxP site.
Modified from (Lewandoski 2001)

2 Aim of the Study

It is the aim of the study to unravel the role of Notch1 signaling in pancreatic homeostasis using conditional, pancreas-specific knockout of the Notch1 receptor in mice utilizing the Cre/loxP system. The study is divided into two parts:

1) In the first part, the specific role of Notch1 receptor signaling on proliferation, apoptosis, differentiation and morphogenesis during embryonic pancreatogenesis as well as in juvenile and adult mice is examined.
2) The second part explores the function of Notch signaling on apoptosis, proliferation, and regeneration during cerulein-induced acute pancreatitis.
   a) First, to investigate whether the demonstrated upregulation of Notch elements during regeneration after cerulein-induced pancreatitis has a functional effect, a more general disruption of the Notch signaling pathway was induced through inhibition of the γ-secretase.
   b) Subsequently, the specific role of Notch1 receptor signaling on this process is examined through conditional disruption of Notch1 in the pancreas.

3 Material

3.1 Equipment and Devices

Chromatography Paper	Whatman
Centrifuge	Zentrifuge 5415R, Eppendorf
Counter	Totalizer T 120, BaumerIVO
Cryostat	Microm International, # HM 560
Digital camera	AxioCam HRc, Zeiss
Digital Imaging software	AxioVision, Zeiss
X-ray film	Amersham Hyperfilm ECL, GE Healthcare, #RPN3103K
Film developer	Amersham Hyperprocessor, GE Healthcare
Fluorescence Microscope	Axiovert 200M, Zeiss
Heater	Labtherm, Liebisch
Homogenizer	Heidolph Diax 900, Heidolph Instruments
Imaging software	AxioVision, Zeiss
Light Microscope	Axio Imager.A1, Zeiss, # 490801-0001-000
Microtome	Microm International, # HM 355S
Molecular Imager Gel Doc XR System	Bio-Rad
Mounting Glasses	Roth, # H877; 1871
pH-meter	MP220 pH-meter, Mettler-Toledo
Photometer (Protein)	Anthos reader 2001, Anthos
Pipettes	Eppendorf Research (Variable), Eppendorf
Photometer (RNA, DNA)	Nanodrop ND 1000, PEQLab
Scale	Sartorius, # BP2100S
TaqMan	ABI Prism® 7700 Sequence detection system, Perkin Elmer Biosystems,
Thermocycler	Primus 96 plus; MWG Biotech
Transfer Membrane	Immobilon-P Transfer Membrane, Millipore, # IPVH 00010

3.2 Chemicals

Acrylamide	Rotiphorese gel 30 Roth, # 3029.2
Acetic acid 100%	Merck, # 100063
β-mercaptoethanol	Sigma, # M7522
BrdU	Sigma-Aldrich, #B5202-5G
Cerulein	Sigma, # C9026
DNA Ladder + Loading Buffer	PEQLab # 25-2040
Eosin	Croma, # 2C-140
Ethidiumbromide	Sigma, # E1510
Glycine	Promega, # H-5073
Goat serum	Sigma, # G9023
Haematoxilin	Merck, # 105174
HCl	Merck, # 109057
HEPES	Sigma, # H7523
Histoclear	Roti-Histol, Roth, # 6640.1
Hydrogen peroxide 30%	Merck, # 108597
Isoflurane	Forene, Abbott, # B506
LE Agarose	Biozym, # 840.004
Methanol	Roth, # 4627.5
Mounting medium	Pertex, Medite, # PER 20000
PBS	PBS, Biochrom, # L182-50
Ponceau red	Fluka, # 09189
Protein Assay Dye Reagent Concentrate	Bio-Rad, # 500-0006
Protein standard	Bio-Rad # 161-0373
Rabbit serum	Sigma, # R9133
SDS	ICN, # 811030
Skim-milk powder	Fluka, # 70166, 500g
SYBR Green Buffer	Applied Biosystems, # 4309155
TEMED	Fluka, # 87689
Tissue Freezing Medium	Tissue-Tec, Sakura, # 4583
Tris-Base	Roth # 5429.2
Tween-20	Roth, # 9127.1
Tween 80	Sigma-Aldrich # P1754

3.3 Buffers and Solutions

10x PBS	10 M PBS
PBS-T	1x PBS, 0.1 % v/v Tween-20,
50x TAE	2 M Tris-acetate, 50 mM EDTA, pH = 8.3
TBE	0.89 M Tris-Base, 0.89 M Boric Acid, 0.02 M EDTA
TBS	10 mM Tris-Base, 150 mM NaCl
TBS-T	1x TBS, 0.1 % v/v Tween-20.
HEPES	1 M HEPES, pH adjusted to 7.9 with 1 M NaOH

3.3.1 X-gal Staining

Washing solution	0.1M PBS, 2mM $MgCl_2$
Staining solution	1 mg/ml X-gal, 5 mM $K_3Fe(CN)_6$, 5mM $K_4Fe(CN)_6$ - 3 H_2O dissolved in washing buffer

3.3.2 Western Blot

3.3.2.1 SDS PAGE

Separating Gel Buffer	1,5 M Tris-Base, pH 8,9 adjusted with HCl
Assemble Gel Buffer	0,5 M Tris-Base, pH 8,9 adjusted with HCl
Separating Gel (10 %)	4.1 ml aqua dest., 2.6 ml Separating Gel Buffer, 3.3 ml 30 % Acrylamide,100 µl10 % SDS, 50 µl 20 % APS, 15 µl TEMED
Stacking Gel	3.0 ml aqua dest., 1,3 ml Assemble Gel Buffer, 750 µl 30 % Acrylamide, 50 µl 10 % SDS, 25 µl 40 % APS, 5 µl, TEMED
SDS Running Buffer	25 mM Tris base, 192 mM Glycine, 0.1 % w/v SDS
Laemmli Loading Buffer	0.35 M Tris-Base pH 6.8, 36 % Glycerin, 10.28 % SDS, 0.6 M DTT, 0.012 % bromphenol blue The buffer was prepared 5x concentrated and stored in aliquots at -20°C

3.3.2.2 Protein Transfer and Immunological Detection

Transfer Buffer	25 mM Tris-Base pH 8.3, 150 mM Glycin, 10 % Methanol
Blocking Buffer	Skim milk 5 % w/v in TBS/T

3.3.3 Cell Lysis

IP-Buffer	50 mM HEPES pH 7.9, 150 mM NaCl, 1 mM EDTA, 0.5 % NP-40, 10 % Glycerol

3.3.4 Digestion of Mouse Tail

Cell Lysis Buffer	5 mM EDTA, 10 mM Tris-Base pH 8.0, 0.4 M NaCl
Proteinase K Buffer	10 mM Tris-Base pH 7.5, 20 mM $CaCl_2$, 50 % Glycerol, 1 % w/v Proteinase K (lyophilized)

3.3.5 Immunohistochemical Staining

Peroxidase Blocking Solution	100 µl H_2O_2 30 %, 900 µl dH2O
Blocking Solution	5 % v/v serum in 1x PBS

3.3.6 Treatment of Mice

BrdU stock solution	BrdU stock solution with a concentration of 20 mg/ml in 0.9 % NaCl was prepared. 100 µl aliquots were stored at -20°C
Cerulein stock solution	1 mg cerulein was dissolved in 1 ml dH_2O (1 mg/ml), 40 µl aliquots were stored at -20°C
DBZ stock solution	DBZ was custom-synthesized to more than 99.9 % purity by Syncom [Netherlands]. DBZ was suspended in 0.5 % (w/v) hydroxypropyl-methylcellulose [Methocel E4], 1 % (v/v) ethanol and 0.1 % (w/v) Tween in water.

4 Methods

4.1 Animal Model

4.1.1 Animals

Floxed *Notch1*$^{f/f}$ mice were generously provided by F. Radtke (1999). Mice were of mixed 129SV/C57BL/6J genetic background and were backcrossed to C57BL/6J background for 2-4 generations. *Ptf1a*$^{+/Cre(ex1)}$ mice were generated in our laboratory by Nakhai et al (2007). *Gt(ROSA)26Sor*^{tm1sor} (*ROSA26* reporter) mice have been described before (Soriano 1999). Transgenic Notch1-GFP reporter mice have been described before and were generously provided by W. Gao (Lewis 1998). For all DBZ experiments, C57BL/6 mice were used.

Animals were maintained in the animal facility of the II. Medizinische Klinik, Klinikum rechts der Isar, Technical University Munich, on a 12-hour light and 12-hour dark schedule. They had free access to food and drinking water.

Mouse protocols and experiments were approved by the Faculty of Medicine, Technical University Munich.

4.1.2 Induction of Pancreatitis

Acute pancreatitis in mice was induced by repeated intraperitoneal injections of cerulein according to the following protocol described by Jensen et al. (2005):

- Dilution of cerulein stock solution 1:100 with PBS; final concentration: 10 µg/ml
- 200 µl per injection
- 8 injections per day, one every hour, on two consecutive days

Mice were sacrificed 24 hours (1d), 3 days (3d) and 7 days (7d) after final injection of cerulein.

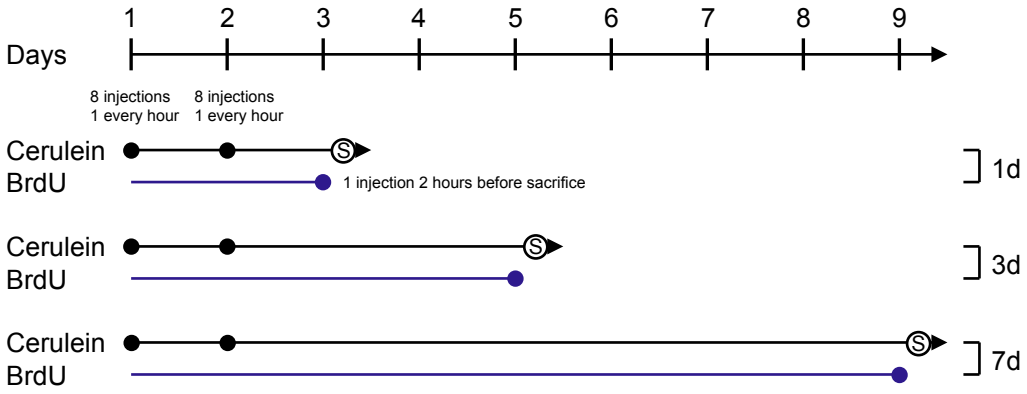

4.1.3 DBZ Treatment

To inhibit the activity of the γ-secretase complex, dibenzazepine (DBA) was injected into the intraperitoneal cave. Injections were performed according to the following protocol described before (van Es 2005):

- 10 μmol/kg BW
- 1 injection per day
- Injections were started on the same day as cerulein injections and were continued until the day of sacrifice of the mice

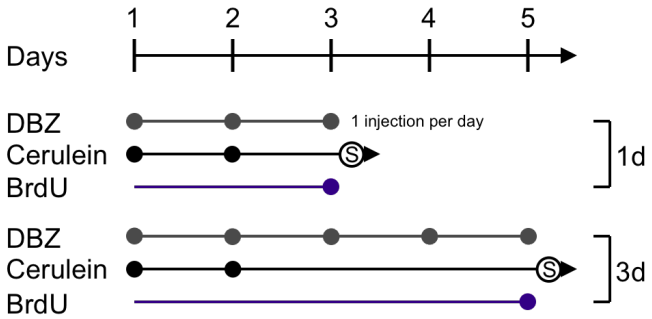

4.1.4 BrdU Treatment

5-bromo-2-deoxyuridine (BrdU) is a thymidine analogue that is inserted into replicating DNA of proliferating cells and can be detected by immunohistochemistry.
For detection and quantitation of proliferating cells, intraperitoneal (i.p.) injections were performed according to the following protocol:

- Dilution of BrdU stock solution 1:10 with 0,9 % NaCl, final concentration: 2 mg/ml
- Injection of 20 mg/kg BW 2 hours before sacrifice (see figures above).

4.2 Collection of Tissue Samples

4.2.1 Embryos

Embryos of the desired age were obtained through timed breeding by leaving one male with several female for one night. On the desired day of pregnancy, the female was anesthetized with Isoflurane and sacrificed by rapid dislocation of the cervical spine. Embryos were retrieved by opening the uterus, taking out and opening the

amniotic sac containing the embryos. Amniotic sacs were collected for genotyping. Embryos were transferred into chilled (4°C) 4 % PFA and left at 4°C for overnight fixation. The embryos were processed in the Institute for Pathology, Klinikum rechts der Isar, and embedded in paraffin.

4.2.2 Newborn Mice

Newborn mice were sacrificed in Isoflurane. To allow for better penetration of PFA and paraffin, head, arms and legs were cut off and the gastrointestinal cavity opened. Part of the tail was taken for genotyping. Mice were transferred into chilled 4 % PFA for overnight fixation at 4°C. Newborn mice were processed in the Institute for Pathology, Klinikum rechts der Isar, and embedded in paraffin.

4.2.3 Adult Mice

Mice were anesthetized with Isoflurane and sacrificed by rapid dislocation of the cervical spine. Bodyweight of the mice was documented. Mice were disinfected with 70 % ethanol, the abdomen opened, the pancreas exposed and the organs examined for macroscopic alterations.

To keep the effect of autodigestive and degrading processes at a minimum, small tissue samples for RNA and protein were taken from three different regions immediately after exposure of the pancreas.

Samples for RNA were transferred into a cryo tube containing 1200 µl RLT buffer (RNeasy Mini Kit [Qiagen, #74106]) supplemented with 1 % v/v β-mercaptoethanol, homogenized with a homogenizer and snap frozen in liquid nitrogen.

Pancreas samples for protein were transferred into a cryotube and either snap frozen in liquid nitrogen or immediately processed. The pancreas was then dissected from the surrounding tissue and the weight documented.

For paraffin embedding, the pancreas, and other organs were put into a cassette for overnight fixation in 4°C PFA (4 %). Samples were processed in the Institute for Pathology and embedded in paraffin. For cryo sectioning, tissue samples were embedded in Tissue Freezing Medium and snap frozen in liquid nitrogen. A small part of the tail was taken for genotyping.

Samples for RNA, Protein and cryo sectioning were stored in -80°C, the tail was stored in -20°C and the paraffin blocks were either stored at 4°C or at -20°C for later processing.

4.3 Genotyping of Mice

4.3.1 Digestion of Tail or Amniotic Sac

Tails or amniotic sacs were transferred into 300 µl cell-lysis-buffer supplemented with 10 µl proteinase K and heated overnight at 50°C.

4.3.2 DNA Isolation and Purification

100 µl of 6 M NaCl were added, the vial vortexed and centrifuged at 14.000 rpm for 20 minutes. To precipitate the DNA, the supernatant was transferred into a new vial and mixed with isopropanol (1:1). The vial was centrifuged at 14.000 rpm for 10 min and the supernatant discarded. The DNA pellet was washed twice with 500 µl chilled 70 % ethanol (4°C) followed by centrifugation at 14.000 rpm and 4°C. Pellets were left at room temperature for approximately 20 min to allow for the ethanol to evaporate. Finally, pellets were dissolved in 30 µl TE buffer. Vials were heated to 50°C for 2 h to let the DNA unfold and make sure that there was no residual ethanol. DNA was stored at 4°C for later processing.

4.3.3 PCR

Isolated DNA was subject to PCR analysis for the genes of interest with the respective primer (Table 4-1), using the "RedTaq ReadyMix PCR REACTION MIX" [Sigma, R-2523] according to the manufacturer's protocol. Primers were purchased from MWG Biotech AG.

Table 4-1: Sequence of primers used for genotyping

Primer	Sequence 5' – 3'	
Notch1	Forward	CTG ACT TAG TAG GGG GAA AAC
	Reverse	AGT GGT CCA GGG TGT GAG TGT
Cre recombinase	Forward	ACC AGC CAG CTA TCA ACT CG
	Reverse	TTA CAT TGG TCC AGC CAC C
$Ptf1a^{+/Cre(ex1}$	Forward	GTC CAA TTT ACT GAC CGT ACA CCA A
	Reverse	CCT CGA AGG CGT CGT TGA TGG ACT GCA

4.3.3.1 Cycling Conditions

Initial denaturation		95°C	1 min.
Cycles 1 – 40	Denaturation	94°C	30 sec.
	Annealing	58°C	30 sec.
	Elongation	72°C	1 min. 30 sec.
Substrate clearance		72°C	10 min.
Storage		4°C	

4.3.4 Agarose Gel Electrophoresis

LE Agarose was dissolved in 1x TBE by boiling. After cooling down, 0.01 % v/v ethidiumbromide was added, and the gel poured into the gel tray with the gel comb set in. PCR products with the DNA samples were loaded onto the hardened gel. A voltage of 80 V was applied until the sample had completely diffused into the gel. The voltage was then increased to 130 V until bands were clearly discernible.

4.3.5 Visualization

DNA bands were made visible and documented under UV-light with the Molecular Imager Gel Doc XR System.

4.4 X-gal Staining

The midgut region from newborn wt mice and pancreata from 6 week-old *N1KO* mice were dissected from the peritoneal cavity and immersed in 4 % PFA for 1 hour for fixation. Tissue samples were washed 3 times in washing solution for 5 minutes. For staining, tissue samples were incubated overnight in staining solution in the dark. Macroscopic pictures were taken with a digital camera.

For microscopic analysis, stained tissue samples were dehydrated, embedded and cut into 3.5 to 4.5 µm thin sections with a Microtome as described below.

4.5 Histology

4.5.1 Preparation of Slides

4.5.1.1 Paraffin Embedded Samples

Paraffin embedded tissue samples were cooled down to -20°C, cut into 3.5 µm thin sections with a Microtome and fixed on mounting glasses.
Slides were deparaffinized and rehydrated according to the following protocol:

- 2x 5 min. Histoclear
- 2x 5 min.100 % ethanol
- 2x 5 min. 96 % ethanol
- 2x 5 min.80 % ethanol
- 1x 5 min. water

4.5.1.2 Cryo Sections

Tissue samples for cryo sectioning were cut into 7-8 µm thin slides in a cryotome at -20°C and fixed on mounting glasses. Slides were left at RT overnight and incubated in chilled acetone (-20°C) for 10 minutes for fixation.

4.5.2 H&E Staining

Rehydrated paraffin slides or cryo slides were immersed into Mayer's Haemalaun for 5 minutes, washed with tap water for 10 minutes and immersed into ethanolic Eosin (0.33 % v/v) for 5 minutes.

4.5.3 Immunohistochemistry (IHC)

For antigen retrieval, rehydrated paraffin slides or cryo slides were boiled in 10 mM sodium-citrate buffer [Antigen Unmasking Solution, Vector Laboratories, # H-3300] for 10 minutes in a microwave oven, left at room temperature for 30 minutes to cool down and washed 3 times with PBS. To block endogenous peroxidase activity, slides were incubated in 3 % v/v H_2O_2 solution for 30 minutes in the dark and washed 3 times 5 minutes with PBS. To avoid nonspecific binding of secondary antibody, serum from the species from which the secondary antibody was derived was added to PBS (5 % v/v). Nonspecific endogenous biotin sites were blocked by adding avidin to the blocking solution [Avidin/Biotin Blocking Kit, Vector Laboratories, #SP-2001]. Slides were incubated in blocking solution for 30 minutes at room temperature and

washed 3 times with PBS. Nonspecific endogenous biotin binding sites and the available biotin binding sites on the avidin were blocked by adding biotin to the blocking solution [Avidin/Biotin Blocking Kit, Vector Laboratories, #SP-2001].
Primary antibody was added to the solution in the desired concentration (Table 4-2). Slides were incubated in the solution for the time indicated in the protocol and washed 3 times with PBS. Secondary antibody was added to the blocking solution in the desired concentration (Table 4-2). Slides were incubated in the solution for 30 minutes at room temperature and washed 3 times with PBS.
Bound antibodies were detected using the avidin-biotin-complex (ABC) peroxidase method [ABC Elite Kit, Vector Laboratories, # PK-6100]. For final staining, DAB solution was prepared according to the manufacturer's protocol **[**Vector Laboratories, # SK-4100**]**. Slides were incubated in the solution either until a brown stain became visible, but at most for 3 minutes, and then transferred into distilled water. Nuclei were counterstained with hematoxilin for 1 second followed by washing in tap water. Alternatively, cytoplasm was counterstained with eosin for 10 seconds. Slides were dehydrated according to the following protocol:

- 2x 1 min.80 % ethanol
- 2x 1 min. 96 % ethanol
- 2x 1 min.100 % ethanol
- 2x 3 min. Histoclear

Slides were mounted with mounting medium and covered with mounting glasses.

Table 4-2: Antibodies used for IHC

Primary antibody	Species	Dilution	Blocking solution	Incubation time	Company
Amylase	Goat	1:1000	5 % v/v Rabbit serum	1 h RT 18 h 4°C	Santa Cruz # sc-31869
Carboxypeptidase A	Rabbit	1:2000	5 % v/v Goat serum	1 h RT 18 h 4°C	Biotrend # 1810-0006
Insulin	Guinea pig	1:500	5 % v/v Goat serum	1 h RT 18 h 4°C	R&D Systems # MAB1417
Glucagon	Guinea pig	1:500	5 % v/v Goat serum	1 h RT 18 h 4°C	Linco # 4031-01F
Somatostatin	Rabbit	1:500	5 % v/v Goat serum	1 h RT 18 h 4°C	ICN # 64714

Pancreatic polypeptide	Rabbit	1:500	5 % v/v Goat serum	1 h RT 18 h 4°C	Chemicon # AB939
DBA		1:200		1 h RT 18 h 4°C	Vector Laboratories # B-1035
BrdU	Rat	1:250	5 % v/v Rabbit serum	1 h RT 18 h 4°C	Serotec # MCA2060
Cleaved Caspase-3	Rabbit	1:500	5 % v/v Goat serum	1 h RT 18 h 4°C	Cell Signaling # 9661S
HES1	Rabbit	1:200	5 % v/v Goat serum	1 h RT 18 h 4°C	Gift from T. Sudo
Clusterin	Goat	1:500	5 % v/v Rabbit serum	1 h RT 18 h 4°C	Santa Cruz sc-6420
PDX1	Rabbit	1:10000	5 % v/v Goat serum	1 h RT 18 h 4°C	Gift from C.V. Wright
CD45	Rat	1:50	5 % v/v Rabbit serum	1 h RT 18 h 4°C	BD # 550539
F4/80	Rat	1:300	5 % v/v Rabbit serum	1 h RT 18 h 4°C	Serotec # MCAP497
CD8	Rat	1:100	5 % v/v Rabbit serum	1 h RT 18 h 4°C	Pharmingen # 550281
CD4	Rat	1:100	5 % v/v Rabbit serum	1 h RT 18 h 4°C	Pharmingen # 550278
Ly6 (Gr1)	Rat	1:100	5 % v/v Rabbit serum	1 h RT 18 h 4°C	BD # 550291
Secondary antibody					
Anti-rabbit Biotin conjugate	Goat	1:500	5 % v/v Goat serum	30 min. RT	Vector Laboratories # BA-1000
Anti-goat Biotin conjugate	Rabbit	1:500	5 % v/v Rabbit serum	30 min. RT	Vector Laboratories # BA-5000
Anti-Rat Biotin conjugate	Rabbit	1:500	5 % v/v Rabbit serum	30 min. RT	Vector Laboratories # BA-4000
Anti-Guinea-pig	Goat	1:500	5 % v/v Goat serum	30 min. RT	Dianova 106-065-003

4.5.4 Immunofluorescence

Antigen retrieval and serum-block was done as described before. Primary antibody was diluted in 5 % blocking solution to the desired concentration (Table 4-3). Sections were incubated overnight at 4°C and washed 3 times 5 minutes with PBS. Secondary antibody conjugated to a fluorochrome was diluted in 5 % blocking solution to the desired concentration (Table 4-3). Sections were incubated for 30 minutes at RT and washed 3 times 5 minutes with PBS. For multiple staining, slides were incubated with another primary antibody for 1 hour at RT, washed 3 times with PBS and incubated with a suitable secondary antibody conjugated with a fluorochrome different from the other secondary antibody for 1 hour at RT.

For nuclear counterstaining and mounting, slides were covered with Vectashield mounting medium with DAPI [Vector, #H-1200] and covered with mounting glasses. The edges were sealed with nail polish and dried.

Table 4-3: Antibodies used for Immunofluorescence

Primary antibody	**Species**	**Dilution**	**Blocking solution**	**Incubation time**	**Company**
Amylase	Goat	1:1000	5 % v/v Rabbit serum	1 h RT 18 h 4°C	Santa Cruz # sc-31869
β-catenin	Rabbit	1:1000	5 % v/v Goat serum	1 h RT 18 h 4°C	BD # 610153
E-cadherin	Goat	1:200	5 % v/v Rabbit serum	1 h RT 18 h 4°C	R&D Systems # AF748
Secondary antibody					
Anti-rabbit Biotin conjugate	Goat	1:500	5 % v/v Goat serum	30 min. RT	Vector Laboratories # BA-1000
Anti-goat Biotin conjugate	Rabbit	1:500	5 % v/v Rabbit serum	30 min. RT	Vector Laboratories # BA-5000
Anti-goat Alexa555 conjugate	Rabbit	1:500	5 % v/v Rabbit serum	30 min. RT	Invitrogen # A21431
Anti-rabbit Alexa555 conjugate	Goat	1:500	5 % v/v Goat serum	30 min. RT	Invitrogen # A21428
Streptavidin Alexa488 conjugate		1:500	5 % v/v BSA	30 min. RT	Invitrogen # S32354

4.6 Quantitation of Proliferation

4.6.1 Embryos

BrdU positive cells were counted and the area of the developing pancreas determined with a digital imaging software. The ratio of proliferating cells to total pancreatic area was calculated and multiplied by 10,000.

4.6.2 Adult mice

High-resolution photographs of 3-4 randomly chosen visual fields of BrdU stained slides were taken with a digital camera at a 200x magnification. BrdU positive nuclei and unstained nuclei of pancreatic acinar cells were counted, and the percentage of proliferating cells was calculated.

4.7 Quantitation of Apoptosis

Pancreatic acinar cells stained for cleaved Caspase-3 were counted in multiple visual fields through a microscope at 200x magnification and the ratio of apoptotic cells per visual field was calculated. Visual fields were chosen to cover the entire pancreas on a slide. No less than 5 visual fields were screened.

4.8 Quantitation of Acinar Regeneration

To quantitate the extent of acinar regeneration in cerulein treated mice, high-resolution photographs of 3-8 randomly chosen visual fields of amylase stained slides were taken with a digital camera at a 100x magnification. The number of acini was counted and the area of the examined visual field determined with a digital imaging software. The ratio of number of acini to pancreatic area was calculated and multiplied by 10,000.

4.9 Detection of Proteins

4.9.1 Protein Isolation from Pancreatic Tissue

Tissue samples were supplemented with 450 µl IP buffer and lysed with a homogenizer. Lysed samples were centrifuged at 14.000 rpm for 10 min at 4°C. Supernatant was transferred to a new vial and immediately chilled on ice.

4.9.2 Protein Quantitation by the Method of Bradford

Protein Assay Dye Reagent Concentrate was diluted 1:5 with water and transferred into microcuvettes. Standard dilution series of known concentration were made by adding BSA stock solution to the microcuvettes. Test Samples with unknown concentration were added to the remaining cuvettes, vortexed and incubated at room temperature for 1 minute. The absorbance was measured with the Photometer at 595 nm vs. water reference, a standard curve was obtained and the sample protein concentration calculated. Samples were adjusted to a concentration of 5 µg/µl with IP buffer.

4.9.3 Western Blot Analysis

4.9.3.1 SDS Gel Electrophoresis

Whole cell lysates were supplemented with 5x Laemmli-Buffer and heated to 95°C for 5 minutes to denature the proteins and mask their intrinsic electric charge, making the migration of the proteins solely dependent on their size. Samples were loaded on a stacking-gel placed on top of a suitable separating-gel. Gels were placed in SDS-Running-Buffer and a voltage of 120-150 V was applied.

4.9.3.2 Protein Transfer from SDS Gels to a PVDF Membrane

PVDF-Membranes were activated in methanol at room temperature for one minute. Gels and PVDF-Membranes were washed in distilled water, equilibrated in transfer-buffer at room temperature for one minute, and placed in the appropriate layer in the transfer sandwich. The transfer sandwich was prepared as follows:

1. Fiber pad soaked in transfer buffer
2. Three pieces of Whatman-paper soaked in transfer-buffer
3. PVDF membrane
4. SDS-Gel
5. Three pieces of Whatman-paper soaked in transfer-buffer
6. Fiber pad soaked in transfer buffer

The transfer-sandwich was placed in a semi-dry blotting chamber, and a current of 150 mA per gel was applied for 45 minutes.

Alternatively, the transfer sandwich was immersed in transfer-buffer, and a current of 350 mA was applied for 2,5 h. To prevent the buffer from overheating, an ice tank was placed in the wet blot tank.

4.9.3.3 Immunological Detection of Proteins

To block unspecific sites, the membrane was incubated in 5 % skim milk for 30 minutes. The membrane was incubated with the primary antibody diluted in skim milk in the respective concentration (Table 4-4) overnight on a shaker at 4°C. Membranes were washed with PBS-T three times 10 for minutes, followed by incubation with the secondary antibody labeled with horseradish peroxidase, diluted in skim milk for one hour on the shaker at room temperature. Membranes were washed with PBS-T three times for 10 minutes.

Chemiluminescent substrate was prepared by using Amersham ECL Western Blotting Detection Reagents [GE Healthcare, #RPN2106] according to the manufacturer's protocol. If chemifluorescent signal was low, detection was performed using Amersham ECL plus Western Blotting Detection Reagents [GE Healthcare, #RPN2132] according to the manufacturer's protocol.

Membranes were placed in a plastic sheet. A film was placed on top of the membrane in a film cassette and exposed for an appropriate period of time. The film was developed and fixed in red light [Amersham Hyperprocessor, GE Healthcare].

Table 4-4: Antibodies used for western blot

Primary antibody	**Species**	**Dilution**	**Blocking solution**	**Incubation time**	**Company**
Notch1 IC	Mouse	1:1000	5% skim milk	18h 4°C	Pharmingen # 552466
β-catenin	Rabbit	1:1000	5% skim milk	18h 4°C	BD # 610153
ERK 1/2	Rabbit	1:1000	5% skim milk	18h 4°C	Santa Cruz # sc-101760
Secondary antibody					
Anti-rabbit IgG HRP conjugate	Donkey	1:500	5% skim milk	1 h. RT	GE Healthcare # NA934
Anti-mouse IgG HRP conjugate	Sheep	1:500	5% skim milk	1h. RT	GE Healthcare # NA931

4.9.3.4 Stripping

Membranes were stripped in 0,1 M Glycine with 1 % v/v SDS at pH 2,0 and room temperature for 30 minutes, washed in TBS-T 3 x 10 minutes and blocked in skim milk for 30 minutes at room temperature.

4.10 Detection and Quantitation of Gene Transcription

4.10.1 Isolation of mRNA from Pancreatic Tissue

Lysed tissue samples for RNA extraction were thawed on ice. 600 µl were taken for RNA extraction using the RNeasy Mini Kit [Qiagen, #74106] according to the manufacturer's protocol, including the optional DNase step with the RNase-Free DNase Set [Qiagen, #79254]. After final centrifugation with RNase free water provided by the manufacturer, samples were instantly stored on ice.

4.10.2 cDNA Synthesis

cDNA synthesis was performed with 15 µg of the RNA sample using SuperScript™ III Reverse Transcriptase [Invitrogen, # 18080-093] or SuperScript™ II Reverse Transcriptase [Invitrogen, #18064-022] according to manufacturer's protocol. The following components were added:
dNTP [Sigma, #D7295]
Random primer [Promega, #C1181]
RNase Inhibitor [SUPERase In, Ambion, #AM2694]
The cDNA was aliquoted into 8 PCR-tubes and stored at -20°C.

4.10.3 Real-Time Quantitative RT-PCR (Real-Time qRT-PCR)

4.10.3.1 Primer Design

Primers were designed using Primer Express software (Applied Biosystems) considering the following parameters:

- The amplicon length should range from 50-150 base pairs.
- Both primers should be approximately 18-25 nucleotides long.
- The melting temperatures (T_m) should be 58-60°C. The T_m of primers used in one reaction should be compatible.

- All four bases should be evenly distributed (45-55 % G/C content) and long stretches of identical nucleotides (especially runs of four or more Gs) should be avoided.
- The last nucleotide at the 3' end should preferably be a G or C for tighter binding at the priming site, but the five nucleotides at the 3' end should have no more than two G and/or C bases.

Primers and probes were tested for possible dimer formation, secondary structures and selfcomplementarities by computational tools. At least one primer spanned an intron in order to exclude amplification of genomic DNA.

4.10.3.2 Real-Time qRT-PCR

Real-time qRT-PCR analyses for sample mRNAs were performed using the ABI PRISM 7700 Sequence Detection System instrument and software. The sequences of the PCR primer pairs for each gene are shown in Table 4-5. Primers were purchased from MWG Biotech AG.

Real-time qRT-PCR was performed using the SYBR Green method. SYBR Green is a cyanine dye that binds to double stranded DNA. The resulting complex absorbs blue light and emits green light. The intensity of fluorescence is directly proportional to the amount of complex formation.

5 µl of cDNA, 900 nM of primers and 12.5 µl of 2x SYBR Green Buffer were used in a 25 µl final master mix.

Table 4-5: Sequence of primers used for real-time qRT-PCR

Primer	**Sequence 5' – 3'**	
Cyclophilin	Forward	ATG GTC AAC CCC ACC GTG T
	Reverse	TTC TGC TGT CTT TGG AAC TTT GTC
Notch1	Forward	ACA TCC GTG GCT CCA TTG TCT A
	Reverse	TCT TGT AAG GAA TAT TGA GGC TGC
Notch2	Forward	GCC TCC CAT CGT GAC TTT CC
	Reverse	GGG CAA CTG GAC TGC GTC
Hes1	Forward	AAA ATT CCT CCT CCC CGG TG
	Reverse	TTT GTT TTG TCC GGT GTC G
Hey1	Forward	CAC TGC AGG AGG GAA AGG TTA TT
	Reverse	GCC AGG CAT TCC CGA AAC

Dll1	Forward	CGG CTC TTC CCC TTG TTC TAA C
	Reverse	CCA CAT TGT CCT CGC AGT ACC T
Amylase	Forward	TGG TCA ATG GTC AGC CTT TTT C
	Reverse	CAC AGT ATG TGC CAG CAG GAA G
Insulin	Forward	GGA CCT TCA GAC CTT GGC GTT
	Reverse	GTT GCA GTA GTT CTC CAG CTG GTA G
CK19	Forward	ACC CTC CCG AGA TTA CAA CCA
	Reverse	GGC GAG CAT TGT CAA TCT GT
Vimentin	Forward	GCC TCT GCC AAC CTT TTC TT
	Reverse	CAT CTC TGG TCT CAA CCG TCT T
F4/80	Forward	CTT TGG CTA TGG GCT TCC AGT C
	Reverse	GCA AGG AGG ACA GAG TTT ATC GTG

4.10.3.3 Quantitation of Gene Expression

Relative expression levels of amplified target genes were calculated using the $2^{-\Delta\Delta Ct}$ method. Cyclophilin was used as the internal control gene to account for differences in starting amount of mRNA and compensate inter PCR variations (Thellin 1999; Livak 2001; Pfaffl 2001). Wildtype mice served as the calibrator. To compare different mice, Ct values from the target genes were subtracted from Ct values from cyclophilin (ΔCt). To compare wildtype animals with *N1KO* animals, the mean Ct value was calculated for wildtype mice and subtracted from the Ct value of each *N1KO* mouse ($\Delta\Delta$Ct) (Livak 2001). Relative expression levels were calculated using the following formula:

- Relative expression = $2^{-\Delta\Delta Ct}$

4.11 Statistical analysis

Correlation between different groups was calculated using the unpaired, two sided students T-test, using SPSS 17.0 for Apple Macintosh. Assumption of equal variances was based upon the “Levene’s Test for Equality of Variances”, using SPSS 17.0 for Apple Macintosh. $p < 0.05$ was considered significant.

5 Results

5.1 Generation of Pancreas-Specific Conditional *Notch1*-Knockout Mice

To study the role of Notch1 signaling in pancreatic development, proliferation, differentiation, and regenerative capabilities, pancreas-specific conditional *Notch1*-knockout (*N1KO*) mice were generated using the Cre/loxP approach. In order to obtain mice with conditionally deleted Notch1 receptors in the pancreatic tissue, two mouse lines are required:

a) A knock-in mouse line harboring the Cre recombinase driven by the promoter of *Ptf1a*, also known as p48 (hereafter *Ptf1a*$^{+/Cre(ex1)}$) (Fig. 5-1 A).
b) One mouse line in which both alleles of the Notch1 signal peptide including the putative promoter are flanked by loxP sites (floxed), (Notch1$^{f/f}$) (Fig. 5-1 B).

Crossing of these two mouse lines generates offspring harboring the Cre recombinase and floxed *Notch1* alleles in their genome. This leads to excision and recombination of the *Notch1* signal peptide and the putative promoter in cells expressing the Cre recombinase, hence in cells expressing *Ptf1a*. Therefore, *Notch1* expression is exclusively eradicated in cells in which *Ptf1a* is activated. Successfully recombined *Notch1* alleles in pancreatic progenitor cells are subsequently inherited by their progeny.

Mice with homozygously floxed *Notch1* alleles that do not harbor the Cre recombinase (*Ptf1a*$^{+/+}$/*Notch1*$^{f/f}$) and mice harboring the *Ptf1a*/*Cre* knock-in construct without floxed *Notch1* alleles (*Ptf1a*$^{+/Cre(ex1)}$/*Notch1*$^{+/+}$) showed no phenotype (this study and (Krapp 1998) and were used as wildtype control mice hereafter referred to as wt.

A

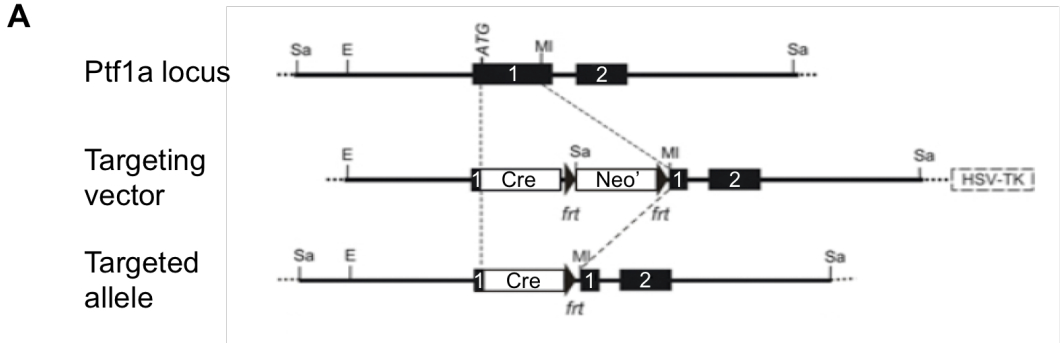

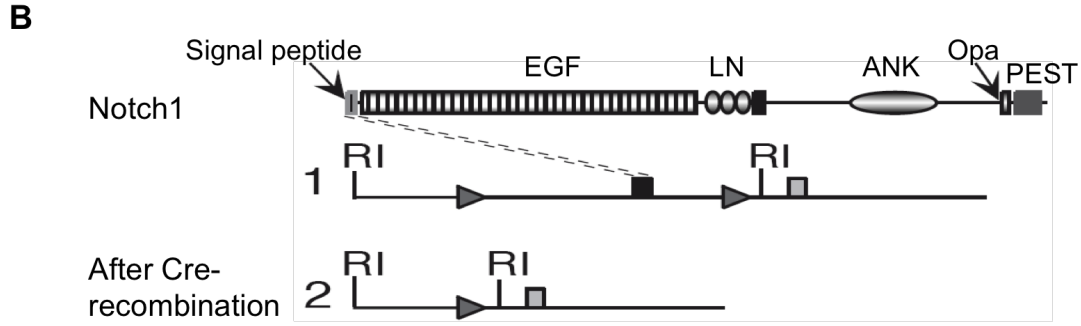

Fig. 5-1: Cre/loxP mediated conditional knockout of the Notch1 receptor

A) Knock-in Cre recombinase driven by the promoter of *Ptf1a*. Black boxes represent exons 1 and 2, open boxes indicate Cre recombinase (Cre) and neomycin resistance gene (*neo*^{r}). Insertion of the Cre recombinase into the first exon results in one *Ptf1a* null allele.
Modified from Nakhai (2007).
B) Schematic structure of the murine Notch1 receptor and the corresponding location on the DNA are shown (1). The black box represents the exon coding for the signal peptide and the putative promoter. Triangles represent localization and orientation of the loxP sites. Cre-mediated excision and recombination of the loxP sites results in deletion of the floxed sequences, leading to a truncated *Notch1* gene lacking the signal peptide and putative promoter (2). From Lutolf (2002)

5.1.1 Confirmation of Cre Recombinase Activity

To monitor Cre recombinase activity, *Ptf1a*$^{+/Cre(ex1)}$ mice were first crossed to *Gt(ROSA)26Sor*^{tm1sor} (*ROSA26* reporter) mice, which carry a lox-STOP-lox (LSL) sequence followed by a modified *lacZ* gene under the promoter of the cell type-independent, ubiquitously transcribed *ROSA26R* gene (Soriano 1999). In the offspring from this cross, *Ptf1a*-driven expression of Cre recombinase excises the floxed stop cassette upstream of *lacZ*, thereby activating expression of β-galactosidase. Consequently, expression of β-galactosidase marks cells in which *Ptf1a* has been activated, a trait that is inherited by their progeny. These cells can be visualized by staining with 5-bromo-4-chloro-3indolyl-β-D-galactosidase (X-gal) (Kawaguchi 2002; Fukuda 2006).

First, lineage-tracing studies with X-gal staining were performed on wt mice to examine two aspects of the *Ptf1a*$^{+/Cre(ex1)}$ construct:

a) Efficiency of the Cre mediated recombination within the pancreas
b) Pancreatic specificity of the *Ptf1a*-driven Cre expression

Staining of embryonic stages (E11.5 and E18.5) were done by Nakhai et al. (2007; 2008a) and revealed Cre mediated recombination to be efficiently and homogeneously executed in the pancreas.

Macroscopic inspection of dissected gastrointestinal tract of newborn wt pups after X-gal staining showed uniform, homogeneous β-galactosidase expression of the entire pancreatic tissue, confirming the inheritance of the Cre mediated recombination in the progeny from the progenitor cells. In the gastrointestinal tract, expression of β-galactosidase was strictly limited to the pancreatic tissue and did not extend to the surrounding organs (Fig. 5-2).

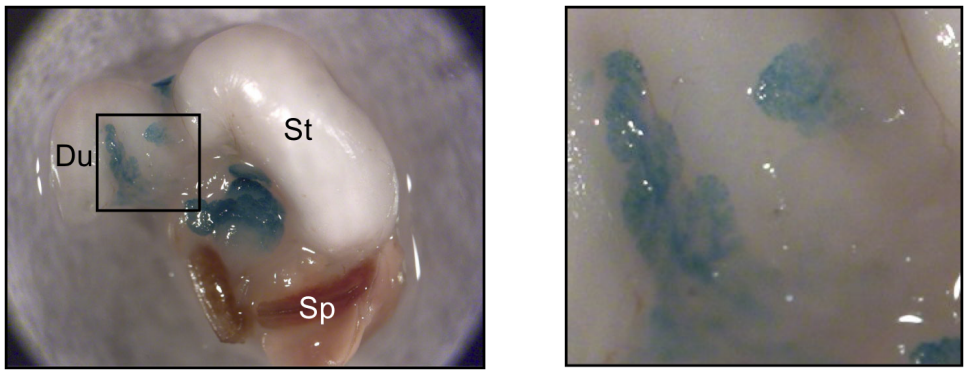

Fig. 5-2: X-gal staining of pancreatic tissue in newborn wt mice

X-gal staining of the dissected midgut region showed uniform expression of β-galactosidase in the entire pancreas (blue), slightly covering the duodenum (Du). Expression was limited to pancreatic tissue and did not extend to surrounding tissue like stomach (St) and spleen (Sp). Magnification (right) showed pancreatic tissue with its lobular structure in the duodenal C and scattered pancreatic tissue in the pyloric area. Extrapancreatic tissue did not stain blue.

5.2 Murine *Notch1* and *Ptf1a* are Located on Chromosome 2

After confirmation of efficient and pancreas specific Cre recombinase activity, generation of *N1KO* mice was attempted by breeding *Ptf1a*$^{+/+}$/ *Notch1*$^{f/f}$ mice to *Ptf1a*$^{+/Cre(ex1)}$/*Notch1*$^{+/f}$ mice. However, this breeding scheme did not follow a Mendelian ratio, as breeding *Ptf1a*$^{+/+}$/ *Notch1*$^{f/f}$ mice to *Ptf1a*$^{+/Cre(ex1)}$/*Notch1*$^{+/f}$ mice led to the birth of approximately 50 % *Ptf1a*$^{+/+}$/*Notch1*$^{f/f}$ mice and 50 % *Ptf1a*$^{+/Cre(ex1)}$/*Notch1*$^{+/f}$, but never to *Ptf1a*$^{+/Cre(ex1)}$/*Notch1*$^{f/f}$ (*N1KO*) mice (Fig. 5-3). This was in contradiction with the expected Mendelian ratio of 25% *Ptf1a*$^{+/+}$/*Notch1*$^{f/f}$, 25 % *Ptf1a*$^{+/+}$/*Notch1*$^{+/f}$, 25 % *Ptf1a*$^{+/Cre(ex1)}$/*Notch1*$^{+/f}$ and 25 % *N1KO* offspring. *Notch1*$^{f/f}$ alleles together with *Ptf1a*$^{+/Cre(ex1)}$ alleles in one mouse appeared to be mutually exclusive events.

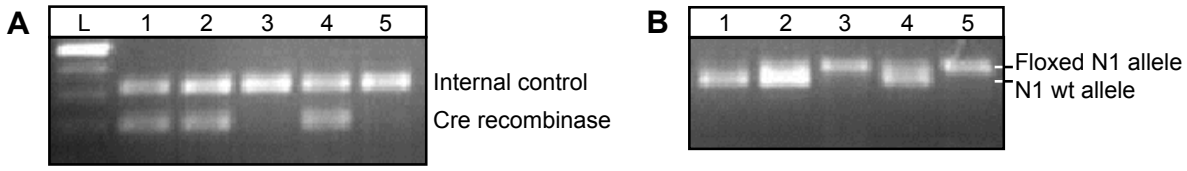

Fig. 5-3: PCR analysis of genomic DNA from mouse-tails from newborn mice

Notch1$^{f/f}$and *Ptf1a*$^{+/Cre(ex1)}$ appeared to be mutually exclusive events.
PCR analysis of offspring from a *Ptf1a* $^{+/Cre(ex1)}$; *Notch1*$^{+/f}$ female bred with a *Ptf1a* $^{+/+}$; *Notch1*$^{f/f}$ male.
A) Analysis of the *Ptf1a* alleles: Upper bands represent the internal positive control, lower bands denote presence of the Cre recombinase.
B) Analysis of the *Notch1* alleles: Upper bands with a size of 334 bp represent targeted *Notch1* allele with the loxP sites, lower bands with a size of 298 bp represent the wildtype *Notch1* allele. Mice with a single upper band are homozygous for the floxed *Notch1* alleles (lanes 3 and 5), mice with a single lower band are homozygous for the wildtype alleles, and mice with one upper and one lower band are heterozygous for the *Notch1* allele (lanes 1,2,4), bp = base pairs.
Offspring were either *Ptf1a* $^{+/Cre(ex1)}$; *Notch1*$^{+/f}$ (lane 1, 2, 4), or *Ptf1a* $^{+/+}$; *Notch1*$^{f/f}$ (lane 3, 5), but never *Ptf1a* $^{+/Cre(ex1)}$; *Notch1*$^{f/f}$ (*N1 KO*). This result with a ratio of 1:1 for the two indicated genotypes is representative for multiple breedings and contradicts the expected Mendelian ratio of 25% *N1KO* offspring.
Lane L: DNA ladder

This finding can be explained by the fact that both genes are located on chromosome 2 in relatively close proximity to each other (Fig. 5-4 A). Furthermore, the *Ptf1a*/Cre construct was originally inserted into a chromosome carrying a wildtype *Notch1* allele. Hence, mice carrying the *Ptf1a*/Cre construct will forcedly carry a wildtype *Notch1* allele, precluding the possibility of homozygously floxed *Notch1* alleles. Conversely, mice homozygous for the floxed *Notch1* allele cannot carry the *Ptf1a*/Cre construct. Consequently, in this setting, *Notch1*$^{f/f}$ alleles together with *Ptf1a*$^{+/Cre(ex1)}$ alleles are indeed mutually exclusive events (Fig. 5-4 B).

Only the event of homologous recombination through crossing over between the *Notch1* locus and the *Ptf1a* locus in *Ptf1a*$^{+/Cre(ex1)}$/*Notch1*$^{+/f}$ mice could therefore lead to the desired genotype of having both the *Ptf1a*-Cre construct and the floxed *Notch1* allele together on one chromosome. This crucial event is a prerequisite, as only the resulting genotype can lead to the successful generation of *N1KO* mice (Fig. 5-4 C).

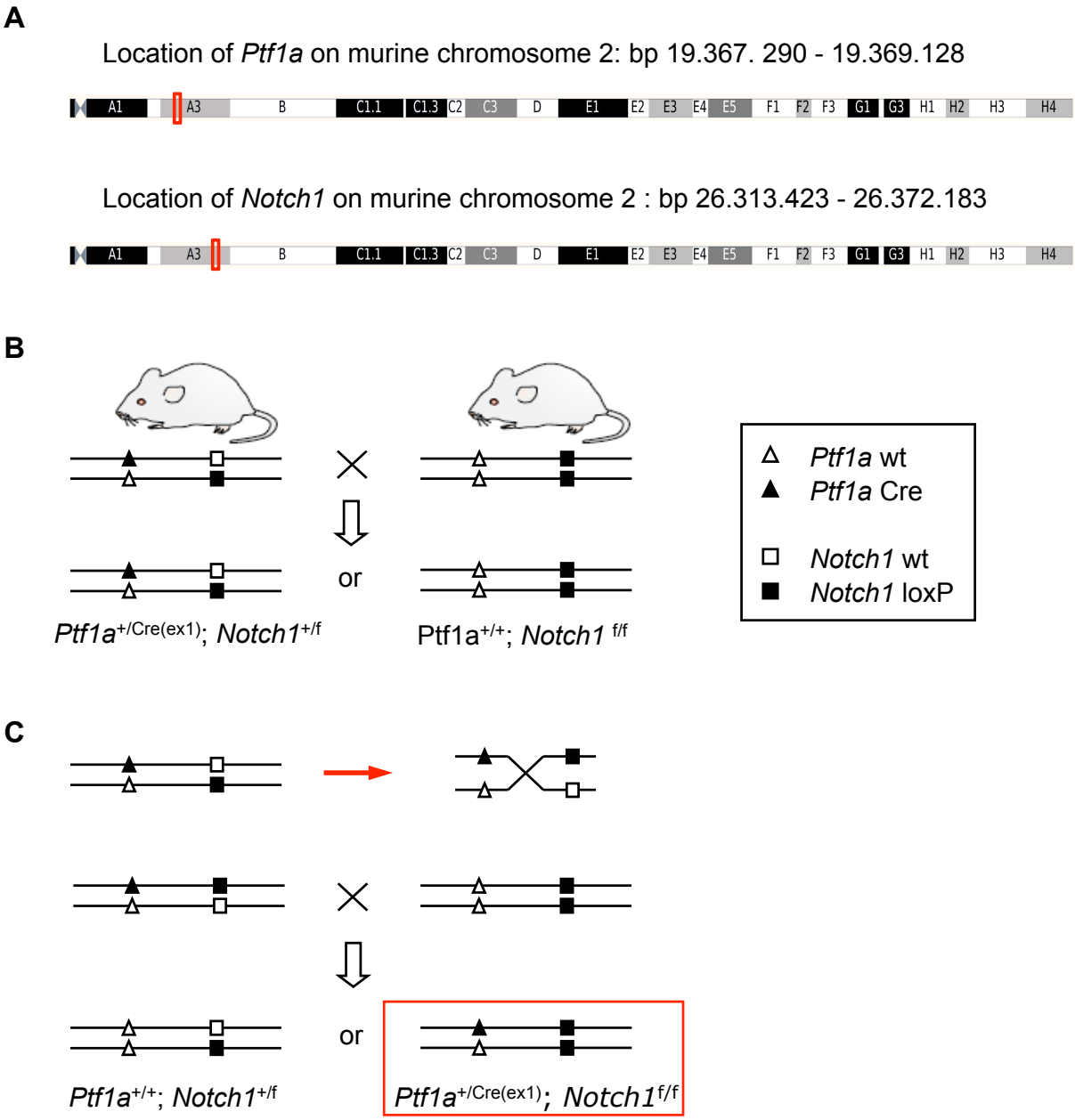

Fig. 5-4: Location of *Ptf1a* and *Notch1* on the murine chromosome 2, breeding scheme and homologous recombination

A) In mice, the genes encoding *Ptf1a* and *Notch1* are located in close vicinity to each other on chromosome 2. *Ptf1a* is located in band A3 from bp 19.367.290 to 19.369.128 (red box), *Notch1* is located in band A3 from bp 26.313.423 to 26.372.183 (red box). bp = basepairs (From Ensembl release 57 [www.ensembl.org])
B) Schematic representation of the breeding event and the possible genotypes from the offspring as shown in Fig. 5-3. With the indicated genotypes, only $p48^{+/Cre(ex1)}$; $Notch1^{+/f}$, or $p48^{+/+}$; $Notch1^{f/f}$ offspring with an expected ratio of 1:1 are possible (compare to Fig. 5-3). $p48^{+/Cre(ex1)}$; $Notch1^{f/f}$ (*N1KO*) cannot be obtained.
C) Only the event of homologous recombination through crossing over renders $p48^{+/Cre(ex1)}$ and $Notch1^{f/f}$ to be placed on the same chromosome (red arrow). This is the prerequisite for obtaining *N1KO* mice (red box) (filled triangle: *Ptf1a*/Cre allele, filled rectangle: floxed *Notch1* allele; empty objects: wildtype alleles)

5.3 Confirmation of Functional *Notch1*-Knockout

5.3.1 Genotyping

The genotype was determined by PCR analysis of genomic DNA isolated from a small part of the mouse-tail for adult mice and the amniotic sac for embryos, respectively.

Wildtype *Notch1* alleles showed an amplification product with a size of 298 bp, whereas floxed *Notch1* alleles showed a band with a higher size of 332 bp due to the inserted loxP site. The *Ptf1a/Cre* knock-in could be identified through an amplification product with a size of 1032 bp.

Embryos/mice showing a single band at 332 bp in the *Notch1* PCR and a band at 1032 bp in the *Ptf1a/Cre* PCR were considered *N1KO* (Fig. 5-5). Wt and *N1KO* embryos and adult mice were born at the expected Mendelian ratio of 50 % wt and 50 % *N1KO*. To confirm functional ablation of the Notch1 receptor in pancreatic tissue, *Notch1* expression tests were performed.

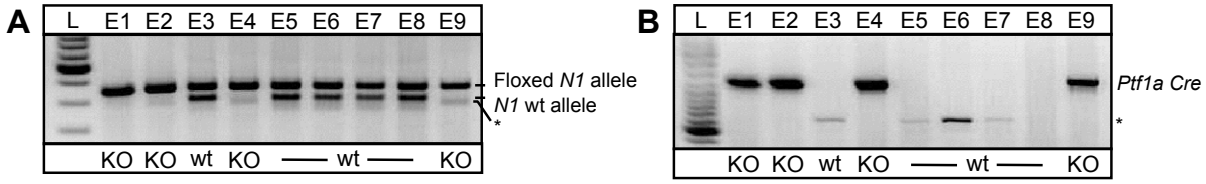

Fig. 5-5: PCR analysis of genomic DNA from amniotic sacs from E14.5 embryos

A) Analysis of the *Notch1* alleles: Upper bands represent the floxed *Notch1* allele; lower bands represent the wildtype *Notch1* allele.
B) Analysis of the targeted *Ptf1a* allele with the inserted Cre recombinase. Size of the product: 1032 bp.
Ptf1a$^{+/Cre(ex1)}$, *Notch1*$^{f/f}$ (*N1KO*): Embryos E1-E2, E4, E9
Ptf1a$^{+/+}$, *Notch1*$^{+/f}$ (wt): Embryos E3, E5-E8
Unspecific bands are marked with an asterisk; Lane L: DNA ladder

5.3.2 Confirmation of Cre Recombinase Activity in *N1KO* Mice

As described for wt mice before, X-gal staining was performed on *N1KO* mice. In 6 week-old knockout mice, β-galactosidase was expressed in all acinar cells and the majority of the ductal and endocrine cells, confirming broad Cre recombinase mediated excision of floxed sites in the pancreas of *N1KO* mice (Fig. 5-6). The incomplete β-galactosidase expression in ductal and islet cells has been described before (Kawaguchi 2002).

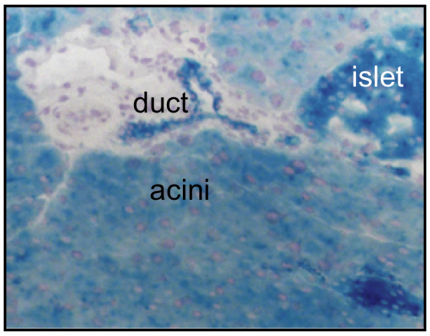

Fig. 5-6: X-gal staining of pancreatic tissue from *N1KO* mice:

Staining of the pancreas of a 6 week-old *N1KO* mouse revealed uniform expression of β-galactosidase in the entire acinar compartment and the majority of the ductal cells and islets of Langerhans

5.3.3 Real-Time qRT-PCR and Western Blot

To investigate the efficiency of the *Notch1* knockout construct on gene transcription, real-time qRT-PCR was performed on cDNA transcribed from pancreas whole cell lysates from *N1KO* and wt mice. *Cyclophilin* was used as the internal control gene to account for differences in amplification efficiency and starting amount of mRNA. Relative quantitation of *Notch1* expression levels using the $2^{-\Delta\Delta ct}$ method revealed a significant reduction of *Notch1* mRNA expression of 91 % in *N1KO* mice compared to wt mice (Fig. 5-7 A)

To assess whether the reduced mRNA expression of *Notch1* had an effect on the efficacy and amount of Notch1 protein expression, western blot analysis of pancreatic whole cell lysates was performed. Notch1 protein was below limit of detection in *N1KO* mice as compared to wt mice, indicating a marked decrease of Notch1 receptor expression (Fig. 5-7 B).

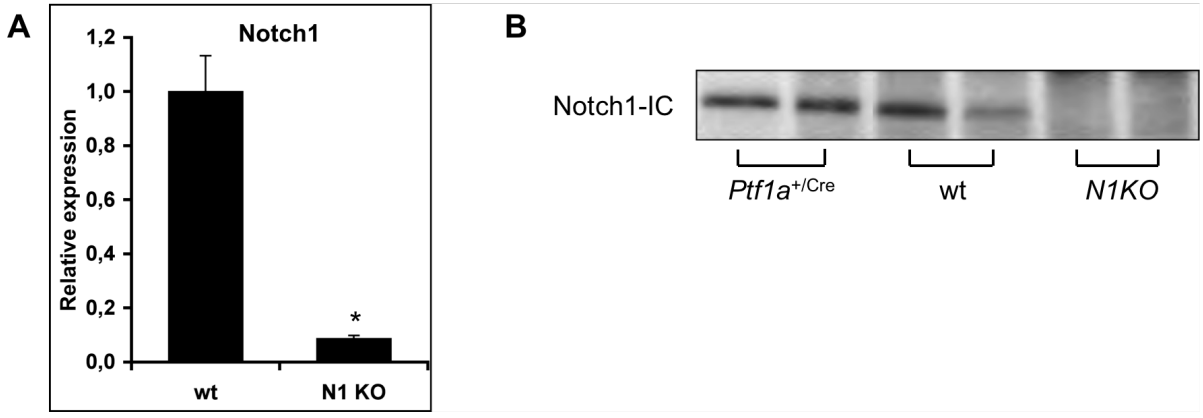

Fig. 5-7: Gene expression analysis of the Notch1 receptor

A) qRT-PCR: Comparison of Notch1 mRNA expression levels of *N1KO* mice to wt mice demonstrated a 91 % reduction of Notch1 receptor expression in knockout pancreata compared to wildtype pancreata. Relative expression levels were calculated using the $2^{-\Delta\Delta Ct}$ method. $p<0.001$. Results represent mean values from two independent experiments with n= 3 for wt, and n= 4 for *N1KO* in both experiments. Results are normalized to cyclophilin with wt = 1. Error bars indicate SEM.
B) Western blot analysis of pancreatic whole cell lysates showed that Notch1-IC protein is below limit of detection in *N1KO* mice. Blotting membrane was stained with ponceau-red and revealed equal loading amounts of protein (not shown).

5.3.4 Conclusion

The combined evidence from the above methods strongly argues in favor of the complete absence, or at least significant decrease, of Notch1 receptor expression in all, or at least the vast majority of, pancreatic cells in *Ptf1a*$^{+/Cre(ex1)}$;*Notch1*$^{f/f}$ mice. Thus it appears justified to consider these mice pancreas specific conditional *Notch1*-knockout mice (*N1KO*).

5.4 Phenotype of Notch1-Knockout Mice

5.4.1 Embryogenesis

To investigate the effect of *Notch1* deficiency in embryonic pancreatogenesis, embryos of different developmental stages were generated by timed breeding. Two time points were chosen for studying different aspects:

Age of embryos:

a) E14.5, representing a stage during second transition.
b) E16.5, representing a stage following the second transition.

Characteristics of interest:

a) Gross morphology
b) Histomorphology
c) Expression of markers specific for the exocrine, endocrine and ductal lineage,
d) Proliferation and apoptosis

5.4.1.1 Macroscopic Morphology

N1KO and wt embryos taken out of the amniotic sac did not display any obvious distinctive feature. They appeared viable, were of approximately the same size, had the same complexion and gross morphology. The difference in genotype was not reflected in altered macroscopic phenotype at either time point.

5.4.1.2 Histomorphology

H&E staining of sagittal tissue sections of whole mount embryos were prepared to compare the histomorphology of the developing pancreata. Developing acinar, as well as ductal structures were well defined and appeared normal in development. No striking histomorphological differences of the pancreas between *N1KO* and wt mice could be detected at either time point (Fig. 5-8).

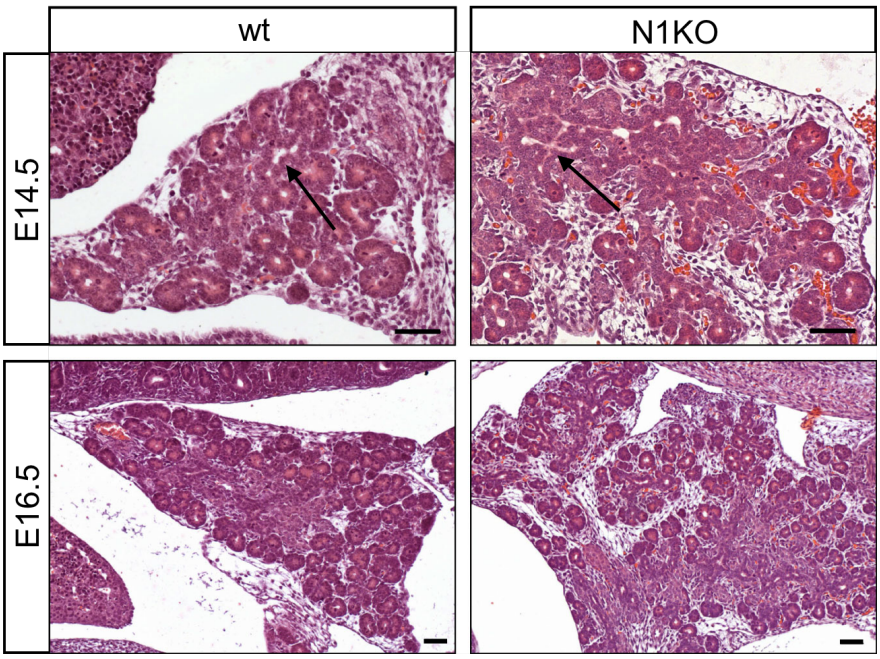

Fig. 5-8: Histomorphology of embryonic wt and *N1KO* pancreas

Histomorphology of E14.5 embryos showed beginning acinar formation around primary tubular complexes (arrows). E16.5 embryos showed continued acinar development in wt and *N1KO* mice. Scale bars: 50 µm

5.4.1.3 Expression of Exocrine and Endocrine Markers

To compare the development of exocrine, endocrine, and ductal structures, sagittal tissue sections of whole mount embryos were stained with antibodies against amylase and carboxypeptidase A (CPA), insulin, glucagon, somatostatin (SS), and pancreatic polypeptide (PP), and Dolichos biflorus agglutinin (DBA), respectively.

In E14.5 embryos, staining for amylase and CPA showed beginning expression of exocrine markers in developing acinar formations, arranged around centrally located, tubular structures (Fig. 5-9 A).

Immunostaining for endocrine markers revealed cell clusters with strong expression of insulin and glucagon, scattered randomly throughout the developing pancreas.

Expression of somatostatin was less pronounced and detectable only in single cells, whereas pancreatic polypeptide was not detectable at this stage (Fig. 5-9 B).

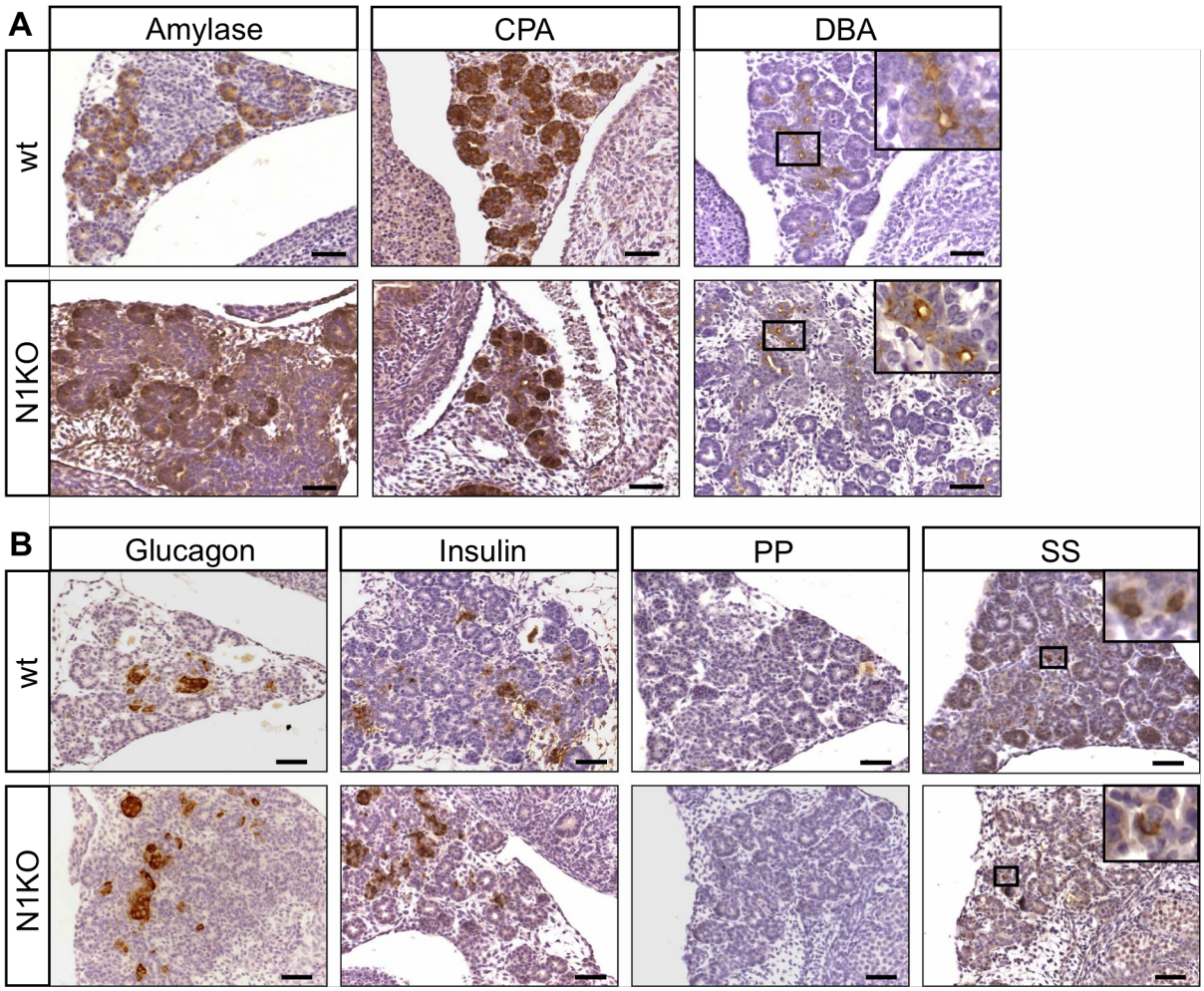

Fig. 5-9: Expression of exocrine and endocrine markers in E14.5 embryos

A) Staining for exocrine markers amylase and CPA showed beginning differentiation of acini in both wt and *N1KO* mice. Staining for the ductal marker DBA showed developing ductal structures. No apparent difference was detectable.
B) Staining for endocrine markers showed beginning expression of hormones in both groups PP was not detectable, SS was detectable in single cells (insert).
Scale bars: 50 µm

In E16.5 embryos, staining for amylase and CPA also showed well defined and evenly distributed development of acinar structures arranged around centrally located ducts as seen in DBA staining (Fig. 5-10 A).

Immunostaining for endocrine markers revealed strong expression of insulin and glucagon. At E16.5, PP was also detectable. Furthermore, the typical distribution pattern and quantity of the four endocrine cell types was sporadically visible,

indicating the beginning aggregation of the endocrine compartment into islets of Langerhans. β-cells showed the strongest staining, consistent with its predominant appearance in the endocrine compartment. (Fig. 5-10 B).

Comparison of sections from different embryos showed great interindividual variations in intensity of endocrine staining, and comparison of two sections from the same embryo showed great intraindividual differences. Hence, definite answers as to possible alterations in endocrine development are difficult to make.

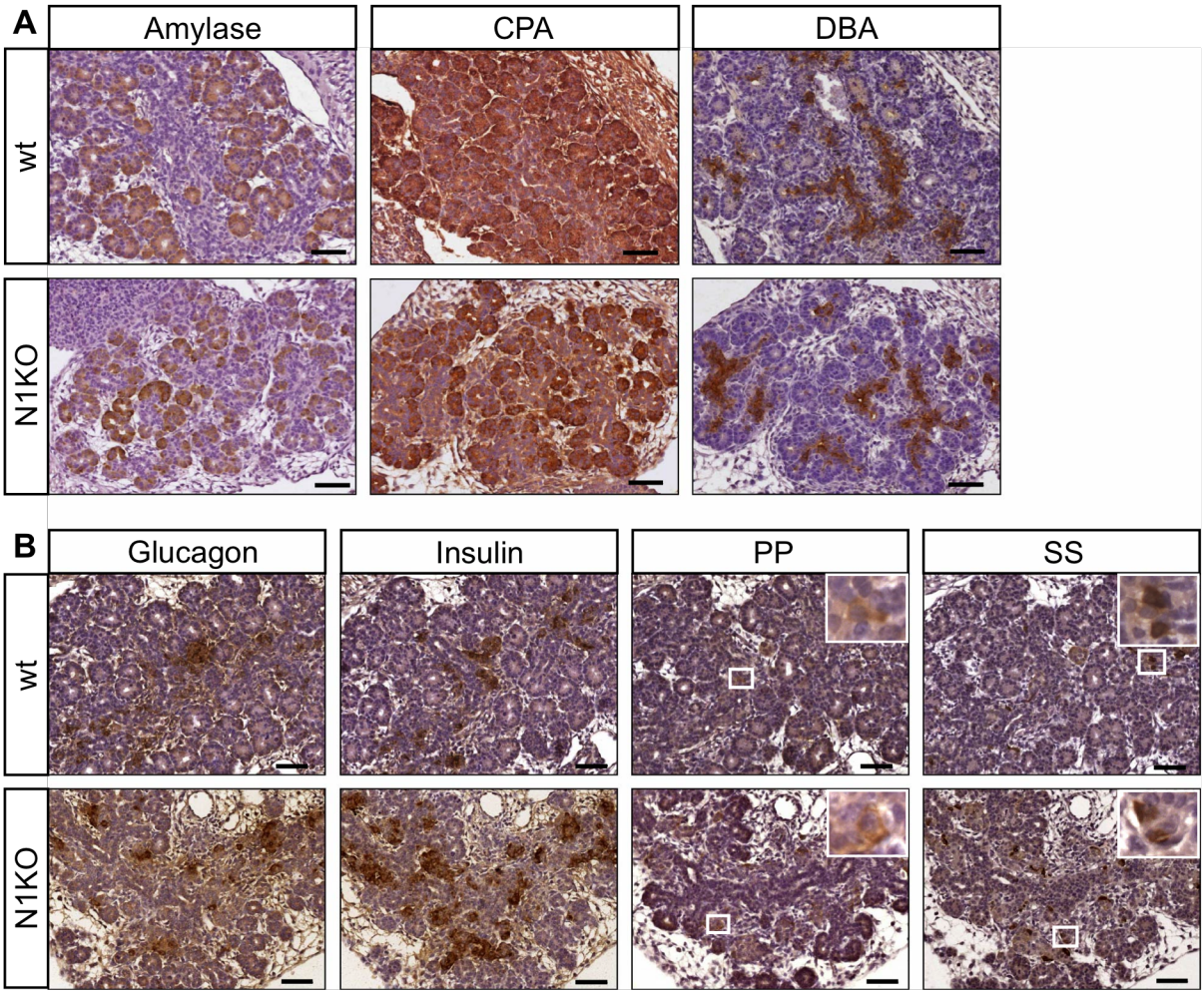

Fig. 5-10: Expression of exocrine and endocrine markers in E16.5 embryos

A) Staining for exocrine markers showed continued development of acini with uniform expression of amylase and CPA in both groups. Staining for DBA showed branching ductal structures.
B) Staining for endocrine markers revealed continued development of the endocrine compartment. At this developmental stage, PP was also detectable (insert).
Scale bars: 50 µm

5.4.1.4 Proliferation and Apoptosis

To assess the proliferative activity in the developing pancreas, BrdU tracing experiments were performed and BrdU stained nuclei were counted. The number of positively stained nuclei was related to the area of the pancreas.

Embryos of both ages showed a very high proliferative activity evenly distributed throughout the entire pancreas in wt as well as *N1KO* embryos (Fig. 5-11 A). Proliferation was slightly lower in E16.5 embryos compared to E14.5 embryos. There was no significant difference in quantity and distribution between wt and *N1KO* mice at either time point (Fig. 5-11 B, C).

Apoptosis was not detectable in both groups in any of the slides as judged by staining for cleaved caspase 3 at either time point (data not shown).

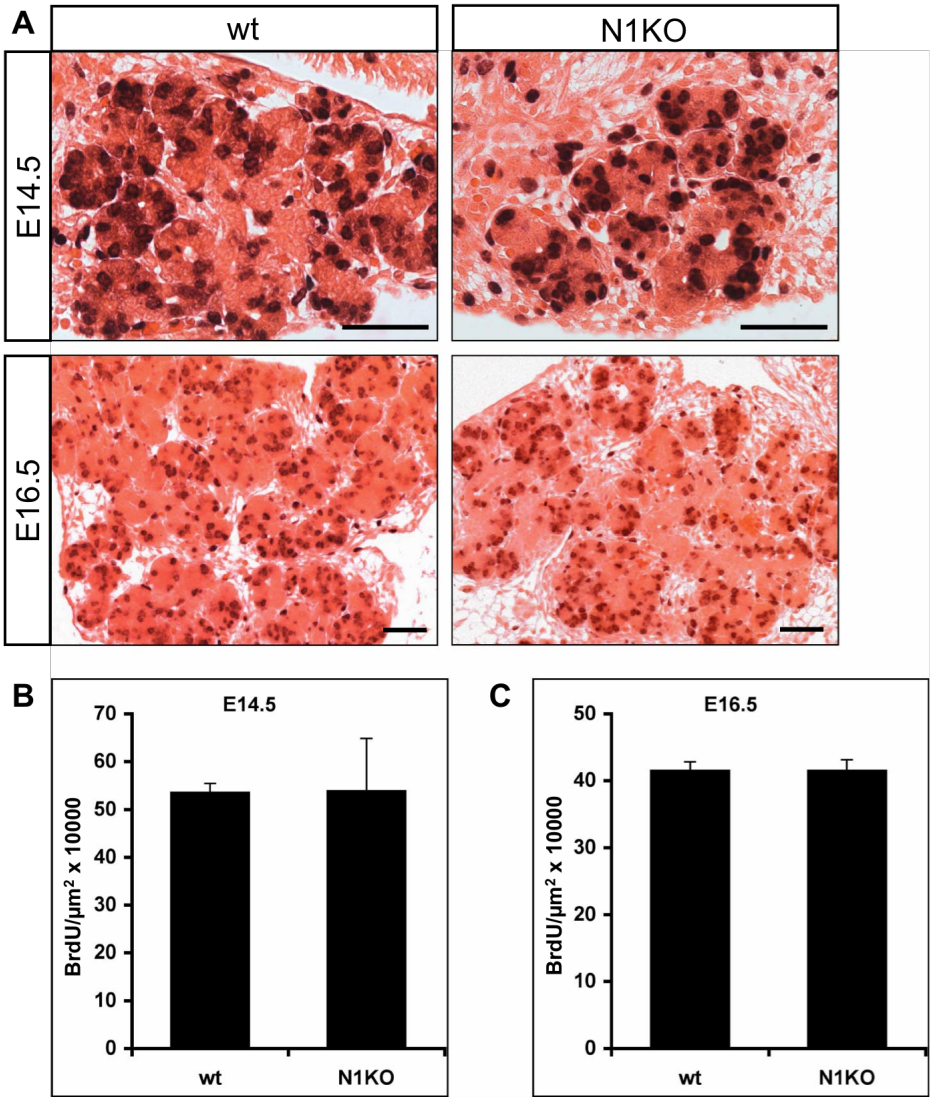

Fig. 5-11: Evaluation of proliferation in E14.5 and E16.5 embryos

A) Representative slides from E14.5 and E16.5 embryos stained for BrdU. Cytoplasm was counterstained with eosin. Scale bars: 50 µm
B, C) Counting of proliferating cells revealed no difference in proliferation between *N1KO* and wt mice at either time point. Proliferation was slightly higher in E14.5 embryos.
n=2 for E14.5 embryos and n=4 for E16.5 embryos. Error bars indicate SEM

5.4.1.5 Conclusion

Taken together, it can be inferred from the above data that the capacity of the embryonic pancreas to proliferate and differentiate into acinar, endocrine and ductal structures is not affected, at least not severely, by a deficiency in the Notch1 receptor, and that a defective Notch1 receptor does not have an impact on apoptotic activity.

5.4.2 Juvenile and Adult Mice

Two time points were chosen to study the effect of ablation of Notch1 signaling on the pancreatic development post partum.

Age of mice:

a) 5.5 weeks, representing a developmental stage just prior to onset of sexual maturation.
b) 9.5 weeks, representing a sexually matured adult mouse.

Characteristics of interest:

a) Gross morphology
b) Histomorphology
c) Body weight, pancreatic weight and pancreatic weight index
d) Expression of markers specific for the exocrine, endocrine and ductal lineages
e) Proliferation and apoptosis
f) Gene expression of Notch pathway and cell lineage markers

5.4.2.1 Macroscopic Appearance

Inspection of littermates did not reveal any clues with respect to the genotype. Mice of both groups appeared equal in development, nourishment, size, appearance of the fur, gross morphology and behavior.

Likewise, the pancreas did not look altered upon inspection. It had a light grey appearance, was of a soft, squishy texture with an amorphous structure and situated in the proper place. The size did not appear visibly altered. Other organs in the peritoneal cavity and retroperitoneum did not show any alteration either.

5.4.2.2 Histomorphology

For histomorphological analysis, H&E staining of paraffin embedded pancreatic tissue was performed. Staining revealed evenly distributed, normal looking acinar structures with islets of Langerhans scattered randomly between the acini. Eosin staining of the cytoplasm appeared equal in strength, suggesting comparable amounts of zymogen granules in wt and *N1KO* mice. Furthermore there was no observable difference between 5.5 week-old mice and 9.5 week-old mice. Thus, no visible histomorphological difference could be detected (Fig. 5-12).

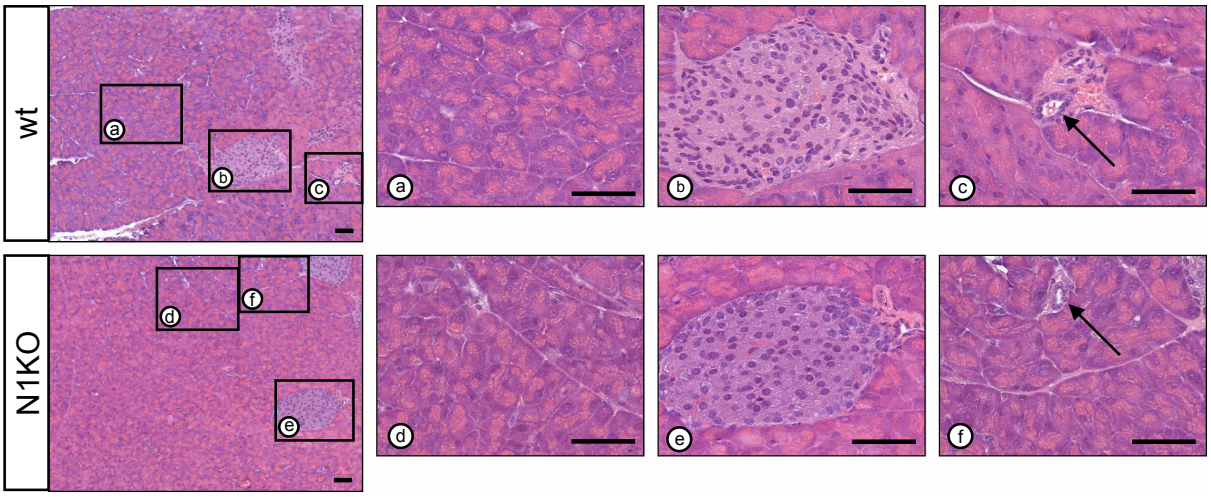

Fig. 5-12: Histomorphology of adult wildtype and *N1KO* pancreas

In wt and *N1KO* mice, acini (a, d), islets (b, e) and ducts (c, f, arrows) developed normally. These results are representative for juvenile and adult mice. Scale bars: 50 µm

5.4.2.3 Body Weight, Pancreatic Weight and Pancreatic Weight Index

Analysis of 5.5 week-old and 9.5 week-old mice showed no difference in body weight between the wt and *N1KO* group. 9.5 week-old wt mice showed a slight, not significant increase in body weight compared to 5.5 week-old mice, suggesting an appropriate nourishment and progressive development of the mice in this group. The body weight did not change in the *N1KO* group (Fig. 5-13 A, D).

Comparison of the pancreatic weight of 5.5 week-old mice revealed a lower pancreatic weight in *N1KO* mice. This finding was not statistically significant (Fig. 5-13 B). However, comparison of the pancreatic weight normalized to the body weight (pancreatic weight index) revealed a statistically significant reduction in *N1KO* mice (Fig. 5-13 C). This reduction was not detectable at age 9.5 weeks anymore.

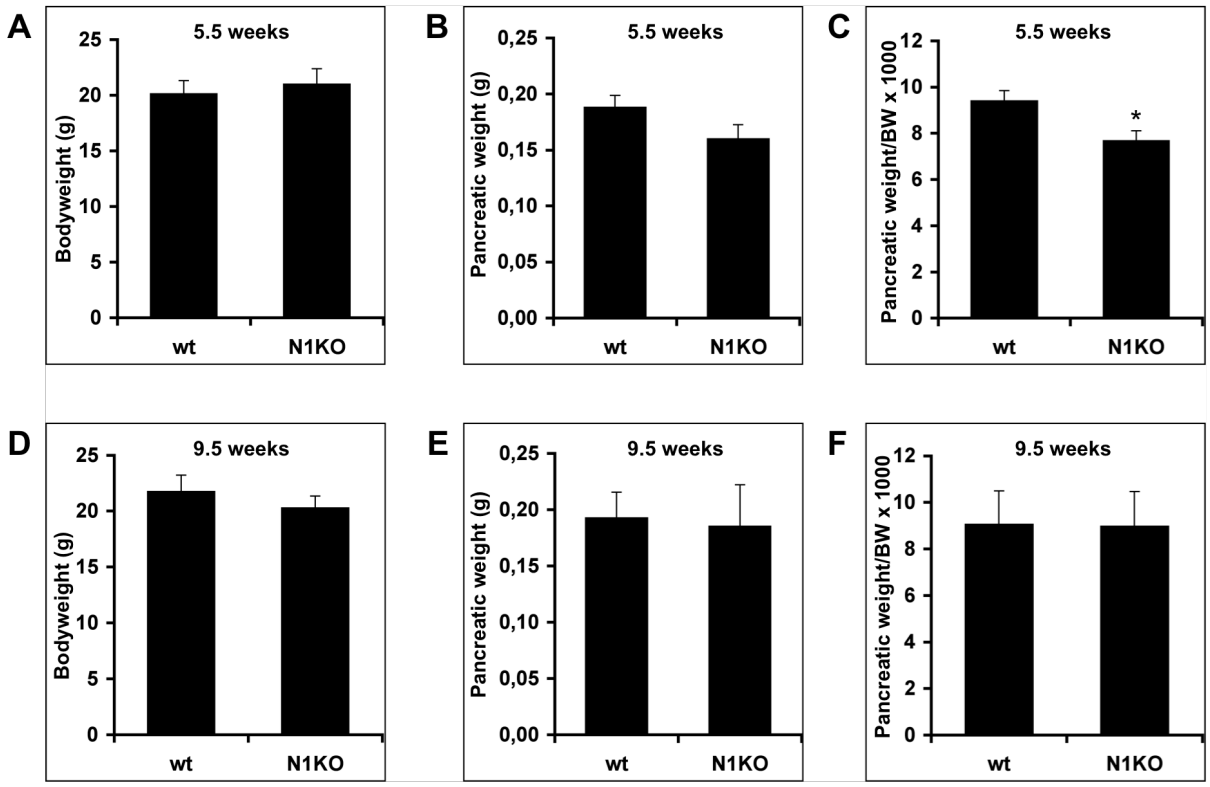

Fig. 5-13: Body weight, pancreatic weight and pancreatic weight index

A, D) Body weight of 5.5 week-old and 9.5 week-old wt and *N1KO* mice showed no difference in body weight. The body weight of wt mice had increased slightly compared to the 5.5 week group, whereas the body weight of *N1KO* mice did not change
B) The pancreatic weight of 5.5 week-old *N1KO* mice was reduced compared to wt mice.
C) In the *N1KO* group, the pancreatic weight index was reduced statistically significant compared to wt mice (p=0.0246) (Compare to panel B).
E) In contrast to 5.5 week-old mice, there was no difference in pancreatic weight in 9.5 week-old mice. The pancreatic weight had slightly increased in both groups. However, the increase was stronger in the *N1KO* group.
F) The pancreatic weight index in 9.5 week-old mice had balanced.
n=6 for 5.5 week-old mice and n= 4 for 9.5 week-old mice. Error bars indicate SEM.

5.4.2.4 Expression of Exocrine and Endocrine Markers

To evaluate the expression of exocrine and endocrine markers, sections from paraffin embedded pancreatic tissue were stained with the same antibodies used for embryonic analyses. Additionally, an antibodiy against CK19 was used to stain the ductal structures, and an antibody against HES1 was used for detecting centroacinar cells with active Notch signaling.

Immunostaining for amylase and CPA showed uniform expression of exocrine markers arranged in acini throughout the whole pancreas. Ductal structures, stained by DBA and CK19, revealed a branched system of ducts dispersed in the entire

pancreas. Centroacinar cells were visible in the expected areas of the pancreas as seen by nuclear staining of HES1 (Fig. 5-14 A).

Islets of Langerhans stained positive for all endocrine markers in the expected pattern: Insulin expressing β-cells formed a core and made up the majority of the islet. Glucagon expressing α-cells, somatostatin expressing δ-cells, and pancreatic polypeptide expressing PP-cells were located around the core, with cell number decreasing from α-cells to PP-cells (Fig. 5-14 B).

In summary, no alteration in expression of exocrine and endocrine markers could be detected, nor was there a difference in quantity or distribution of ductal and centroacinar structures between wt and *N1KO* mice.

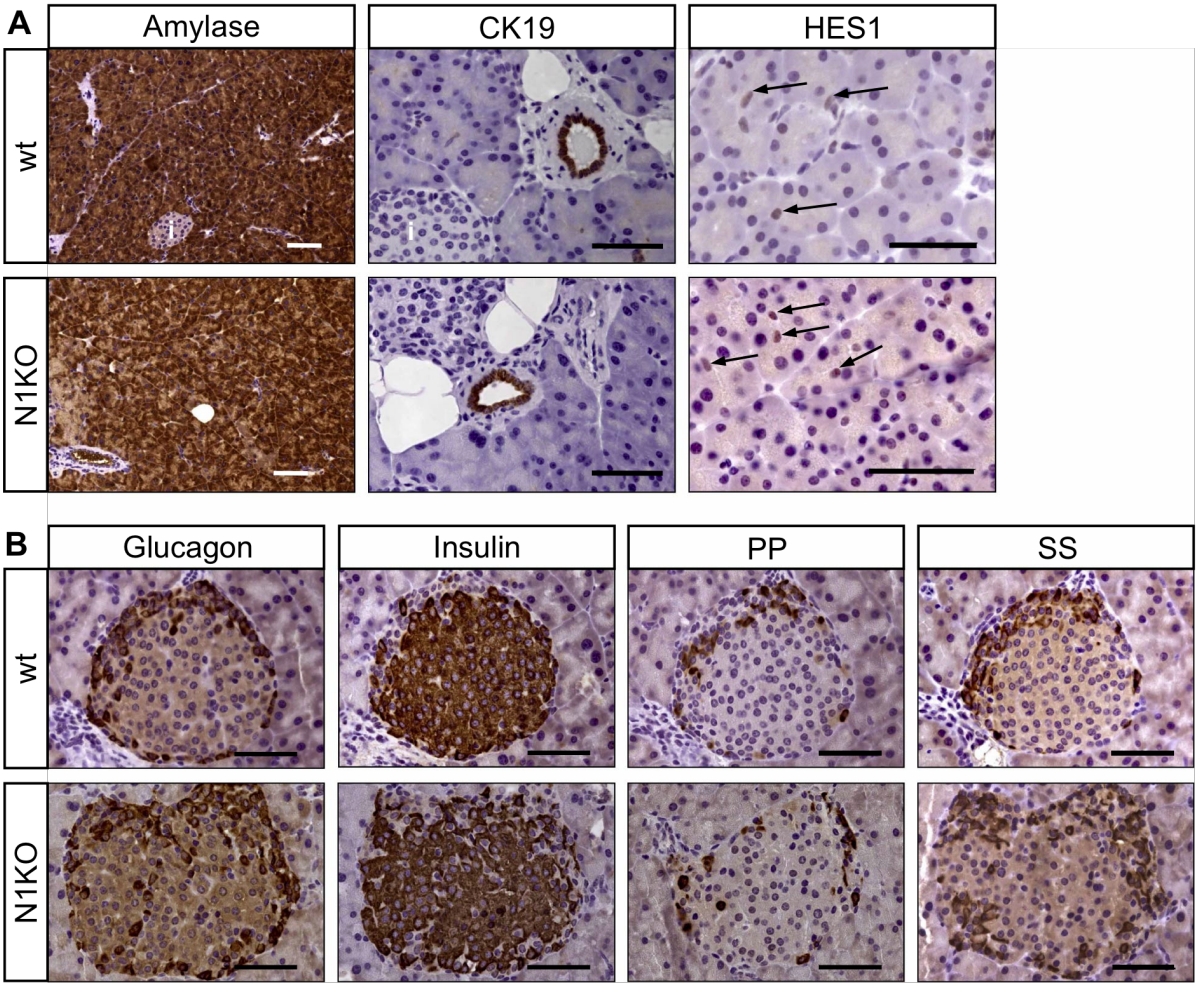

Fig. 5-14: Expression of exocrine and endocrine markers in adult mice

A) Staining for amylase and CK19 revealed equal amount of acini and no apparent difference in ductal structures. Staining for Hes1 shows centroacinar cells (arrows). i: Islets
B) Serial sections stained for insulin, glucagon, pancreatic polypeptide and somatostatin revealed equal amount and typical distribution of endocrine markers in islets of Langerhans. Scale bars: 50 µm.

5.4.2.5 Immunohistological Staining for β-catenin

Since β-catenin is a marker for the maturation status of acinar cells, immunofluorescence staining of acini for this marker was performed to compare the differentiation and maturation status of wt and *N1KO* mice.

Staining for β-catenin revealed higher expression and elevated cytoplasmic location in *N1KO* mice. Double immunofluorescence analysis of amylase with β-catenin revealed a moderate increase of cytoplasmic location of β-catenin in some acinar cells (Fig. 5-15).

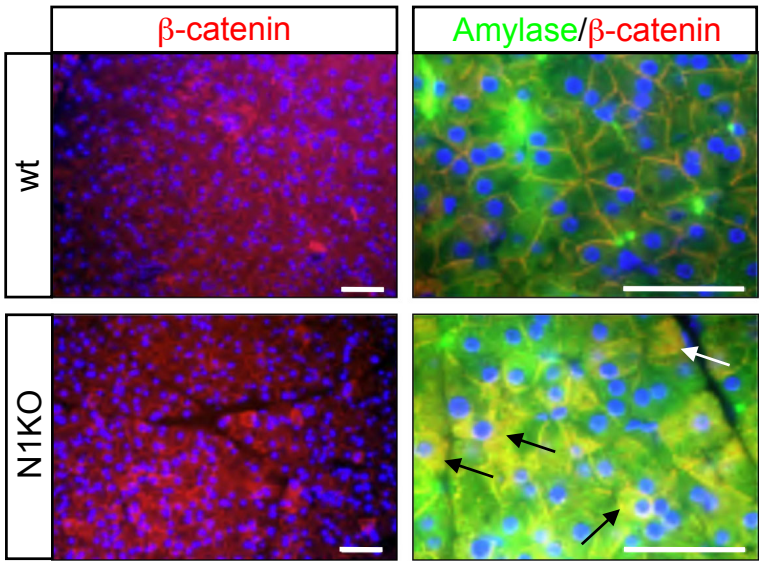

Fig. 5-15: Expression of β-catenin in wt and *N1KO* mice

Immunofluorescence staining for β-catenin showed elevated expression and enhanced cytoplasmic localization in *N1KO* mice (left panels). Double immunofluorescence staining for amylase (green) and β-catenin (red) at a higher magnification (right panels). Yellow areas indicate colocalization. β-catenin expression was higher in *N1KO* mice and showed colocalization with amylase (arrows). Nuclei were counterstained with DAPI (blue).
Scale bars: 50 µm

5.4.2.6 Proliferation and Apoptosis

Proliferative activity was evaluated by immunohistological staining with antibodies against BrdU (Fig. 5-16 A). Counting of 23,742 nuclei revealed a proliferation rate of 2.1 % in wt mice and 1.9 % in *N1KO* mice. There was no significant difference between both groups (Fig. 5-16 C).

Apoptosis rate was evaluated by immunohistological staining with antibodies against cleaved caspase 3 (Fig. 5-16 B). Apoptotic rate was barely detectable, only solitary apoptotic cells were visible in stained slides. Counting of 8 to 24 different visual fields

per slide from 4 wt and 3 *N1KO* mice revealed no significant difference between wt and knockout mice at either time point (Fig. 5-16 D).

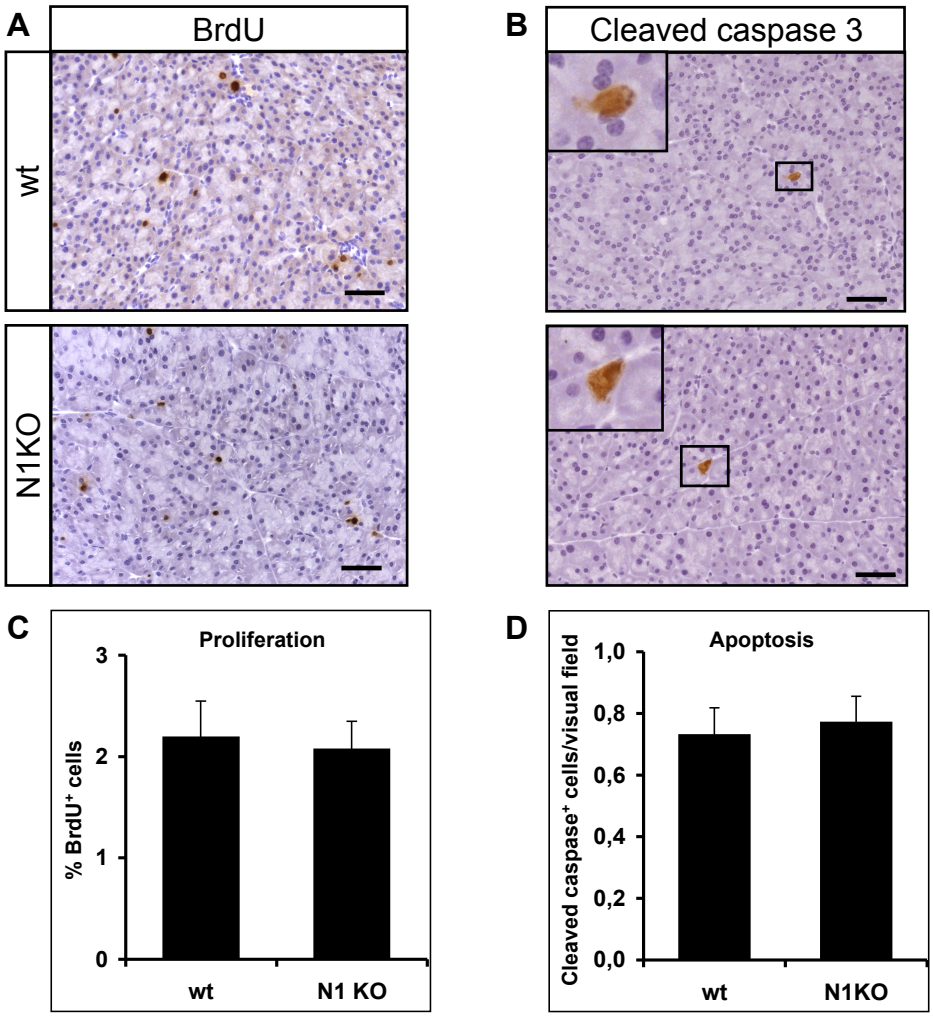

Fig. 5-16: Evaluation of proliferation and apoptosis

A) Staining for BrdU revealed proliferating cells scattered randomly throughout the pancreas. Results are representative for juvenile and adult mice. Scale bars: 50 µm.
B) Staining for cleaved caspase 3 revealed only singular apoptotic cells. Results are representative for juvenile and adult mice. Scale bars: 50 µm
C) Counting of BrdU stained nuclei revealed no difference in proliferation between wt and *N1KO* mice. Bars indicate the percentage of BrdU positive nuclei of a total of 23,742 nuclei counted. n=6 for wt and for *N1KO* mice. Error bars are expressed in SEM.
D) Counting of apoptotic cells revealed no difference in apoptosis between wt and *N1KO* mice. n=4 for wildtype mice, n=3 for knockout mice. A minimum of 8 visual fields per mouse were counted. Error bars indicate SEM.

5.4.2.7 Gene Expression Analysis

To examine the gene expression of various Notch pathway elements and lineage markers, real-time qRT-PCR was performed on RNA extracted from samples of pancreatic tissue.

a) Notch pathway elements

Analysis of expression levels of the other epithelially expressed Notch receptor Notch2 and of the ligand Dll1 revealed no significant alteration. Also, the Notch target gene *Hes1* showed no striking variation, whereas *Hey1* was upregulated, albeit at very low levels. In summary, none of the findings were statistically significant (Fig. 5-17 A-D).

b) Lineage markers

Analysis of the exocrine marker amylase, the endocrine marker insulin and the ductal marker CK19 showed a reduced expression in *N1KO* mice, pointing towards a reduced function in all three compartments. For amylase, this finding was statistically significant. For insulin, however, expression levels showed great variations between mice. Furthermore, expression of Pdx1 was not altered, arguing against striking alterations in the endocrine cell mass (Fig. 5-17 E-G).

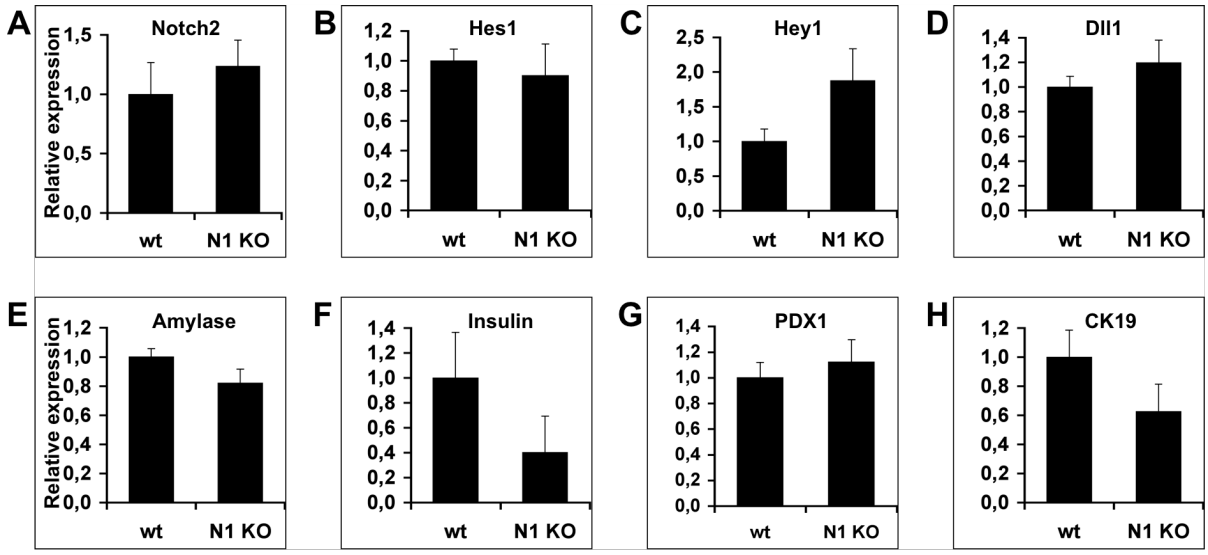

Fig. 5-17: Gene expression analysis of Notch pathway elements and lineage markers

A-D) Expression of Notch2 was slightly elevated in *N1KO* mice. Notch target gene *Hes1* was slightly reduced whereas *Hey1* was elevated. Notch ligand Dll1 was also slightly elevated. None of the findings were statistically significant.
E-F) Expression levels of exocrine and endocrine markers were decreased in *N1KO* mice,
G) PDX1 expression was not altered.
H) CK19 expression was reduced in *N1KO* mice.
n=5 for wt and *N1KO* mice for Notch2; n=4 for wt and *N1KO* mice for the other genes. Bars represent fold expression normalized to cyclophilin with wt = 1. Error bars indicate SEM.

5.5 Cerulein Induced Acute Pancreatitis

To investigate the expression and role of Notch1 signaling in pancreatic diseases involving regenerative and redifferentiation processes, acute pancreatitis was induced by repeated application of the CCK analogue cerulein at supramaximal doses into the peritoneal cave of mice as described in methods.

5.5.1 Expression Analysis of Notch1 During Acute Pancreatitis

5.5.1.1 Immunofluorescence

To assess the expression of Notch1 during the course of acute pancreatitis, expression analysis was performed using transgenic *Notch1-GFP* mice (Lewis 1998). Immunofluorescence analysis on day 1 after induction of pancreatitis showed only weak staining, whereas on day 3 GFP expression was clearly detectable in acinar cells, suggesting gradually increasing Notch1 expression in the course of cerulein induced acute pancreatitis (Fig. 5-18). Expression of Notch1 was not detectable in ductal cells. Evaluation of Notch expression with *Notch1-GFP* transgenic mice was done in cooperation with Dr. Clara Lubeseder-Martellato.

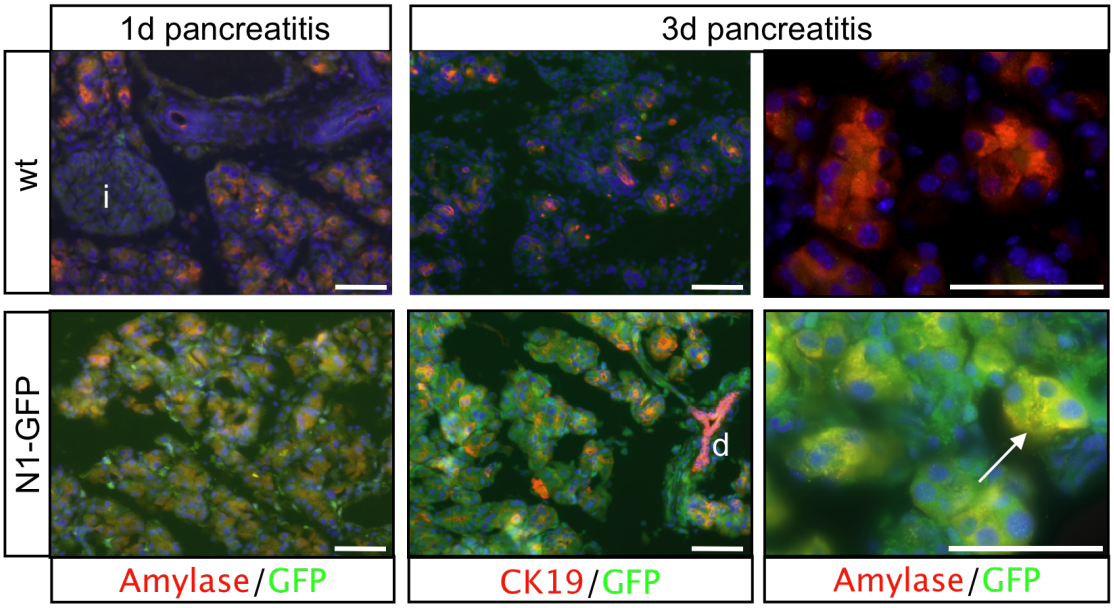

Fig. 5-18: Immunohistochemical analysis of Notch1 expression in acute pancreatitis

Notch1-GFP mice revealed low expression of Notch1 one day after induction of pancreatitis and elevated expression of Notch1 three days after induction. Arrow indicates coexpression of Notch1 and amylase in acinar cells (yellow). d: duct, i: islet. Scale bars: 50 µm

5.5.1.2 Gene Expression Analysis

TaqMan analysis of Notch pathway members supported the immunohistochemical finding. Notably, *Notch1* showed a marked decrease in expression on day 1 in wt mice (Fig. 5-19 A). This contradictory finding can be explained when considering that during the course of acute tissue reaction, the normal acinar structures expressing *Notch1* are severely destroyed and strongly infiltrated by inflammatory cells. On day 3 and day 7 expression of *Notch1* was significantly upregulated compared to day 1 in wt mice. *Notch2* was strongly upregulated in wt and *N1KO* mice, and upregulation was significantly elevated in *N1KO* mice compared to wt mice on day 3 (Fig. 5-19 B). *Notch2* expression decreased significantly on day 7, but was still elevated compared to unstimulated pancreata. Expression analysis of the Notch target genes *Hes1* and *Hey1* demonstrated upregulation of both genes on day 3, denoting functional Notch signaling (Fig. 5-19 C, D). For *Hes1*, upregulation on day 3 was significant for wildtype and *N1KO* group. For *Hey1*, upregulation on day 3 was significant only for the *N1KO* group. Upregulation of both target genes was higher in the *N1KO* group, albeit not significant.

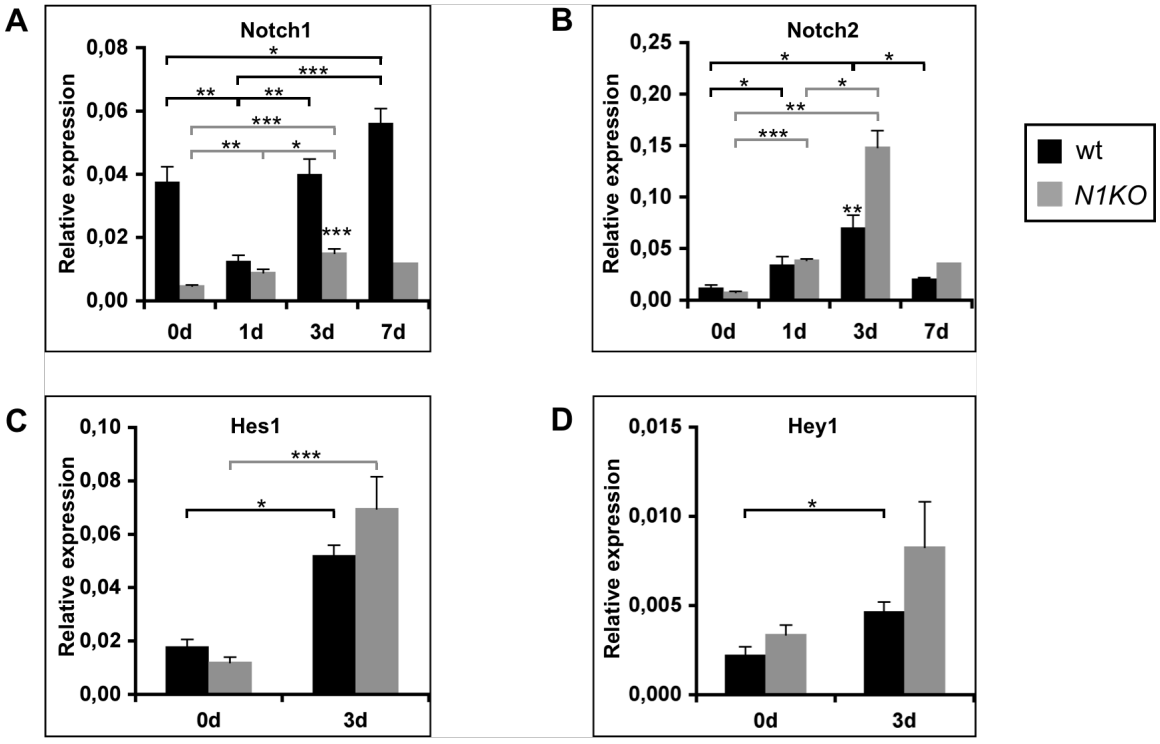

Fig. 5-19: Gene expression analysis of Notch pathway members

A) *Notch1* expression decreased on day 1 in wt mice. Since acinar structures expressing Notch1 are severely damaged during initial acute tissue reaction, this finding is not

surprising. The remaining expression level most likely reflects background expression (compare to *N1KO*) and possibly expression of *Notch1* in infiltrating inflammatory cells. Expression of *Notch1* increased significantly on day 3 and day 7 compared to day 1. On day 7, *Notch1* expression was significantly higher compared to day 0 in wt mice.
B) *Notch2* was upregulated on day 1 and day 3. Upregulation was significantly higher in *N1KO* mice compared to wt mice on day 3. On day seven, *Notch2* expression decreased significantly but remained above levels of unstimulated pancreata.
C, D) Upregulation of *Hes1* and *Hey1* on day 3 demonstrates active Notch signaling
Bars represent relative expression levels normalized to cyclophilin. Error bars indicate SEM. *: $p < 0.05$; **: $p < 0,01$; ***: $p < 0.005$

5.5.2 DBZ Treated Mice

To study whether the upregulation of Notch pathway elements had any functional effect, Notch signaling was more broadly abrogated through repeated intraperitoneal injection of the recently described γ-secretase inhibitor Dibenzazepine (DBZ), leading to inhibition of S3 cleavage and thus to disruption of NIC formation and silencing of Notch signaling (Milano 2004). Pancreata were analyzed 1 day (1d) and 3 days (3d) after induction of pancreatitis.

5.5.2.1 Confirmation of DBZ Effect

In DBZ treated mice, PAS-staining of the small intestine showed a massive conversion of crypt cells into goblet cells, demonstrating the previously described effect of DBZ administration thus confirming the Notch-inhibiting effect of DBZ in vivo (Fig. 5-20) (van Es 2005).

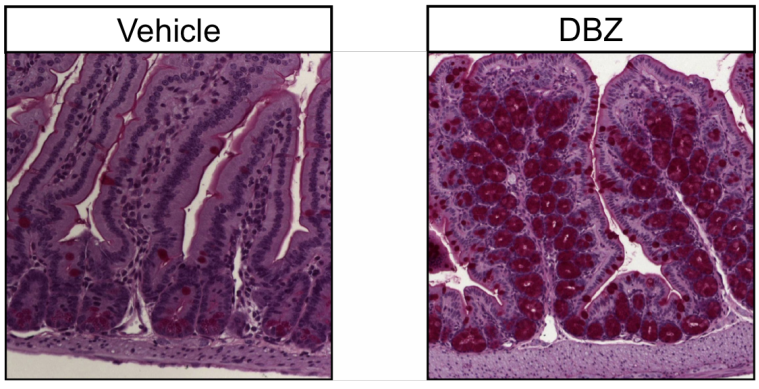

Fig. 5-20: Confirmation of DBZ effect

Crypt cells of the small intestine are converted into goblet cells following administration of DBZ, demonstrating functionality of γ-secretase inhibition. PAS staining.

5.5.2.2 Histomorphology

On day 1, DBZ and vehicle treated mice displayed comparable acute tissue reactions with edema, acinar cell death and inflammatory cell reaction (Fig. 5-21 A). On day 3 however, significant histomorphological differences were visible between pancreata of DBZ and vehicle treated mice. Vehicle treated mice revealed large areas with almost complete exocrine regeneration and only focal post inflammatory residues. Only few lobules with incompletely regenerated tissue remained, with the extent varying interindividually and between experiments.

In DBZ treated mice, pancreata showed large areas with an almost complete absence of normal acinar architecture. Furthermore, eosinophilic staining was reduced, indicating a decrease of zymogen granules (Fig. 5-21 B).

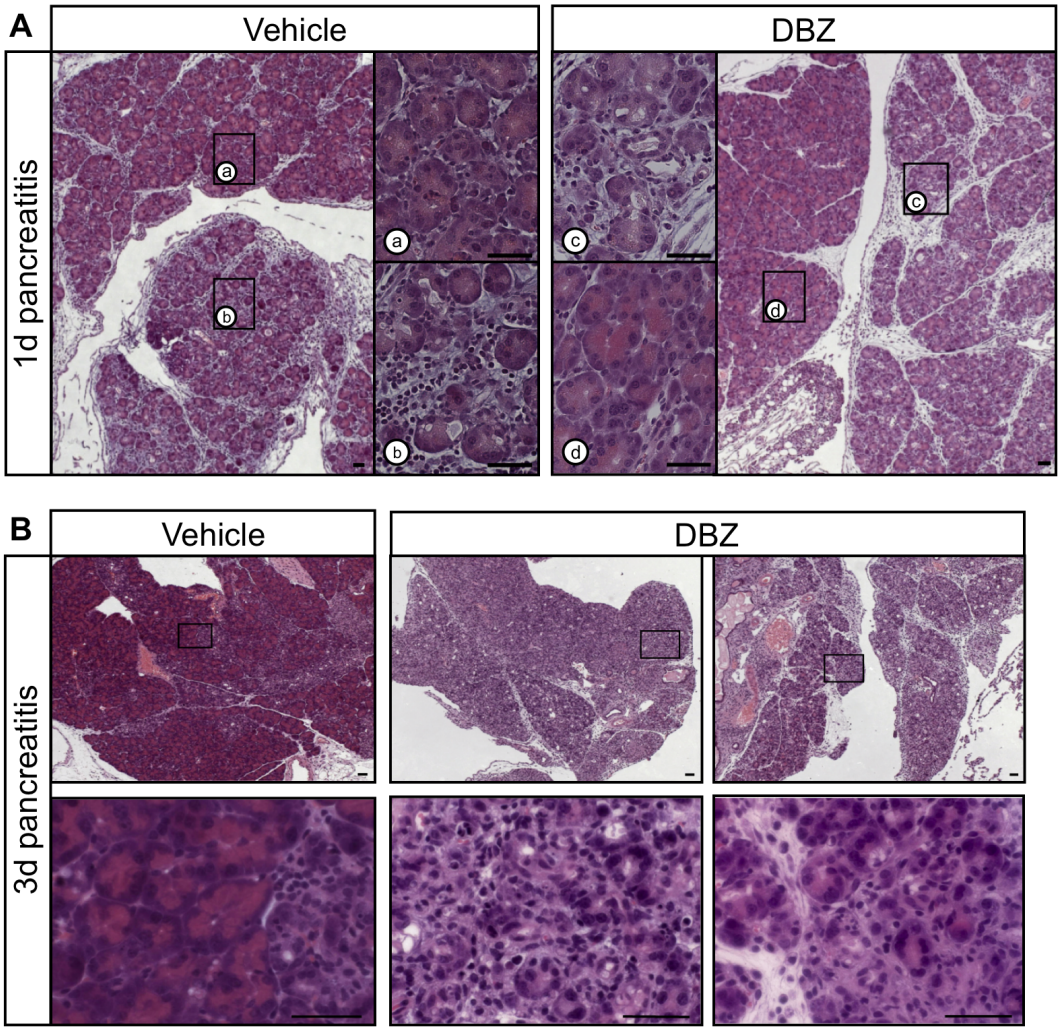

Fig. 5-21: Pancreatic histomorphology during acute pancreatitis

A) Comparison of histomorphology on day 1 revealed similar acute tissue reaction in vehicle- and DBZ treated mice. Inserts show magnification with infiltrating cells between acini.

B) On day 3, vehicle treated mice showed largely regenerated areas with small inflammatory residues. In contrast, DBZ-treated mice showed impaired regeneration with large areas of destructed acini. Inserts show magnification with details of regenerating acinar structures. Scale bars: 50 µm

5.5.2.3 Proliferation and Apoptosis

Evaluation of proliferation revealed a slightly reduced activity in DBZ treated mice on day 1 compared to vehicle treated mice. However, on day 3, proliferation was significantly reduced in DBZ treated mice (Fig. 5-22 A).

Apoptosis was significantly increased in DBZ treated mice on day 3 (Fig. 5-22 B).

5.5.2.4 Quantitation of Acinar Regeneration

To quantitate and compare the extent of acinar regeneration in DBZ and vehicle treated mice, the number of acini was counted in slides stained for amylase. This number was related to the area of the section examined.

On day 1, there was no statistically significant difference in the number of acini between both groups, although the number of acini was slightly reduced in DBZ treated mice. On day 3, the number of acini decreased in vehicle and DBZ treated mice compared to day 1. However, the decrease was more pronounced in the DBZ group, leading to a significant reduction in acini in DBZ treated mice compared to vehicle treated control mice (Fig. 5-22 C). This increased loss in acinar tissue in the DBZ group is well in accordance with the elevated apoptosis rate and reduced proliferation in this group on day 1 and day 3.

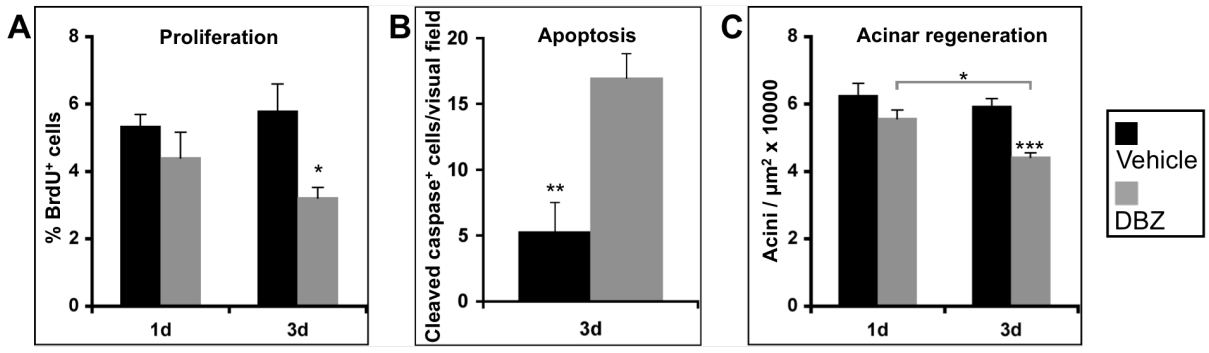

Fig. 5-22: Evaluation of proliferation, apoptosis and acinar regeneration

A) On day 1, proliferation was slightly reduced in DBZ treated mice. On day 3, the reduction was statistically significant. $p = 0.036$

B) On day 3, apoptosis was significantly elevated in DBZ treated mice. $p = 0.0059$

C) Morphometric analysis of acini revealed a slight reduction in DBZ treated mice on day 1. On day 3, the reduction was statistically significant. $p < 0.005$. Error bars denote SEM.

5.5.2.5 Immunohistochemical Staining and Immunofluorescence

To further characterize the nature of the cells within the non-regenerated areas, sections of pancreata from day 3 were analyzed using various markers. Almost none of the cells stained positive for exocrine (amylase), endocrine (insulin, glucagon), and ductal (DBA) markers. However, PDX1 and clusterin expression was detectable, suggesting the appearance of un- or dedifferentiated pancreatic cells. Furthermore, CD45 and F4/80 positive cells were detectable, revealing the presence of leukocytes and macrophages (Fig. 5-23 A).

To further analyze the epithelial and differentiation status of the exocrine cells, the expression pattern of E-cadherin and β-catenin was analyzed by double immunofluorescence staining with amylase. In vehicle treated mice, regenerated acinar cells showed strong staining for amylase and a membrane bound localization of E-cadherin and β-catenin, whereas in DBZ treated mice, staining for amylase was reduced and expression of E-cadherin and β-catenin was increased and colocalized in the cytoplasm (Fig. 5-23 B). This expression patterns are reminiscent of undifferentiated acinar cells.

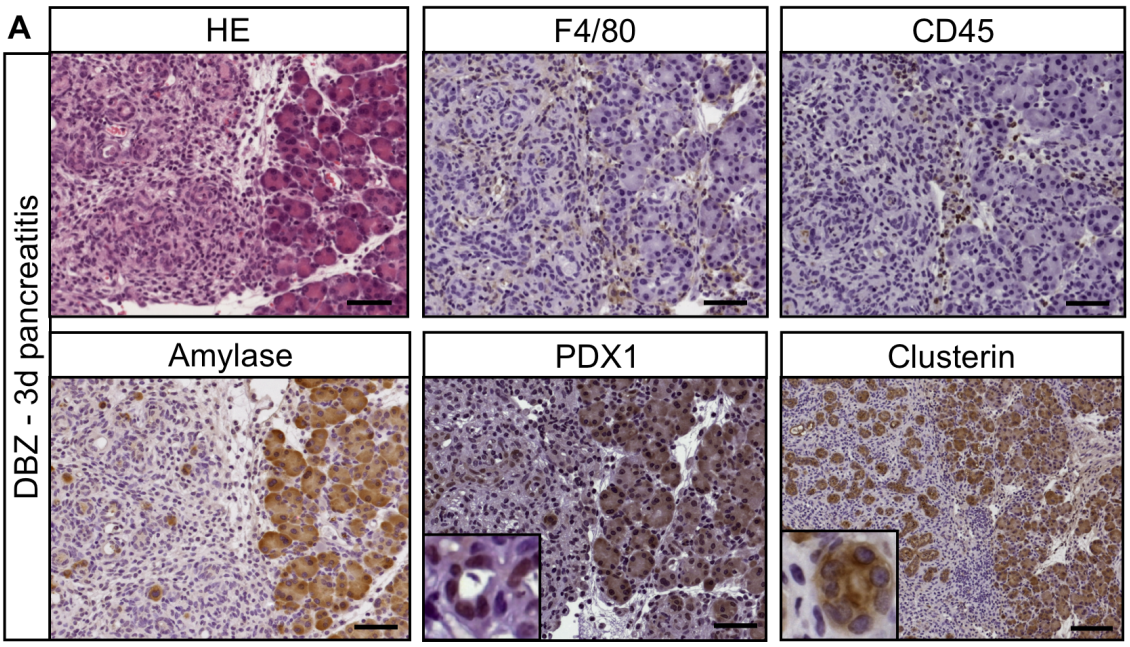

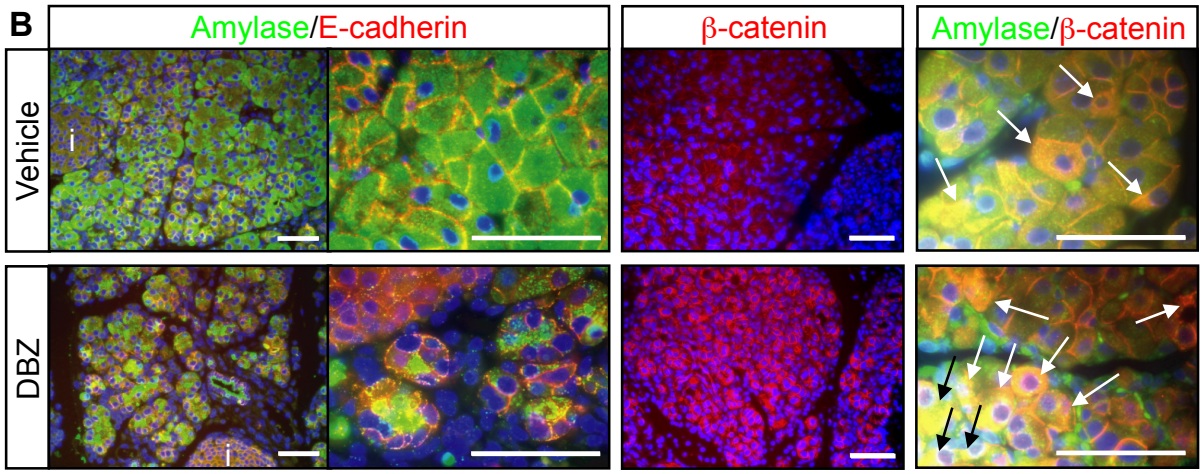

Fig. 5-23: Characterization of cells in non-regenerated pancreatic areas

A) H&E staining showed a pancreatic section containing an area with impaired regeneration and neighboring regenerated acini. Immunochemical staining for CD45 and F4/80 showed infiltrating leukocytes and macrophages. Only residual amylase staining was detectable in the non-regenerated areas. Cells in this area stained positive for PDX1 and clusterin, resembling cells in an immature status.
B) Double immunofluorescence staining for amylase (green) and E-cadherin (red) of pancreata of vehicle treated mice revealed strong expression of amylase, expression of E-cadherin was confined to the cell membrane. In DBZ treated mice, expression of amylase was strongly reduced, E-cadherin showed cytoplasmic localization.
Staining for β-catenin (red) also showed strong cytoplasmic localization in DBZ treated mice.
Double immunofluorescence staining for amylase (green) and β-catenin (red) revealed increased colocalization of β-catenin with amylase in DBZ-treated mice (yellow, arrows). Nuclei were counterstained with DAPI (blue); i = islet, scale bars: 50µm.

5.5.3 Notch1 Knockout Mice

Having demonstrated a functional role of the Notch signaling pathway in the course of pancreatic regeneration after acute cellular injury, the individual impact of the Notch1 receptor was studied through induction of acute pancreatitis in *N1KO* mice using the same protocol as before.

5.5.3.1 Body Weight and Pancreatic Weight

The body weight was documented on the indicated days after final injection of cerulein. One day after induction of pancreatitis, the body weight was slightly reduced in *N1KO* mice as compared to wt mice (Fig. 5-24 A, 1d). Between day 1 and day 3, the body weight in both groups remained stable, with the body weight of the *N1KO* mice being slightly reduced compared to the wt mice (Fig. 5-24 A, 3d). On day 7, the body weight of *N1KO* mice decreased whereas the body weight of wt mice did not change (Fig. 5-24 A, 7d).

The pancreatic weight was documented on the indicated days after final injection of cerulein. There was no significant difference in pancreatic weight 24 hours after cerulein treatment (Fig. 5-24 B, 1d). After 3 days, there was a statistically significant decrease in the pancreatic weight in *N1KO* mice and in wt mice (Fig. 5-24 B, 3d). The decrease was a little more pronounced in wt mice. Seven days after cerulein stimulation, the pancreas in wt mice gained weight, indicating recovery from the injury, whereas the pancreas in *N1KO* mice continued to diminish (Fig. 5-24 B, 7d).

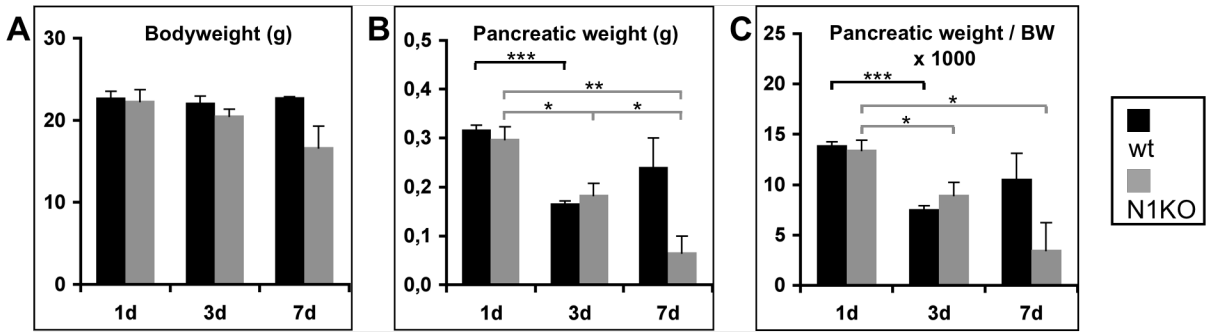

Fig. 5-24: Body weight, pancreatic weight and pancreatic weight index

A) The body weight of *N1KO* mice was slightly lower compared to the wt group at all time points. Whereas the body weight remained stable in the wt group at all time points, the body weight in the *N1KO* group showed a decrease on day 7.
B) On day 1 there was no significant difference in pancreatic weight between wt and *N1KO* mice. On day 3, the pancreatic weight showed a statistically significant decrease in both groups compared to day 1. On day 7, the pancreatic weight in wt mice increased whereas the pancreatic weight in the *N1KO* mice continued to drop.
C) On day 3, the pancreatic weight index decreased in both groups. On day 7 it increased in wt mice whereas it continued to decrease in the *N1KO* group.
For wt mice, n= 5; 4; 2 and for *N1KO* mice, n= 4; 6; 2 for day 1, day 3 and day 7 respectively
Error bars indicate SEM. *: $p < 0.05$; **: $p < 0,01$; ***: $p < 0.005$

5.5.3.2 Histomorphology

On day 1, comparable histomorphological alterations resulting from acute tissue reactions to the cerulein treatment were observable in *N1KO* as well as wt mice. In both groups, edema, inflammatory cell reaction with infiltrating neutrophils and macrophages and cell death could be detected. No obvious histomorphological differences between wt and *N1KO* mice were detectable in the acute phase of pancreatitis on day 1 (Fig. 5-25 A).

On day 3, during the course of pancreatic regeneration, substantial morphological differences between the pancreata of wt and *N1KO* mice were observable. Wt mice showed large areas of almost completely regenerated acinar tissue with normal

appearing eosinophilic staining. In these areas only minor post-inflammatory alterations could be noted. A few lobules showed incomplete regeneration with infiltrating cells and an impaired acinar architecture.

In *N1KO* mice, the normal acinar architecture was almost completely absent and the acini showed decreased eosinophilic staining. Those areas that were reminiscent of normal acinar tissue showed less intercellular adhesions. (Fig. 5-25 B).

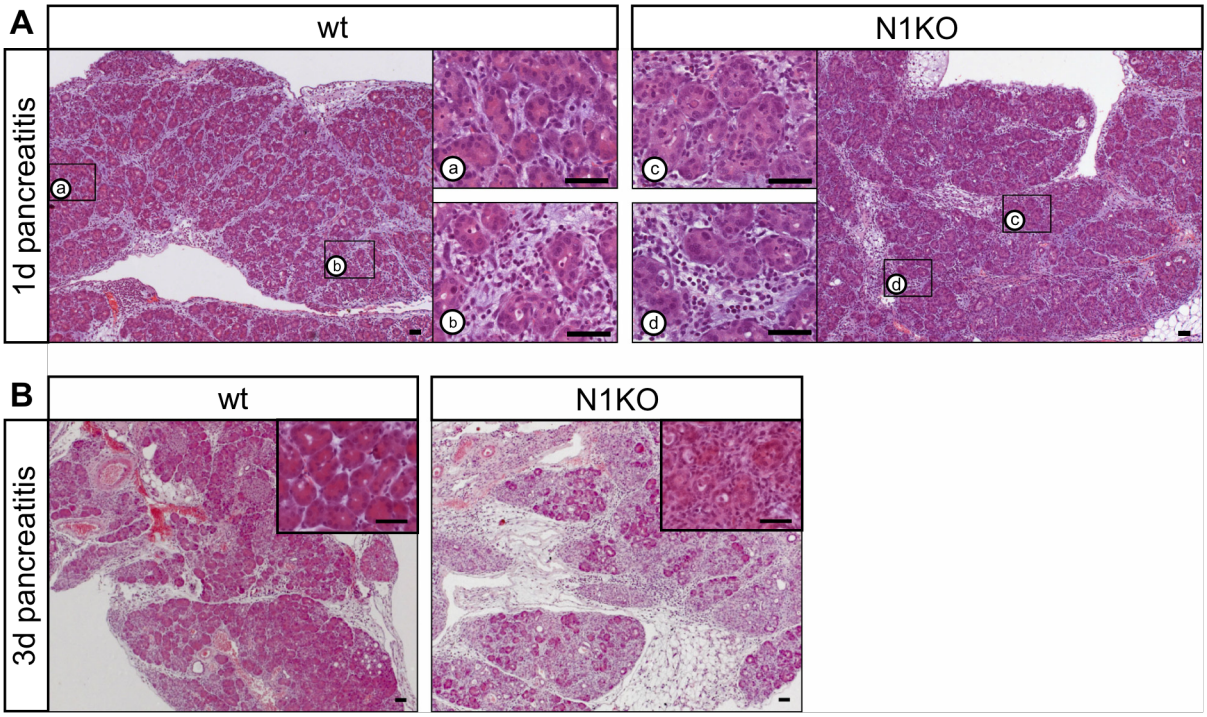

Fig. 5-25: Pancreatic histomorphology during acute pancreatitis

A) Comparison of histomorphology on day 1 revealed similar acute tissue reaction in wt and *N1KO* mice. Inserts show magnification with infiltrating cells between acini.
B) On day 3, wt mice showed largely regenerated areas with small inflammatory residues. In contrast, *N1KO* mice showed impaired regeneration with large areas of destructed acini. Inserts show magnification with details of regenerating acinar structures.
Scale bars: 50µm

5.5.3.3 Immunohistochemical Staining for Different Markers

To further characterize the cells in the non-regenerated exocrine pancreas of *N1KO* mice on day 3, immunohistochemical staining was performed for various markers. As in DBZ treated mice, cells in these areas stained negative for exocrine (amylase), endocrine (insulin) and ductal (DBA) markers (Fig. 5-26 A), but positive for markers denoting precursor cells as clusterin and PDX1 (Fig. 5-26 B). Staining for leukocyte markers showed the presence of lymphocytes and macrophages (Fig. 5-26 C).

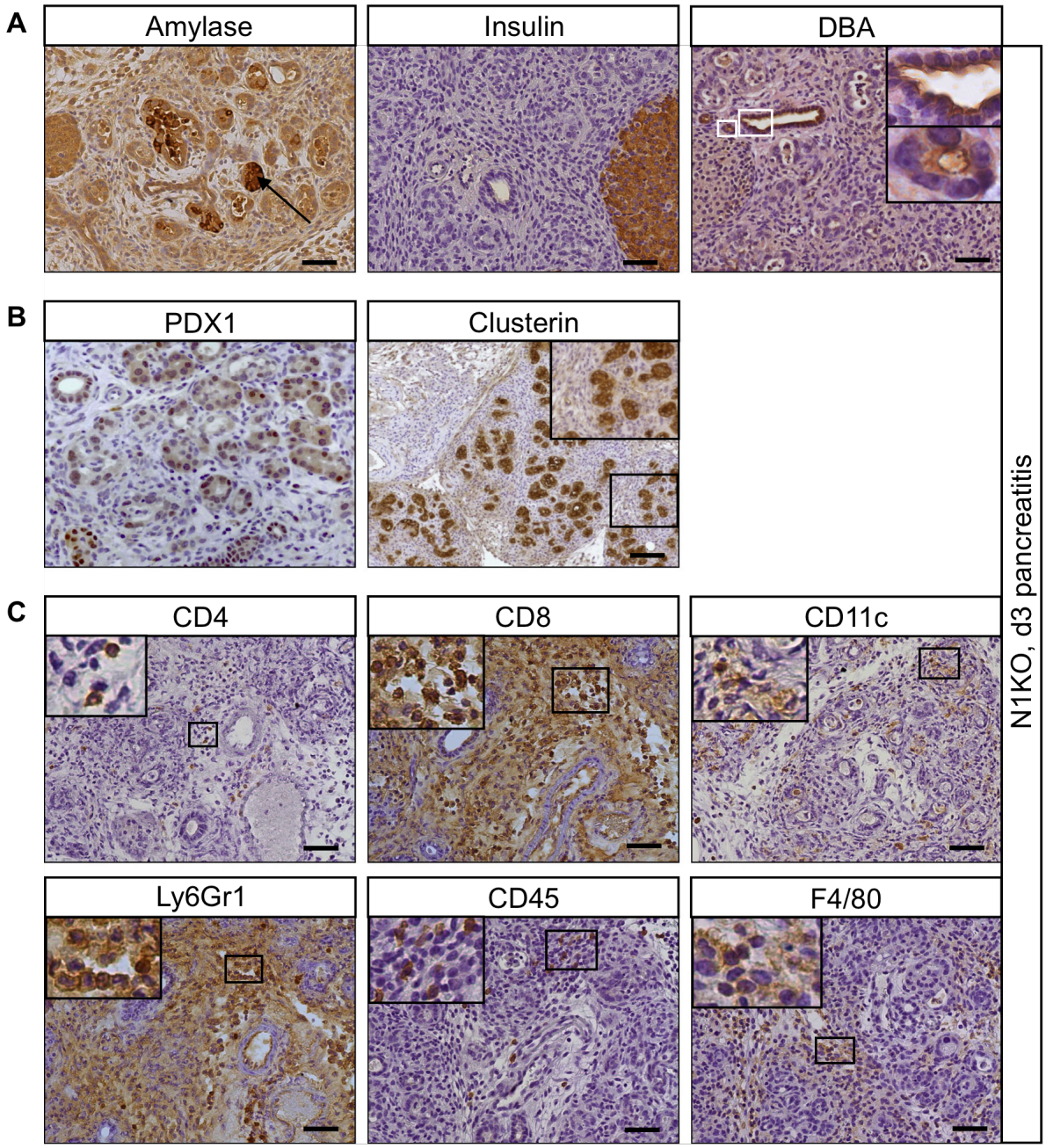

Fig. 5-26: Characterization of cells in non-regenerated pancreatic areas

A) Immunostaining of destructed areas for exocrine differentiation marker amylase revealed only residual amylase$^+$ acini (arrow). The majority of the cells did not express amylase. Immunostaining for insulin revealed that expression is confined to islets. Staining for DBA labeled ductal structures only.
B) Immunostaining for PDX1 and clusterin showed strong staining, indicating that most of the cells were immature pancreatic precursor cells. Insert shows magnification expression of clusterin in pancreatic cells.
C) Immunostaining for different leukocyte markers showed infiltration of inflammatory cells.
Scale bars: 50 µm

5.5.3.4 Proliferation and Apoptosis

Counting of 65,185 exocrine cells revealed a slightly increased proliferation in *N1KO* mice one day, and a significantly increased proliferation in *N1KO* mice three days after induction of pancreatitis. 7 days after induction of pancreatitis, proliferation dropped by 82 % in wt mice compared to day 3. However, in *N1KO* mice proliferation remained significantly elevated on day 7 compared to wt mice (Fig. 5-27 A).

Counting of 5 to 23 visual fields revealed an elevated apoptosis rate in *N1KO* mice compared to wt mice at all time points. On day 1, apoptosis was 4.6-fold higher in *N1KO* mice compared to wt mice (Fig. 5-27 B, 1d). In wt mice, the apoptotic rate nearly doubled from day 1 to day 3, but then decreased 3.7-fold between day 3 and day 7 (Fig. 5-27 B). In *N1KO* mice, the apoptosis rate showed a continuous decrease from day 1 to day 7, reaching about 50 % apoptotic rate on day 3 compared to day 1. On day 7, apoptosis was still elevated 4.6-fold in *N1KO* mice compared to wt mice (Fig. 5-27 B, d7).

5.5.3.5 Quantitation of Acinar Regeneration

To quantitate and compare the extent of acinar regeneration in wt and *N1KO* mice, the number of acini was counted in slides stained for amylase. This number was related to the area of the section examined.

On day 1, there was no statistically significant difference in number of acini between wt and *N1KO* mice, although the number of acini was slightly reduced in *N1KO* mice (Fig. 5-27 C, 1d). On day 3, the number of acini increased in wt mice, whereas the number of acini decreased in *N1KO* mice, leading to a statistically significant reduction in acini in *N1KO* mice compared to wt mice (Fig. 5-27, 3d). This continued loss in acinar tissue is well in accordance with the elevated apoptosis rate in *N1KO* mice on day one and three, and also explains the continued loss of pancreatic weight on day 7.

On day 7, amylase staining of *N1KO* pancreas revealed a mostly regenerated pancreas. Only residual signs of inflammatory reactions as infiltrating cells and slightly loosened interlobular adhesions were left (not shown).

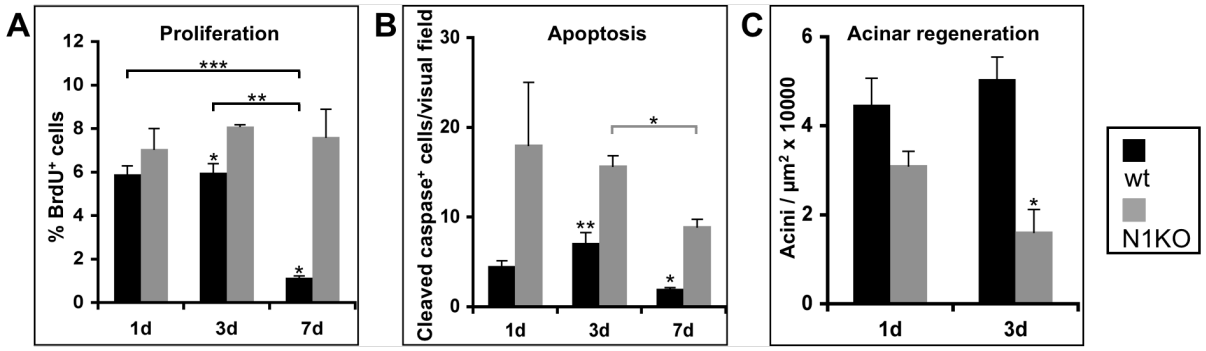

Fig. 5-27: Evaluation of proliferation, apoptosis and acinar regeneration

A) Counting of BrdU positive cells revealed a slightly increased proliferation in *N1KO* mice on day 1, and a significant increase on day 3 and day 7. On day 7, the proliferation rate decreased in the wt group. Proliferation in *N1KO* mice remained 6.7-fold higher.
A total of 65,185 cells were counted.
B) On day 1, apoptosis was 4.6 fold higher in *N1KO* mice. On day three, apoptosis rate increased in wt mice, reaching a peak. In *N1KO* mice, apoptosis dropped slightly. On day 7, apoptosis decreased 3.7-fold in wt mice. In the *N1KO* group, apoptosis continued to drop but was still 4.6-fold elevated compared to the wt group. On day 3 and day 7, the elevated apoptosis was statistically significant. 5 to 23 visual fields per mouse were counted.
C) On day 1, *N1KO* mice displayed a lower number of acini. On day 3, wt mice showed a slightly elevated number of acinar structures compared to day 1. The number of acinar structures decreased further in *N1KO* mice compared to day 1. On day 3, the difference between wt and *N1KO* mice was statistically significant.
Error bars are expressed in SEM. *: $p < 0.05$; **: $p < 0,01$; ***: $p < 0.005$

5.5.3.6 Gene Expression Analysis

Gene expression analysis of exocrine (amylase) and endocrine (insulin) lineage markers by quantitative real-time qRT-PCR reflected the destruction of normal pancreatic tissue one day after induction of pancreatitis, and the subsequent regeneration on day 3 and day 7. On day 1, amylase expression was hardly detectable. On day 3, amylase expression increased about 10-fold in wt mice, whereas expression in *N1KO* mice lagged behind reaching a mere 3.8-fold elevation. On day 7, recovery continued in both groups with *N1KO* progress still lagging behind, reaching only 50 % of expression levels of wt mice. (Fig. 5-28 A)

Analysis of insulin expression showed a marked decrease on day 1 in wt and *N1KO* mice. On day 3, insulin expression reached levels of unstimulated pancreata in wt mice. In *N1KO* mice insulin expression surpassed that of unstimulated mice. On day 7, insulin levels normalized in *N1KO* mice. (Fig. 5-28 B)

On day 1, the ductal marker CK19 increased 11-fold and 13-fold in wt and *N1KO* mice, respectively. On day 3, CK19 expression decreased 71 % in wt mice, whereas

it increased further in *N1KO* mice. On day 7, CK19 expression reached levels of unstimulated pancreata (Fig. 5-28 C).

Expression analysis of the mesenchymal marker vimentin showed strong upregulation on day 1. On day 3, upregulation remained high in *N1KO* mice, whereas in the wt group it dropped to less than 50 %. On day 7, vimentin expression decreased further. Of note, the decrease was more pronounced in *N1KO* mice such that the expression levels became equal in wt and *N1KO* mice (Fig. 5-28 D). Analysis of the macrophage marker F4/80 revealed a strong increase on day 1. On day 7, expression levels decreased in wt pancreata but remained elevated in *N1KO* pancreata (Fig. 5-28 E).

Immunofluorescence of E-cadherin and β-catenin revealed stronger staining in *N1KO* mice. Western blot analysis of β-catenin in pancreatic whole cell lysates showed elevated protein expression, confirming the upregulation of β-catenin expression in *N1KO* mice (Fig. 5-28 F, G).

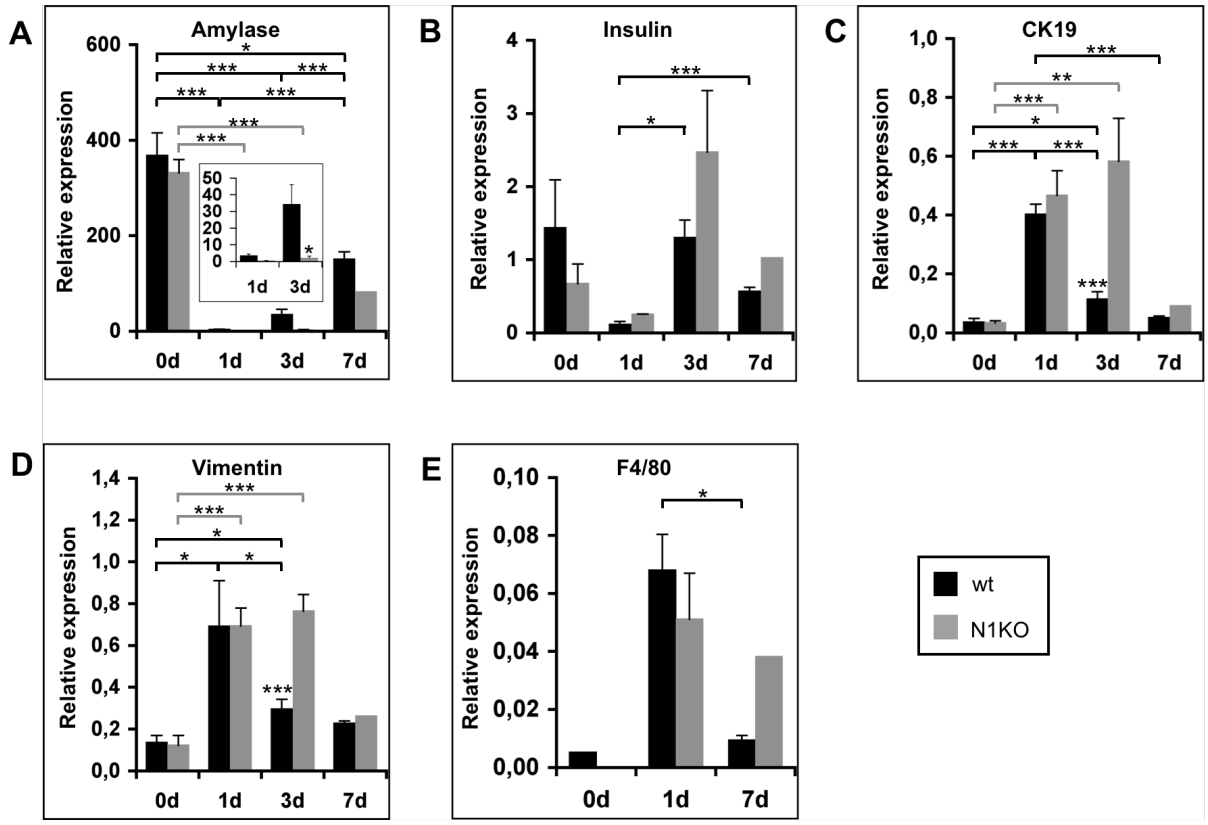

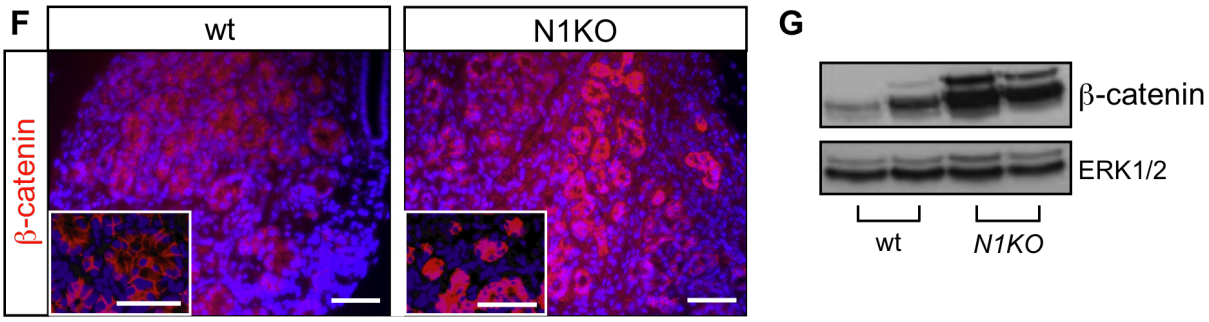

Fig. 5-28: Gene expression analysis

A) Expression analysis of amylase reflected the destruction of pancreatic tissue. Amylase expression was barely detectable on day 1. On day 3, amylase expression increased about 10-fold in wt mice, whereas the increase in *N1KO* mice was merely 3,8-fold (insert). Regeneration of amylase expression continued on day 7, with *N1KO* mice still lagging behind wt mice. Insert shows amylase expression on day 1 and day 3 in a different scale.
B) Expression analysis of insulin showed strong reduction on day 1. In contrast to amylase expression, insulin expression recovered completely on day 3, suggesting a faster regeneration process of the endocrine compartment.
C) Expression of CK19 was upregulated 11-fold and 13-fold in wt and *N1KO* mice, respectively. On day 3, expression decreased in wt mice and continued to increase in *N1KO* mice. On day 7, expression reached normal levels.
D) Vimentin was strongly upregulated on day 1 in wt and *N1KO* mice. On day 3, expression decreased in wt mice and remained elevated in *N1KO* mice. On day 7, expression approximated normal levels.
E) Expression of the macrophage marker F4/80 increased strongly on day 1. On day 7 expression levels decreased in wt pancreata but remained elevated in *N1KO* mice.
Error bars indicate SEM. *: $p < 0.05$; **: $p < 0,01$; ***: $p < 0.005$
F) Immunohistochemistry for β-catenin revealed elevated expression in *N1KO* compared to wt mice. Inserts show that localization of β-catenin in wt mice is confined to plasma membrane, as opposed to elevated cytoplasmic localization in *N1KO* mice. Nuclei were counterstained with DAPI (blue). Scale bar: 50µm
G) Western blot analysis revealed increased protein levels of β-catenin in *N1KO* mice. Staining for ERK1/2 shows equal protein loading.

6 Discussion

This study investigated the role of Notch signaling and specifically of Notch1 on morphogenesis, proliferation and apoptosis during pancreatic organogenesis and its function in regenerative processes during acute pancreatitis, using a pancreas-specific conditional *Notch1*-deficient mouse model and a chemically induced inhibition of Notch signaling.

6.1 Efficiency of Genetical Ablation of Notch Signaling

Expression analyses of *Notch1* mRNA and protein were done for adult mice only, since Nakhai et al. previously showed homogeneous Cre-recombination and early excision of the floxed *Notch1* allele in embryonic pancreata at E11.5 and 18.5 (Nakhai 2007; 2008a). These data suggest that the floxed *Notch* alleles are recombined early after Cre recombinase expression, and that this recombination occurs in all *Ptf1a* positive cells. Protein and real-time qRT-PCR analysis of whole pancreatic tissue revealed a reduction of *Notch1* expression in pancreatic tissue of 91 %. The remaining 9 % *Notch1* mRNA in the pancreas can most likely be attributed to three factors:

- Incomplete Cre mediated recombination of the targeted *Notch1* alleles in pancreatic cells
- *Notch1* expression in cells within the pancreas that have not expressed *Ptf1a* during pancreatic development
- *Notch1* expression in extrapancreatic cells within the whole cell lysates

As X-gal staining revealed high efficiency and homogeneous distribution of Cre recombinase activity in the exocrine tissue, either non-recombined islets or non-pancreatic cells from the connective tissue or vascular endothelium most likely contribute to the residual *Notch1* expression.

6.2 Notch1 During Pancreatic Organogenesis

6.2.1 Embryogenesis

This study did not detect any manifest differences in pancreatic development in the intrauterine phase. Histomorphological analysis of the exocrine, endocrine and ductal development as well as pancreatic proliferation and apoptosis during this period

showed no differences in wt and *N1KO* mice. This result is unexpected, as several studies have demonstrated *Notch1* expression during pancreatic organogenesis and that loss of as well as induction of Notch-signaling resulted in severe exocrine and endocrine developmental anomalies and early embryonic death of mice with homozygous deletions of genes of the Notch pathway (Apelqvist 1999; Jensen 2000b; Lammert 2000; Hald 2003; Hart 2003; Murtaugh 2003; Norgaard 2003; Fukuda 2006; Ahnfelt-Rønne 2007; Zecchin 2007). Several explanations have to be considered that account for this finding:

1) Different modes of Notch signaling disruption:
   Previous studies that utilized conditional ablation of Notch signaling in the pancreas did not target one single receptor but induced a broader disruption of the pathway either through ablation of the nuclear transducer of Notch signaling *Rbpj* or the Notch target gene *Hes1*.
2) Different timing of Notch signaling ablation:
   In many of the previous studies mentioned above, Notch signaling ablation was inherent in the embryos from the moment of conception.

The broadest approach to disrupt Notch signaling specifically in the pancreas was achieved by ablation of the intranuclear transducer of Notch signaling, *Rbpj,* affecting signaling through all Notch receptors (Apelqvist 1999; Fujikura 2006; Nakhai 2008a). In the first study, *Rbpj* deficient mice displayed an increased number of cells expressing *Ngn3*, indicating an increased differentiation towards the endocrine lineage. However, these mice died at around E8.5, precluding studies on later stages during embryonic development and potential effects on the exocrine lineage. In the second study, *Rbpj* was conditionally deleted using a *Pdx-Cre* transgenic strain. These mice also displayed a premature increase in *Ngn3* expression, pancreatic hypoplasia caused by a depletion of progenitor cells and the precocious differentiation of endocrine and ductal cells. Thus, ablation of just one receptor as in this study may not be sufficient to recapitulate the severe developmental phenotype, but instead cause either no defects or induce only subtle alterations that evaded detection in this study. A precise quantitation of the endocrine and exocrine compartment in wt and *N1KO* mice as well as gene expression analyses during pancreatogenesis could elucidate the potential existence of such subtle differences in phenotype and/or alterations in the genetic program during this specific developmental period. Other explanations for the unaltered phenotype could be

potential compensatory upregulation of other Notch receptors and partly redundant roles of the different Notch receptors during pancreatic development. Analogous to the finding in this study, a previous study comparing the effect of *Rbpj* and *Notch1* knockout during neurogenesis in mice observed a less severe phenotype in *Notch1* deficient mice (de la Pompa 1997). That finding was also attributed to functional redundancy of the Notch receptors. Several other studies have also demonstrated less severe phenotypes during murine embryogenesis with single receptor knockouts compared to multiple knockouts, arguing in favor of redundancy as a mechanism to compensate for loss of one receptor (Krebs 2000; Cormier 2004; Kitamoto 2005). In this study, gene expression analysis of the other epithelially expressed Notch receptor, Notch2, did indeed display a slight upregulation in adult *N1KO* mice. Although this finding was not significant, it could be indicative of a possible compensatory role of Notch2 during embryogenesis, supporting the hypothesis of compensation/redundancy as a possible mechanism. However, double-knockout *Notch1/2* mice also have no apparent exocrine defect (Nakhai 2008a) suggesting that these receptors are not essential for exocrine development and homeostasis. While compensatory mechanisms through Notch3 and/or Notch4 receptors need also be considered, this scenario appears less likely since these receptors are not expressed in the pancreatic epithelium (Lammert 2000). Indeed, real-time qRT-PCR analyses in adult pancreata of *Notch1/2* double-knockout pancreata showed no upregulation of Notch3 and Notch4 suggesting that these receptors are not involved in compensatory mechanisms during exocrine development and homeostasis.

Studies have shown that RBP-Jκ interacts with PTF1a in a way distinct from Notch and that the resulting PTF1 complex is not dependent on Notch signaling, suggesting a Notch-independent role for *Rbpj* in embryonic pancreas development (Obata 2001; Beres 2006). Additionally, various DNA binding transcription factors have been identified that contain peptide sequences related to *Rbpj* interacting motifs, suggesting possible Notch-independent interactions that would be disrupted in *Rbpj* deficient mice (Beres 2006). Supporting these findings, a Notch-independent role of *Rbpj* has been described in other tissues (Barolo 2000). It should therefore be considered that the phenotype seen in *Rbpj* deficient mice could at least in part result independently from Notch signaling inactivation.

Also, the time point at which *Notch1* ablation is induced through activation of Cre recombinase needs to be considered. PTF1a expression in the pancreas is initiated

approximately on E9.5, leading to a corresponding expression of Cre recombinase in *Ptf1a*$^{+/Cre(ex1)}$ mice. However, effective Cre-mediated recombination was shown to occur with a delay of 1 day, hence approximately on E10.5 (Fujikura 2007). Assuming that the delay between beginning expression of Cre recombinase and effective recombination is an inherent trait of the Cre/loxP system means that inactivation of Notch1 signaling in this study also occurs at around E10.5. It is conceivable that inactivation of Notch1 signaling at that time point is too late to severely affect early pancreatic development. This was also hypothesized by Fujikura et al. (2006; 2007) who found the phenotype more severely affected in mice in which *Rbpj* was deleted by Cre recombinase under control of the *Pdx1* promoter as compared to *Ptf1a*. Since PDX1 expression starts one day earlier than expression of PTF1a, they concluded that the difference in phenotype was due to the difference in timing, and that the impact of Notch signaling on pancreatogenesis declines between E9.5 and E10.5.

Further evidence substantiating that timing of expression is pivotal during murine embryogenesis comes from a study by Heiser et al. (2006). In the study, usage of two different *Pdx1-Cre* transgenic strains, with a difference in Cre expression of 1 day, resulted in fundamentally different pancreatic phenotypes. Additionally, two studies employing overexpression of Notch during pancreatogenesis showed different phenotypes and attributed this finding to differences in the temporal expression pattern (Hald 2003; Murtaugh 2003).

Therefore, to assess the role of Notch1 signaling at earlier time points of embryonic pancreatogenesis, knockout constructs disrupting *Notch1* expression prior to expression of PTF1a would be necessary, e.g. by generation of knock-in mice expressing the Cre recombinase under the control of the endogenous *Pdx1* promoter. This construct would circumvent the difficulties inherent in the transgenic construct of Pdx1-Cre mice used so far. Although *Pdx1* is expressed only one day earlier than PTF1a on E9.5, this difference could potentially result in a more severe phenotype, as was demonstrated by Fujikura et al. (2006). This approach would give a more precise understanding of the physiological role of Notch1 signaling during early embryonic pancreas development. However, mice heterozygous for *Pdx1* show an impaired β-cell function and develop diabetes, aggravating analysis due to effects of *Pdx1* heterozygosity (Brissova 2002; Melloul 2002).

6.2.2 Juvenile and Adult Mice

As in embryonic mice, analysis of the morphology and of the exocrine, endocrine, and ductal lineage as well as evaluation of proliferation and apoptosis in pancreata from 5.5 and 9.5 week old mice did not reveal any difference between wt and *N1KO* mice.

6.2.2.1 Notch Signaling Gene Expression Analysis

Expression of *Notch2* was elevated in *N1KO* mice, suggesting a compensatory upregulation (compare to 6.2.1). Expression of the Notch ligand DLL1 was only slightly elevated, whereas expression levels of the Notch target gene *Hes1* were not altered. Although expression of *Hey1* was upregulated, the levels of *Hey1* transcripts in adult mice were extremely low questioning a functional role of *Hey1* in the pancreas. The finding of unaltered *Hes1* expression supports the hypothesis that loss of Notch1 in adult mice does not result in measurable functional alterations of these Notch target gene expression. While not all members of the *Hes* and *Hey* family of transcription factors were analyzed, it is likely that Notch-independent regulation plays a role in gene expression. Indeed, a recent study on development of hair follicles found β-catenin dependent expression of *Hes* and *Hey* genes, demonstrating Notch-independent regulation of *Hes1* (Ambler 2007). The finding in this study that β-catenin is elevated in *N1KO* could explain the sustained expression of *Hes1* in the absence of *Notch1*. Whether β-catenin is indeed responsible for the maintenance of *Hes1* expression in the adult pancreas needs further investigation.

6.2.2.2 Pancreatic Lineage Gene Expression and Weight Analysis

Expression analysis of exocrine and endocrine lineage markers revealed a downregulation of amylase and insulin, whereas CK19 as a ductal marker was not altered. For amylase, this finding was significant. The reduced amylase mRNA expression could result from a reduced production within acinar cells. On the other hand, it could be the result of a reduced overall exocrine cell mass and thus not implicate an altered phenotype of single acinar cells. Finally, it could be a combination of both. The observed decrease in pancreatic weight in N1KO mice is in agreement with a reduced overall exocrine cell mass, arguing against functional impairment due to loss of Notch-signaling.

Despite the absence of gross differences during embryonic pancreatogenesis, pancreata of 5.5 week-old *N1KO* mice displayed a diminished weight. Even though this finding was statistically not significant, it is suggestive of a mild growth retardation of the pancreas. Relating the pancreatic weight to the body weight further substantiated this finding. Comparison of the pancreatic weight index showed a significant decrease in the *N1KO* group. The growth retardation could occur either during embryonic pancreatogenesis or during the final proliferation process in the first weeks postpartum, or both. Pancreatic weight of newborn mice need to be measured to narrow the developmental period the growth retardation occurs in. However, since the Notch1 receptor is predominantly expressed during the embryonic period, it appears more likely that the impaired pancreatic development leading to the growth retardation occurs during that time. This finding is indeed surprising considering that the parameters influencing the growth and size of an organ documented in this study, proliferation and apoptosis, did not display any detectable difference, neither in all embryos analyzed nor in juvenile mice.

Previous studies have shown that in the absence of Notch signaling, the endocrine compartment differentiates prematurely at the expense of exocrine precursor cells, leading to a depletion of pancreatic precursor cells and development of a pancreas of decreased size (Apelqvist 1999; Jensen 2000b; Fujikura 2006). However, no apparent difference in size, endocrine or exocrine development was notable. Of course, it is possible that the effect of pancreatic Notch1 ablation on apoptosis, proliferation and the number of progenitor cells is too subtle and thus below limit of detection in any of the stages examined, however strong enough in the course of development to accumulate in detectable growth retardation. In fact, the moderate increase in cytoplasmic β-catenin expression in adult *N1KO* pancreata suggests an altered maturation status of acinar cells. Since β-catenin has been implicated in pancreatic development and differentiation of acinar cells (Dessimoz 2005; Murtaugh 2005; Heiser 2006; Nakhai 2008b), this finding could be indicative of a possible residue of an impaired maturation/differentiation process during embryonic pancreatogenesis and could play a role in the observed pancreatic growth impairment evident in young *N1KO* mice.

Another potential explanation for the observed growth retardation could be the heterozygosity for the *Ptf1a* gene in the conditional knockout mice, as *Ptf1a* gives rise to all pancreatic cells and is crucial in exocrine development and specification.

However, data from a study by Krapp et al. (1998) that carefully compared wildtype mice and mice heterozygous for *Ptf1a* during various stages of embryonic pancreas development and in newborn mice did not detect any differences. Therefore, it seems unlikely that the absence of one *Ptf1a* allele alone accounts for the phenotype.
Since interaction between Notch signaling and PTF1a through competition for the binding site to the transcription factor RBP-J has been demonstrated, it is conceivable that at least part of the mechanism by which the phenotype in *N1KO* mice is mediated is through disturbed regulation of Notch - PTF1a - RBP-J interaction.
In 9 week-old adult mice, the difference in pancreatic weight and pancreatic weight index was not detectable any more, implying that the pancreas has the capability of recovering from the initial growth retardation. This finding leads to the conclusion that Notch1 signaling loses its impact on maturing juvenile pancreas cells, and that the ability of pancreatic cells to develop and proliferate normally is reconstituted in adult mice. This finding is consistent with a study that detected pancreatic malformation in *Rbpj* deficient juvenile mice that had disappeared in adult mice (Fujikura 2007). A possible explanation could be the shift in PTF1 composition from RBP-J to RBP-L in adult mice, since only RBP-J but not RBP-L can bind to Notch-IC (Beres 2006).
Expression levels for insulin showed a reduction in *N1KO* mice, however this finding was not significant. Immunohistochemistry revealed the typical expression pattern of endocrine hormones, arguing in favor of normal endocrine function. Furthermore, these mice showed normal blood glucose levels and no impaired glucose tolerance arguing against a reduced endocrine organ function.

6.2.3 Conclusion

Deficiency of Notch1 ablation did not lead to apparent morphologic alterations of pancreata during embryogenesis and in adult mice. This finding was surprising in the light of previous studies showing striking phenotypes after ablation of Notch signaling. Potential compensatory mechanisms of other Notch receptors and the time point of Notch ablation could explain the absence of severe defects. Another possibility is the Notch-independent role of *Rbpj* during pancreatic development. Evaluation of the pancreatic weight index and gene expression analysis for amylase revealed significant differences between wt and *N1KO* mice. Furthermore, the increased expression of cytoplasmic β-catenin in *N1KO* mice points towards an

altered maturation status. Hence, it seems justified to reason that Notch1 signaling does play a role in embryonic pancreas development. Its impact is, however, not strong enough to result in a profound impairment of pancreatogenesis or apparent alterations of the composition of the individual lineages during embryogenesis. Furthermore, the restored weight of the adult pancreas suggests reconstitution of normal pancreatic function during maturation of juvenile mice, also arguing against long-term defects resulting from *Notch1* ablation.

The finding of an apparently normal pancreas in adult *N1KO* mice allows for studying the role of Notch1 in adult homeostasis and in disease states such as acute pancreatitis.

6.3 Notch1 during acute pancreatitis

6.3.1 Upregulation of Notch During Acute Pancreatitis

For the analysis of Notch1 expression during pancreatitis, real-time qRT-PCR analyses and transgenic *Notch1-GFP* mice were employed (Lewis 1998). *Notch1-GFP* mice revealed a weak upregulation of Notch1 on day 1 and strong upregulation on day 3 after induction of pancreatitis. However, real-time qRT-PCR analysis of *Notch1* showed a marked drop in expression on day 1 in wt mice. This apparently contradictory finding could be explained when considering that during the course of acute tissue reaction, the acinar compartment expressing Notch1 is severely damaged and strongly infiltrated by inflammatory cells. In the absence of reliable tissue Notch1 detection, this heterogeneity makes precise deductions as to the temporal expression pattern of Notch1 difficult. Nonetheless, comparison of Notch1 expression between day 1 and day 3 demonstrates a more than 3-fold increase, indicating a significant upregulation of Notch1 in regenerating acinar cells on day 3. The elevated expression level of Notch1 on day 7 compared to unstimulated pancreata also indicates sustained upregulation of Notch1 from the regeneration process. This result is in accordance with a study from Jensen et al. (2005) as well as the *Notch1-GFP* findings from this study that Notch1 upregulation peaks three to four days after induction of pancreatitis and is only faintly initiated on day 1.

Expression analysis of Notch2 revealed a comparable upregulation on day 1 between wt and *N1KO* mice. On day 3, upregulation of Notch2 was significantly higher in *N1KO* than in wt mice, suggesting a compensatory effect for the absence of *Notch1*

during regenerative processes after acute pancreatitis, analogous to the putative mechanism during pancreatogenesis. The decrease of Notch2 expression on day 7 most likely reflects the advanced regeneration process. Expression analysis of the Notch target genes *Hes1* and *Hey1* on day 3 revealed significant upregulation of both genes in wt and *N1KO* mice, denoting functional Notch signaling.

Previous studies investigating expression of Notch pathway members during acute pancreatitis have also found an upregulation of this pathway, however their analyses differed in the temporal pattern of Notch expression. Data from this study are in accordance with the study from Jensen et al (2005) who found upregulation to begin on day 1 and peak on day 3. In contrast, the study by Gomez et al. (2004) detected upregulation of Notch signaling members peaking at 8-12 hours after induction of pancreatitis. Differences between the studies were the mice strains used, the amount of cerulein administered, and the detection method. That these differences account for the divergent findings is likely, yet remains unclear.

6.3.2 DBZ Treated Mice

To study the role of Notch on regenerative processes of the pancreas after cellular insult, the cerulein-induced model of acute pancreatitis was not only induced in *N1KO* mice but also in mice where Notch signaling was chemically ablated using the γ-secretase inhibitor DBZ. Conversion of crypt cells into goblet cells confirmed the functionality of DBZ treatment as previously described (van Es 2005). This double approach had the advantage of studying the specific role of Notch1 as well as the role of all Notch receptors during acute pancreatitis and to compare the resulting phenotypes.

6.3.3 Impaired Regeneration vs. Elevated Susceptibility

Examination of disruption of Notch signaling, either chemically or genetically, during cerulein-induced acute pancreatitis revealed similar tissue reaction on day 1 compared to control mice. However, on day 3, pancreata of Notch deficient mice revealed less thoroughly regenerated pancreatic tissue with large areas of destructed acinar architecture, tubular complexes, infiltration and edema compared to control mice. On day 7, regeneration showed great progress in Notch deficient mice, as exocrine tissue was mostly restored and only small areas of inflammatory residues persisted.

There are two explanations for the observed difference between Notch ablated and control mice:

1) Action of Notch in the initial phase of cellular destruction (e.g. within the first day), resulting in a higher susceptibility of Notch ablated pancreatic cells to cerulein
2) Effects of Notch signaling in the regenerative phase leading to an impaired regeneration and delayed restitution of cellular integrity.

Data from this study support the hypothesis that the initial injury leading to destruction of the acinar architecture and formation of metaplastic ductal lesions is not significantly altered in Notch ablated mice, but that the regeneration of acinar cells and the restoration of the normal acinar architecture are delayed.

As was shown above, Notch1 expression is absent or at least below limits of detection in unstimulated pancreata and barely detectable on day 1 after induction of pancreatitis, but is strongly upregulated in the course of pancreatitis, reaching a peak on day 3 post induction. This observation points towards a role of Notch1 in the regenerative rather than the acute phase of injury after cerulein injection. The fact that upregulation is sustained up to day 7 supports the hypothesis of Notch1 regulating the regenerative acinar tissue process.

The acute tissue reaction in DBZ-treated and *N1KO* mice on day 1 did not display a more severe exocrine damage compared to vehicle-treated and wt mice. In both models, the pancreata showed an identical tissue reaction consisting of edema, inflammatory cell reaction, development of metaplastic ductal lesions, and cell death. Morphometric quantitation of acini revealed no significant differences between *Notch* ablated and control mice on day 1, indicating comparable loss of acinar tissue. On day 3, the number of acini remained stable in vehicle-treated mice and increased in wt mice, whereas Notch ablated mice showed continued loss in acinar structures, indicating impaired regeneration. These findings demonstrate that the *Notch* ablated pancreata are destroyed to the same extent as control pancreata. If the pancreata were indeed more vulnerable to injury, differences in phenotype on day 1 would be expected. Instead, significant differences between Notch ablated and control mice were detected on day 3 and day 7, during the regenerative phase.

Gene expression analyses of exocrine and ductal markers also support the hypothesis of delayed regeneration. On day 1, amylase expression was greatly reduced in all mice. On day 3, amylase expression in wt mice increased 10 fold,

indicating strong recovery of the exocrine compartment, whereas in *N1KO* mice it increased only 3.8 fold. On day 7, regeneration continued in both groups, however, *N1KO* mice were still lagging behind. Expression of CK19 was strongly upregulated on day 1 in *N1KO* and wt mice. This finding could either indicate acinar-to-ductal metaplasia or reflect a relative increase in ductal structures due to the loss of acinar tissue. Two findings argue in favor of the latter explanation. First, ductal cells were found to express BCL2 during pancreatic injury protecting them from apoptosis (Wada 1997). Second, a recent study has found acinar-to-ductal transdifferentiation to play a subordinate role during cerulein-induced pancreatitis (Strobel 2007). In their study, Elastase-CreER^{TM} (*Ela*-*Cre*ER) mice were used to label acinar cells. Subsequent lineage tracing after induction of pancreatitis revealed that only a small percentage of metaplastic lesions were derived from acini, indicating that this mechanism is only marginally involved in the pathophysiology of pancreatitis. Thus, the apoptotic deletion of acinar cells and the persistence of ducts leads to a spatial convergence of ductal structures and could explain the formation of tubular complexes without acinar-to-ductal metaplasia. Consequently, the continued increase of CK19 expression in *N1KO* mice on day 3 is best explained by a relative increase in ductal structures due to continued loss of acinar tissue surrounding the ducts. The strong decline of CK19 expression in wt mice indicates restitution of normal acinar architecture. On day 7, CK19 levels approximated levels of unstimulated pancreata, indicating advanced acinar regeneration in wt mice. In *N1KO* mice, CK19 was still elevated, indicating a sustained reduction of acinar structures.

Comparison of the body weight between *N1KO* mice and wt mice revealed no significant difference on day 1 and day 3. The decrease of the body weight in *N1KO* mice but not in wt mice on day 7 is indicative for a more severe and prolonged pancreatic insufficiency due to an impaired regeneration, resulting in extended maldigestion and thus inefficient nutrition resorption. The pancreatic weight was not altered between *N1KO* and wt mice on day 1 and displayed an equal decrease on day 3, clearly demonstrating a comparable loss of acinar tissue in wt and *N1KO* mice during the phase of acinar destruction. However, on day 7, pancreatic weight increased in wt mice indicating recovery from the injury, whereas in *N1KO* mice pancreatic weight continued to decrease, suggesting that acinar regeneration is impaired, leading to a defective reconstitution of pancreatic exocrine tissue in *N1KO* mice.

Impaired regeneration in Notch ablated mice could result from various mechanisms. In DBZ treated mice, disruption of the Notch pathway in non-pancreatic cells such as stellate, mesenchymal and endothelial cells or fibroblasts in addition to pancreatic cells could lead to an imbalanced Notch signaling network between pancreatic and non-pancreatic cells, thus impairing potentially essential inter- and intracellular signaling. Furthermore, Notch independent effects caused by inhibition of γ-secretase cannot be excluded. However, *N1KO* mice with pancreas-specific deletion of Notch1 displayed essentially the same phenotype compared to DBZ-treated mice, suggesting an important role of Notch1 in exocrine cells during regeneration and argues in favor of a cell autonomous effect of Notch signaling during regeneration of the pancreas. Additionally, since the knockout of the Notch1 receptor has a similarly severe phenotype as that of DBZ-treated mice, it is likely that it is the Notch1 receptor that is of major importance for exocrine Notch signaling during regeneration.

6.3.4 Cellular Origin and Mechanism of Regeneration

Important issues of acute pancreatitis are the cellular origin of as well as the mechanism of regeneration that lead to a complete functional and morphological restoration of the organ after cellular insult. The absence of lineage tracing in this study, precludes definite conclusions as to the cell type in which Notch signaling is required for a normal regenerative process. Several hypotheses are conceivable:

a) Regression of acinar cells into an immature state and subsequent regeneration through redifferentiation into mature acinar cells
b) Death of acinar cells and regeneration through differentiation of another cell type (e.g. islet cells, ductal cells, centroacinar cells)
c) Regeneration through activation and expansion of exocrine progenitor cells

Several in-vitro studies demonstrated considerable plasticity of acinar cells (Rooman 2000; Shen 2000; Means 2005). Other studies have suggested acino-ductal and acino-endocrine transdifferentiation and subsequent redifferentiation to be involved in this process. Recent data, as well as older studies, suggest that restoration of acinar integrity arises primarily from surviving acinar cells and involves a transient alteration in acinar differentiation towards a less differentiated state, at least in the model of cerulein-induced pancreatitis (Iovanna 1992; Reid 1999; Jensen 2005). Two studies that used Cre/loxP mediated lineage tracing of acinar cells revealed that acinar regeneration results primarily from the expansion of preexisting acinar cells, and that

acinar cells are capable of entering the cell cycle in their differentiated state (Desai 2007; Strobel 2007). In light of these lineage tracing studies, the finding in this study of elevated expression of PDX1, clusterin and β-catenin, and the absence of differentiation markers in non-regenerated areas could indeed be interpreted as a regression of mature acinar cells into less differentiated cells after cellular insult, and that these cells regenerate/redifferentiate into mature acinar cells. Therefore, even though this study did not employ lineage tracing of acinar cells, the most likely action of Notch required for normal regeneration lies within previously existing acinar cells that enter the cell cycle in a differentiated state as is hypothesized by Strobel et al. (2007). Thus, a possible role of Notch signaling in controlling regeneration is the regulation of the differentiation status of acinar cells during pancreatitis.

On the other hand, the finding from previous lineage tracing studies that regenerated acinar cells originate from terminally differentiated cells does not preclude the possibility that cell types other than the terminally differentiated acini (e.g. progenitor cells, centroacinar cells) are also dependent on Notch activity. Even though these cells do not appear to be crucially involved in the active regeneration of the acinar compartment, they might play an important role in the regulation of this process through Notch signaling. Indeed, the expression of HES1 in centroacinar cells indicates Notch signaling in these cells and substantiates the hypothesis that these cells could be involved in governing the homeostasis of surrounding acinar and possibly ductal structures via Notch signaling. To study the lineage relation during the regenerative process in *N1KO* mice more thoroughly, lineage-tracing approaches in *Notch1* deficient mice are necessary.

Another possibility that cannot be excluded in this study is that the absence of acinar Notch1 signaling in *N1KO* mice could result in an entirely altered regeneration mechanism of acinar cells, that could eventually lead to an elevated rate of acinar-to-ductal transdifferentiation. This finding would also explain the increase in CK19 expression in *N1KO* mice (see above). The delayed reduction of CK19 expression could then also be interpreted as a possibly delayed reversion of these metaplastic cells to acinar cells. Notch1 signaling would then not only control the regeneration program of acinar cells, but also their lineage fate during regeneration after cellular insult. To clarify whether the ablation of Notch signaling leads to a regeneration program different from wt mice and subsequent alteration in the lineage fate of acinar cells, lineage tracing studies labeling acinar cells, e.g. by employment

of *Ela-Cre*ER mice, in *N1KO* mice during acute pancreatitis are required to address these questions.

Notwithstanding, precise deductions as to the molecular mechanisms that are impaired in the process are not possible. The finding of elevated expression and cytoplasmic location of β-catenin and E-cadherin in Notch ablated mice suggests the Wnt signaling pathway to be involved. Subsequent transfection studies on the pancreatic acinar cell line 266-6 have indeed shown an interaction of Notch and β-catenin such that Notch1-IC was capable of inhibiting transcriptional activity of β-catenin (Siveke 2008). This finding indicates that Notch signaling in concert with the Wnt pathway controls the maturation status of acinar cells. Another role of Notch signaling during acute pancreatitis could be the mediation of resistance to apoptotic stimuli, since the apoptotic rate was elevated on all days examined in *N1KO* and DBZ-treated mice compared to control mice, significantly on day 3 and day 7. This elevation in apoptosis would also explain the delayed regeneration and reduction of pancreatic weight on day 7. The contradictory results regarding proliferation in DBZ-treated and *N1KO* mice are not easily interpretable. The finding that proliferation in the developing pancreas does not differ between *N1KO* and wt embryos supports the hypothesis that Notch signaling is not significantly involved in proliferation of acinar/pancreatic cells.

7 Summary

7.1 Notch During Pancreatic Organogenesis

To investigate the role of Notch1 signaling in pancreatic homeostasis during embryogenesis and in juvenile/adult mice, the Notch1 receptor was conditionally ablated using Cre recombinase under the promoter of the endogenous *Ptf1a* gene. X-gal staining of pancreatic sections from *ROSA26* reporter mice revealed high efficiency in Cre-mediated recombination specifically in the pancreas, and gene expression analysis revealed a 91% decrease in *Notch1* levels in the pancreas.

Investigation of embryonic pancreatogenesis revealed no apparent morphological or functional alterations as evidenced by staining for exocrine, endocrine and ductal markers. Proliferative activity was unaltered and no apoptosis could be detected. Explanations for these unexpected findings could be that ablation of only one receptor is not sufficient to result in severe alterations through compensation or redundancy of other Notch receptors. Slightly elevated expression of the other epithelially expressed Notch receptor Notch2 may suggest such a mechanism. Furthermore, ablation of Notch1 on E10.5 could possibly be too late to severely impact pancreatogenesis, suggesting that Notch1 is not crucially involved in pancreatic organogenesis after that time point. Additionally, alterations in development might have been too subtle and thus eluded detection in this study.

Examination of juvenile and adult mice did not display any histomorphological differences between *N1KO* and wt mice. The body weight was the same in juvenile and adult mice. However, comparison of the pancreatic weight and the pancreatic weight index revealed a significant reduction in the *N1KO* group of 5.5 week old mice. In adult mice, the difference was not evident any more. Immunohistological staining for the exocrine marker amylase revealed strong expression homogeneously distributed within the acini. Immunohistochemistry of the endocrine markers displayed the typical distribution and quantity of pancreatic hormones within the islets of Langerhans. Staining for ductal markers showed no alterations of the ductal tree. However, gene expression analysis of lineage markers revealed reduced expression of amylase. Analysis of β-catenin and E-cadherin expression showed elevated levels and increased cytoplasmic location in *N1KO* mice, indicating a possible alteration in

the maturation status of exocrine cells compared to wt mice. However, data from this study do not point towards a functional exocrine impairment in adult mice.
Therefore, the results from the study on pancreatic organogenesis present evidence that the Notch1 receptor does not play an essential role during pancreatic organogenesis and preservation of adult homeostasis.

7.2 Notch During Acute Pancreatitis

To study the role of Notch signaling on pancreatic regeneration, acute pancreatitis was induced by repeated intraperitoneal injections of supramaximal doses of cerulein. In addition to the genetical *Notch1* knockout construct, Notch signaling was ablated chemically through injection of the γ-secretase inhibitor DBZ.
Expression analysis of Notch signaling members during acute pancreatitis revealed upregulation of Notch1, Notch2, and the target genes *Hes1* and *Hey1*, denoting functional activation of Notch signaling. Upregulation was faintly detectable on day 1 and peaked on day 3. Notch2 expression was significantly higher in *N1KO* mice, suggesting a compensatory mechanism for the absence of Notch1, analogous to the finding in of the pancreata in juvenile/adult mice.
Histomorphological comparison of Notch ablated to control mice revealed similar acute tissue reaction on day 1. However, on day 3, substantial differences were evident. Control mice displayed large areas of regenerated pancreatic tissue, whereas in Notch ablated mice, the majority of the organ consisted of non-regenerated areas with continued infiltration and edema. Immunohistological analysis of non-regenerated areas showed expression of markers indicative of immature acinar cells (e.g. PDX1, clusterin) as well as increased cytoplasmic expression of β-catenin and E-cadherin. Markers labeling differentiated cells (exocrine, endocrine, ductal) could not be detected. Evaluation of apoptosis revealed a higher rate in Notch deficient mice, whereas proliferation showed ambiguous results between DBZ and *N1KO* mice.
Two hypotheses could explain the different phenotype: Importance of Notch in the early phase of cellular destruction rendering the pancreas more susceptible to cellular injury, or action of Notch during the course of regeneration, leading to a delayed restoration of pancreatic integrity. Assessment of body weight, pancreatic weight and acinar regeneration, as well as expression analyses of Notch signaling members and lineage markers during the 7 day course of acute pancreatitis showed

comparable results on day one and divergent findings on day 3 and day 7. This strongly supports the hypothesis that Notch1 is implicated in the course of acinar regeneration rather than the initial phase of acinar destruction.

7.3 Conclusion

Taken together, the results from the study on pancreatic organogenesis and pancreatic injury implicate an important role of Notch1 signaling in the restitution of a balanced and physiologic homeostasis in disease states of the pancreas, and a negligible role in the genesis and maintenance of a physiologic homeostasis.

8 References

Abremski, K. and Hoess, R.: "Bacteriophage P1 site-specific recombination. Purification and properties of the Cre recombinase protein." J. Biol. Chem. 259(3): 1509-14 (1984).

Adler, G., Gerhards, G., Schick, J., Rohr, G. and Kern, H. F.: "Effects of in vivo cholinergic stimulation of rat exocrine pancreas." Am J Physiol 244(6): G623-9 (1983).

Ahlgren, U., Jonsson, J., Jonsson, L., Simu, K. and Edlund, H.: "beta-cell-specific inactivation of the mouse Ipf1/Pdx1 gene results in loss of the beta-cell phenotype and maturity onset diabetes." Genes Dev 12(12): 1763-8 (1998).

Ahnfelt-Rønne, J., Hald, J., Bødker, A., Yassin, H., Serup, P. and Hecksher-Sørensen, J.: "Preservation of proliferating pancreatic progenitor cells by Delta-Notch signaling in the embryonic chicken pancreas." BMC Dev Biol 7: 63 (2007).

Ambler, C. A. and Watt, F. M.: "Expression of Notch pathway genes in mammalian epidermis and modulation by beta-catenin." Dev Dyn 236(6): 1595-601 (2007).

Apelqvist, A., Li, H., Sommer, L., Beatus, P., Anderson, D. J., Honjo, T., Hrabe de Angelis, M., Lendahl, U. and Edlund, H.: "Notch signalling controls pancreatic cell differentiation." Nature 400(6747): 877-81 (1999).

Artavanis-Tsakonas, S., Muskavitch, M. A. and Yedvobnick, B.: "Molecular cloning of Notch, a locus affecting neurogenesis in Drosophila melanogaster." Proc. Natl. Acad. Sci. U.S.A. 80(7): 1977-81 (1983).

Bardeesy, N. and DePinho, R. A.: "Pancreatic cancer biology and genetics." Nat Rev Cancer 2(12): 897-909 (2002).

Barolo, S., Walker, R. G., Polyanovsky, A. D., Freschi, G., Keil, T. and Posakony, J. W.: "A notch-independent activity of suppressor of hairless is required for normal mechanoreceptor physiology." Cell 103(6): 957-69 (2000).

Beatus, P., Lundkvist, J., Oberg, C., Pedersen, K. and Lendahl, U.: "The origin of the ankyrin repeat region in Notch intracellular domains is critical for regulation of HES promoter activity." Mech. Dev. 104(1-2): 3-20 (2001).

Beckers, J., Clark, A., Wünsch, K., Hrabé De Angelis, M. and Gossler, A.: "Expression of the mouse Delta1 gene during organogenesis and fetal development." Mech. Dev. 84(1-2): 165-8 (1999).

Beres, T. M., Masui, T., Swift, G. H., Shi, L., Henke, R. M. and MacDonald, R. J.: "PTF1 is an organ-specific and Notch-independent basic helix-loop-helix complex containing the mammalian Suppressor of Hairless (RBP-J) or its paralogue, RBP-L." Mol. Cell. Biol. 26(1): 117-30 (2006).

Bessho, Y., Miyoshi, G., Sakata, R. and Kageyama, R.: "Hes7: a bHLH-type repressor gene regulated by Notch and expressed in the presomitic mesoderm." Genes Cells 6(2): 175-85 (2001).

Bettenhausen, B.: "Transient and restricted expression during mouse embryogenesis of Dll1, a murine gene closely related to Drosophila Delta." Development 121: 2407-2418 (1995).

Blaumueller, C. M., Qi, H., Zagouras, P. and Artavanis-Tsakonas, S.: "Intracellular cleavage of Notch leads to a heterodimeric receptor on the plasma membrane." Cell 90(2): 281-91 (1997).

Bockman, D. E.: "Morphology of the exocrine pancreas related to pancreatitis." Microsc Res Tech 37(5-6): 509-19 (1997).

Bray, S. J.: "Notch signalling: a simple pathway becomes complex." Nat. Rev. Mol. Cell Biol. 7(9): 678-89 (2006).

Brissova, M., Shiota, M., Nicholson, W. E., Gannon, M., Knobel, S. M., Piston, D. W., Wright, C. V. and Powers, A. C.: "Reduction in pancreatic transcription factor PDX-1 impairs glucose-stimulated insulin secretion." J Biol Chem 277(13): 11225-32 (2002).

Brou, C., Logeat, F., Gupta, N., Bessia, C., LeBail, O., Doedens, J. R., Cumano, A., Roux, P., Black, R. A. and Israel, A.: "A novel proteolytic cleavage involved in Notch signaling: the role of the disintegrin-metalloprotease TACE." Mol Cell 5(2): 207-16 (2000).

Cano, D. A., Hebrok, M. and Zenker, M.: "Pancreatic development and disease." Gastroenterology 132(2): 745-62 (2007).

Cockell, M., Stevenson, B. J., Strubin, M., Hagenbüchle, O. and Wellauer, P. K.: "Identification of a cell-specific DNA-binding activity that interacts with a transcriptional activator of genes expressed in the acinar pancreas." Mol. Cell. Biol. 9(6): 2464-76 (1989).

Conlon, R. A., Reaume, A. G. and Rossant, J.: "Notch1 is required for the coordinate segmentation of somites." Development 121(5): 1533-45 (1995).

Cormier, S., Vandormael-Pournin, S., Babinet, C. and Cohen-Tannoudji, M.: "Developmental expression of the Notch signaling pathway genes during mouse preimplantation development." Gene Expr Patterns 4(6): 713-7 (2004).

De Caro, G. and Improta, G.: "Disappearance of caerulein from circulating blood and its inactivation in vitro by tissue homogenates and blood of dogs and rats." Archives internationales de pharmacodynamie et de thérapie 197(1): 166-74 (1972).

de la Pompa, J. L., Wakeham, A., Correia, K. M., Samper, E., Brown, S., Aguilera, R. J., Nakano, T., Honjo, T., Mak, T. W., Rossant, J. and Conlon, R. A.: "Conservation of the Notch signalling pathway in mammalian neurogenesis." Development 124(6): 1139-48 (1997).

De Strooper, B., Annaert, W., Cupers, P., Saftig, P., Craessaerts, K., Mumm, J. S., Schroeter, E. H., Schrijvers, V., Wolfe, M. S., Ray, W. J., Goate, A. and Kopan, R.: "A presenilin-1-dependent gamma-secretase-like protease mediates release of Notch intracellular domain." Nature 398(6727): 518-22 (1999).

del Amo, F. F., Gendron-Maguire, M., Swiatek, P. J., Jenkins, N. A., Copeland, N. G. and Gridley, T.: "Cloning, analysis, and chromosomal localization of Notch-1, a mouse homolog of Drosophila Notch." Genomics 15(2): 259-64 (1993).

Del Monte, G., Grego-Bessa, J., González-Rajal, A., Bolós, V. and De La Pompa, J. L.: "Monitoring Notch1 activity in development: Evidence for a feedback regulatory loop." Dev. Dyn. 236(9): 2594-614 (2007).

Desai, B. M., Oliver-Krasinski, J., De Leon, D. D., Farzad, C., Hong, N., Leach, S. D. and Stoffers, D. A.: "Preexisting pancreatic acinar cells contribute to acinar cell, but not islet beta cell, regeneration." J Clin Invest 117(4): 971-7 (2007).

Dessimoz, J., Bonnard, C., Huelsken, J. and Grapin-Botton, A.: "Pancreas-specific deletion of beta-catenin reveals Wnt-dependent and Wnt-independent functions during development." Curr Biol 15(18): 1677-83 (2005).

Ellisen, L. W., Bird, J., West, D. C., Soreng, A. L., Reynolds, T. C., Smith, S. D. and Sklar, J.: "TAN-1, the human homolog of the Drosophila notch gene, is broken by chromosomal translocations in T lymphoblastic neoplasms." Cell 66(4): 649-61 (1991).

Esni, F., Ghosh, B., Biankin, A. V., Lin, J. W., Albert, M. A., Yu, X., MacDonald, R. J., Civin, C. I., Real, F. X., Pack, M. A., Ball, D. W. and Leach, S. D.: "Notch inhibits Ptf1 function and acinar cell differentiation in developing mouse and zebrafish pancreas." Development 131(17): 4213-24 (2004).

Fisher, A. and Caudy, M.: "The function of hairy-related bHLH repressor proteins in cell fate decisions." Bioessays 20(4): 298-306 (1998).

Fleming, R. J.: "Structural conservation of Notch receptors and ligands." Semin. Cell Dev. Biol. 9(6): 599-607 (1999).

Fleming, R. J., Purcell, K. and Artavanis-Tsakonas, S.: "The NOTCH receptor and its ligands." Trends Cell Biol 7(11): 437-41 (1997).

Fujikura, J., Hosoda, K., Iwakura, H., Tomita, T., Noguchi, M., Masuzaki, H., Tanigaki, K., Yabe, D., Honjo, T. and Nakao, K.: "Notch/Rbp-j signaling prevents premature endocrine and ductal cell differentiation in the pancreas." Cell metabolism 3(1): 59-65 (2006).

Fujikura, J., Hosoda, K., Kawaguchi, Y., Noguchi, M., Iwakura, H., Odori, S., Mori, E., Tomita, T., Hirata, M., Ebihara, K., Masuzaki, H., Fukuda, A., Furuyama, K., Tanigaki, K., Yabe, D. and Nakao, K.: "Rbp-j regulates expansion of pancreatic epithelial cells and their differentiation into exocrine cells during mouse development." Dev. Dyn. 236(10): 2779-91 (2007).

Fukuda, A., Kawaguchi, Y., Furuyama, K., Kodama, S., Horiguchi, M., Kuhara, T., Koizumi, M., Boyer, D. F., Fujimoto, K., Doi, R., Kageyama, R., Wright, C. V. and Chiba, T.: "Ectopic pancreas formation in Hes1 -knockout mice reveals plasticity of endodermal progenitors of the gut, bile duct, and pancreas." J Clin Invest 116(6): 1484-93 (2006).

Gomez, G., Englander, E. W., Wang, G. and Greeley, G. H.: "Increased expression of hypoxia-inducible factor-1alpha, p48, and the Notch signaling cascade during acute pancreatitis in mice." Pancreas 28(1): 58-64 (2004).

Gorelick, F. S., Adler, G. and Kern, H. F.: "Cerulein-Induced Pancreatitis". In: "The Pancreas: Biology, Pathobiology, and Disease". Chapter: 25. Edited by: V. L. W. Go, E. P. DiMagno et al. New York, Raven Press, Ltd. (1993) p. 501-526

Gu, G., Dubauskaite, J. and Melton, D. A.: "Direct evidence for the pancreatic lineage: NGN3+ cells are islet progenitors and are distinct from duct progenitors." Development 129(10): 2447-57 (2002).

Guz, Y., Montminy, M. R., Stein, R., Leonard, J., Gamer, L. W., Wright, C. V. and Teitelman, G.: "Expression of murine STF-1, a putative insulin gene transcription factor, in beta cells of pancreas, duodenal epithelium and pancreatic exocrine and endocrine progenitors during ontogeny." Development 121(1): 11-8 (1995).

Haass, C. and De Strooper, B.: "The presenilins in Alzheimer's disease--proteolysis holds the key." Science 286(5441): 916-9 (1999).

Habener, J. F., Kemp, D. M. and Thomas, M. K.: "Minireview: transcriptional regulation in pancreatic development." Endocrinology 146(3): 1025-34 (2004).

Hald, J., Hjorth, J. P., German, M. S., Madsen, O. D., Serup, P. and Jensen, J.: "Activated Notch1 prevents differentiation of pancreatic acinar cells and attenuate endocrine development." Dev. Biol. 260(2): 426-37 (2003).

Hale, M. A., Kagami, H., Shi, L., Holland, A. M., Elsässer, H. P., Hammer, R. E. and MacDonald, R. J.: "The homeodomain protein PDX1 is required at mid-pancreatic development for the formation of the exocrine pancreas." Dev. Biol. 286(1): 225-37 (2005).

Hamilton, D. L. and Abremski, K.: "Site-specific recombination by the bacteriophage P1 lox-Cre system. Cre-mediated synapsis of two lox sites." J Mol Biol 178(2): 481-6 (1984).

Han, J. H., Rall, L. and Rutter, W. J.: "Selective expression of rat pancreatic genes during embryonic development." Proc. Natl. Acad. Sci. U.S.A. 83(1): 110-4 (1986).

Hansson, E. M., Lendahl, U. and Chapman, G.: "Notch signaling in development and disease." Semin. Cancer Biol. 14(5): 320-8 (2004).

Hart, A., Papadopoulou, S. and Edlund, H.: "Fgf10 maintains notch activation, stimulates proliferation, and blocks differentiation of pancreatic epithelial cells." Dev. Dyn. 228(2): 185-93 (2003).

Heiser, P. W., Lau, J., Taketo, M. M., Herrera, P. L. and Hebrok, M.: "Stabilization of beta-catenin impacts pancreas growth." Development 133(10): 2023-32 (2006).

Hoess, R. H., Ziese, M. and Sternberg, N.: "P1 site-specific recombination: nucleotide sequence of the recombining sites." Proc. Natl. Acad. Sci. U.S.A. 79(11): 3398-402 (1982).

Holland, A. M., Hale, M. A., Kagami, H., Hammer, R. E. and MacDonald, R. J.: "Experimental control of pancreatic development and maintenance." Proc. Natl. Acad. Sci. U.S.A. 99(19): 12236-41 (2002).

Iovanna, J. L., Lechene de la Porte, P. and Dagorn, J. C.: "Expression of genes associated with dedifferentiation and cell proliferation during pancreatic regeneration following acute pancreatitis." Pancreas 7(6): 712-8 (1992).

Iso, T., Chung, G., Hamamori, Y. and Kedes, L.: "HERP1 is a cell type-specific primary target of Notch." J. Biol. Chem. 277(8): 6598-607 (2002).

Iso, T., Kedes, L. and Hamamori, Y.: "HES and HERP families: multiple effectors of the Notch signaling pathway." J Cell Physiol 194(3): 237-55 (2003).

Jarriault, S., Brou, C., Logeat, F., Schroeter, E. H., Kopan, R. and Israel, A.: "Signalling downstream of activated mammalian Notch." Nature 377(6547): 355-8 (1995).

Jarriault, S. and Greenwald, I.: "Evidence for functional redundancy between C. elegans ADAM proteins SUP-17/Kuzbanian and ADM-4/TACE." Dev Biol 287(1): 1-10 (2005).

Jarriault, S., Le Bail, O., Hirsinger, E., Pourquié, O., Logeat, F., Strong, C. F., Brou, C., Seidah, N. G. and Isra l, A.: "Delta-1 activation of notch-1 signaling results in HES-1 transactivation." Mol. Cell. Biol. 18(12): 7423-31 (1998).

Jensen, J.: "Gene regulatory factors in pancreatic development." Dev. Dyn. 229(1): 176-200 (2003).

Jensen, J., Heller, R. S., Funder-Nielsen, T., Pedersen, E. E., Lindsell, C., Weinmaster, G., Madsen, O. D. and Serup, P.: "Independent development of pancreatic alpha- and beta-cells from neurogenin3-expressing precursors: a role for the notch pathway in repression of premature differentiation." Diabetes 49(2): 163-76 (2000a).

Jensen, J., Pedersen, E. E., Galante, P., Hald, J., Heller, R. S., Ishibashi, M., Kageyama, R., Guillemot, F., Serup, P. and Madsen, O. D.: "Control of endodermal endocrine development by Hes-1." Nat Genet 24(1): 36-44 (2000b).

Jensen, J. N., Cameron, E., Garay, M. V., Starkey, T. W., Gianani, R. and Jensen, J.: "Recapitulation of elements of embryonic development in adult mouse pancreatic regeneration." Gastroenterology 128(3): 728-41 (2005).

Junqueira, L. C. and Carneiro, J.: "Bauchspeicheldrüse, Pankreas". In: "Histologie". Chapter: 21.2, Springer-Verlag. (1996) p. 521-530

Kaneto, H., Miyatsuka, T., Shiraiwa, T., Yamamoto, K., Kato, K., Fujitani, Y. and Matsuoka, T. A.: "Crucial role of PDX-1 in pancreas development, beta-cell differentiation, and induction of surrogate beta-cells." Curr Med Chem 14(16): 1745-52 (2007).

Kato, H., Sakai, T., Tamura, K., Minoguchi, S., Shirayoshi, Y., Hamada, Y., Tsujimoto, Y. and Honjo, T.: "Functional conservation of mouse Notch receptor family members." FEBS Lett. 395(2-3): 221-4 (1996).

Kato, H., Taniguchi, Y., Kurooka, H., Minoguchi, S., Sakai, T., Nomura-Okazaki, S., Tamura, K. and Honjo, T.: "Involvement of RBP-J in biological functions of mouse Notch1 and its derivatives." Development 124(20): 4133-41 (1997).

Kawaguchi, Y., Cooper, B., Gannon, M., Ray, M., MacDonald, R. J. and Wright, C. V.: "The role of the transcriptional regulator Ptf1a in converting intestinal to pancreatic progenitors." Nat. Genet. 32(1): 128-34 (2002).

Kitamoto, T., Takahashi, K., Takimoto, H., Tomizuka, K., Hayasaka, M., Tabira, T. and Hanaoka, K.: "Functional redundancy of the Notch gene family during mouse embryogenesis: analysis of Notch gene expression in Notch3-deficient mice." Biochem Biophys Res Commun 331(4): 1154-62 (2005).

Kovall, R. A. and Hendrickson, W. A.: "Crystal structure of the nuclear effector of Notch signaling, CSL, bound to DNA." EMBO J. 23(17): 3441-51 (2004).

Krapp, A., Knöfler, M., Frutiger, S., Hughes, G. J., Hagenbüchle, O. and Wellauer, P. K.: "The p48 DNA-binding subunit of transcription factor PTF1 is a new exocrine pancreas-specific basic helix-loop-helix protein." EMBO J. 15(16): 4317-29 (1996).

Krapp, A., Knöfler, M., Ledermann, B., Bürki, K., Berney, C., Zoerkler, N., Hagenbüchle, O. and Wellauer, P. K.: "The bHLH protein PTF1-p48 is essential for the formation of the exocrine and the correct spatial organization of the endocrine pancreas." Genes Dev. 12(23): 3752-63 (1998).

Krebs, L. T., Xue, Y., Norton, C. R., Shutter, J. R., Maguire, M., Sundberg, J. P., Gallahan, D., Closson, V., Kitajewski, J., Callahan, R., Smith, G. H., Stark, K. L. and Gridley, T.: "Notch signaling is essential for vascular morphogenesis in mice." Genes Dev 14(11): 1343-52 (2000).

Kuroda, K., Tani, S., Tamura, K., Minoguchi, S., Kurooka, H. and Honjo, T.: "Delta-induced Notch signaling mediated by RBP-J inhibits MyoD expression and myogenesis." J. Biol. Chem. 274(11): 7238-44 (1999).

Kurooka, H., Kuroda, K. and Honjo, T.: "Roles of the ankyrin repeats and C-terminal region of the mouse notch1 intracellular region." Nucleic Acids Res 26(23): 5448-55 (1998).

Kwan, K. M.: "Conditional alleles in mice: practical considerations for tissue-specific knockouts." Genesis 32(2): 49-62 (2002).

Lammert, E., Brown, J. and Melton, D. A.: "Notch gene expression during pancreatic organogenesis." Mech. Dev. 94(1-2): 199-203 (2000).

Lardelli, M., Dahlstrand, J. and Lendahl, U.: "The novel Notch homologue mouse Notch 3 lacks specific epidermal growth factor-repeats and is expressed in proliferating neuroepithelium." Mech. Dev. 46(2): 123-36 (1994).

Lee, J. C., Smith, S. B., Watada, H., Lin, J., Scheel, D., Wang, J., Mirmira, R. G. and German, M. S.: "Regulation of the pancreatic pro-endocrine gene neurogenin3." Diabetes 50(5): 928-36 (2001).

Leimeister, C., Externbrink, A., Klamt, B. and Gessler, M.: "Hey genes: a novel subfamily of hairy- and Enhancer of split related genes specifically expressed during mouse embryogenesis." Mech. Dev. 85(1-2): 173-7 (1999).

Lewandoski, M.: "Conditional control of gene expression in the mouse." Nat. Rev. Genet. 2(10): 743-55 (2001).

Lewis, A. K., Frantz, G. D., Carpenter, D. A., de Sauvage, F. J. and Gao, W. Q.: "Distinct expression patterns of notch family receptors and ligands during development of the mammalian inner ear." Mech Dev 78(1-2): 159-63 (1998).

Lindsell, C. E., Shawber, C. J., Boulter, J. and Weinmaster, G.: "Jagged: a mammalian ligand that activates Notch1." Cell 80(6): 909-17 (1995).

Livak, K. J. and Schmittgen, T. D.: "Analysis of relative gene expression data using real-time quantitative PCR and the 2(-Delta Delta C(T)) Method." Methods 25(4): 402-8 (2001).

Logeat, F., Bessia, C., Brou, C., LeBail, O., Jarriault, S., Seidah, N. G. and Israël, A.: "The Notch1 receptor is cleaved constitutively by a furin-like convertase." Proc. Natl. Acad. Sci. U.S.A. 95(14): 8108-12 (1998).

Lutolf, S., Radtke, F., Aguet, M., Suter, U. and Taylor, V.: "Notch1 is required for neuronal and glial differentiation in the cerebellum." Development (2002).

Matsunami, N., Hamaguchi, Y., Yamamoto, Y., Kuze, K., Kangawa, K., Matsuo, H., Kawaichi, M. and Honjo, T.: "A protein binding to the J kappa recombination sequence of immunoglobulin genes contains a sequence related to the integrase motif." Nature 342(6252): 934-7 (1989).

Means, A. L., Meszoely, I. M., Suzuki, K., Miyamoto, Y., Rustgi, A. K., Coffey, R. J., Wright, C. V., Stoffers, D. A. and Leach, S. D.: "Pancreatic epithelial plasticity mediated by acinar cell transdifferentiation and generation of nestin-positive intermediates." Development 132(16): 3767-76 (2005).

Melloul, D., Tsur, A. and Zangen, D.: "Pancreatic Duodenal Homeobox (PDX-1) in health and disease." J Pediatr Endocrinol Metab 15(9): 1461-72 (2002).

Metzger, D. and Feil, R.: "Engineering the mouse genome by site-specific recombination." Curr Opin Biotechnol 10(5): 470-6 (1999).

Miele, L.: "Notch signaling." Clin. Cancer Res. 12(4): 1074-9 (2006).

Milano, J., McKay, J., Dagenais, C., Foster-Brown, L., Pognan, F., Gadient, R., Jacobs, R. T., Zacco, A., Greenberg, B. and Ciaccio, P. J.: "Modulation of notch processing by gamma-secretase inhibitors causes intestinal goblet cell metaplasia and induction of genes known to specify gut secretory lineage differentiation." Toxicol Sci 82(1): 341-58 (2004).

Miyamoto, Y., Maitra, A., Ghosh, B., Zechner, U., Argani, P., Iacobuzio-Donahue, C. A., Sriuranpong, V., Iso, T., Meszoely, I. M., Wolfe, M. S., Hruban, R. H., Ball, D. W., Schmid, R. M. and Leach, S. D.: "Notch mediates TGF alpha-induced changes in epithelial differentiation during pancreatic tumorigenesis." Cancer Cell 3(6): 565-76 (2003).

Mohr, O. L.: "Character Changes Caused by Mutation of an Entire Region of a Chromosome in Drosophila." Genetics 4(3): 275-82 (1919).

Morgan, T. H.: "The Theory of the Gene." The American Naturalist 51(609): 513-544 (1917).

Mumm, J. S., Schroeter, E. H., Saxena, M. T., Griesemer, A., Tian, X., Pan, D. J., Ray, W. J. and Kopan, R.: "A ligand-induced extracellular cleavage regulates gamma-secretase-like proteolytic activation of Notch1." Mol Cell 5(2): 197-206 (2000).

Murtaugh, L. C.: "Pancreas and beta-cell development: from the actual to the possible." Development 134(3): 427-38 (2007).

Murtaugh, L. C., Law, A. C., Dor, Y. and Melton, D. A.: "Beta-catenin is essential for pancreatic acinar but not islet development." Development 132(21): 4663-74 (2005).

Murtaugh, L. C., Stanger, B. Z., Kwan, K. M. and Melton, D. A.: "Notch signaling controls multiple steps of pancreatic differentiation." Proc. Natl. Acad. Sci. U.S.A. 100(25): 14920-5 (2003).

Muskavitch, M. A.: "Delta-notch signaling and Drosophila cell fate choice." Dev Biol 166(2): 415-30 (1994).

Nagy, A.: "Cre recombinase: the universal reagent for genome tailoring." Genesis 26(2): 99-109 (2000).

Nakhai, H., Sel, S., Favor, J., Mendoza-Torres, L., Paulsen, F., Duncker, G. I. and Schmid, R. M.: "Ptf1a is essential for the differentiation of GABAergic and glycinergic amacrine cells and horizontal cells in the mouse retina." Development 134(6): 1151-60 (2007).

Nakhai, H., Siveke, J. T., Klein, B., Mendoza-Torres, L., Mazur, P. K., Algul, H., Radtke, F., Strobl, L., Zimber-Strobl, U. and Schmid, R. M.: "Conditional ablation of Notch signaling in pancreatic development." Development 135(16): 2757-65 (2008a).

Nakhai, H., Siveke, J. T., Mendoza-Torres, L. and Schmid, R. M.: "Conditional inactivation of Myc impairs development of the exocrine pancreas." Development 135(19): 3191-6 (2008b).

Norgaard, G. A., Jensen, J. N. and Jensen, J.: "FGF10 signaling maintains the pancreatic progenitor cell state revealing a novel role of Notch in organ development." Dev. Biol. 264(2): 323-38 (2003).

Obata, J., Yano, M., Mimura, H., Goto, T., Nakayama, R., Mibu, Y., Oka, C. and Kawaichi, M.: "p48 subunit of mouse PTF1 binds to RBP-Jkappa/CBF-1, the intracellular mediator of Notch signalling, and is expressed in the neural tube of early stage embryos." Genes Cells 6(4): 345-60 (2001).

Offield, M. F., Jetton, T. L., Labosky, P. A., Ray, M., Stein, R. W., Magnuson, M. A., Hogan, B. L. and Wright, C. V.: "PDX-1 is required for pancreatic outgrowth and differentiation of the rostral duodenum." Development 122(3): 983-95 (1996).

Ohlsson, H., Karlsson, K. and Edlund, T.: "IPF1, a homeodomain-containing transactivator of the insulin gene." EMBO J. 12(11): 4251-9 (1993).

Oswald, F., Liptay, S., Adler, G. and Schmid, R. M.: "NF-kappaB2 is a putative target gene of activated Notch-1 via RBP-Jkappa." Mol. Cell. Biol. 18(4): 2077-88 (1998).

Oswald, F., Täuber, B., Dobner, T., Bourteele, S., Kostezka, U., Adler, G., Liptay, S. and Schmid, R. M.: "p300 acts as a transcriptional coactivator for mammalian Notch-1." Mol. Cell. Biol. 21(22): 7761-74 (2001).

Pfaffl, M. W.: "A new mathematical model for relative quantification in real-time RT-PCR." Nucleic Acids Res 29(9): e45 (2001).

Pictet, R. L., Clark, W. R., Williams, R. H. and Rutter, W. J.: "An ultrastructural analysis of the developing embryonic pancreas." Dev. Biol. 29(4): 436-67 (1972).

Poulson, D. F.: "Chromosomal Deficiencies and the Embryonic Development of Drosophila Melanogaster." Proc. Natl. Acad. Sci. U.S.A. 23(3): 133-7 (1937).

Poulson, D. F.: "The effects of certain X-chromosome deficiencies on the embryonic development of Drosophila melanogaster." Journal of Experimental Zoology 83(2): 271-325 (1940).

Prado, C. L., Pugh-Bernard, A. E., Elghazi, L., Sosa-Pineda, B. and Sussel, L.: "Ghrelin cells replace insulin-producing beta cells in two mouse models of pancreas development." Proc. Natl. Acad. Sci. U.S.A. 101(9): 2924-9 (2004).

Radtke, F. and Raj, K.: "The role of Notch in tumorigenesis: oncogene or tumour suppressor?" Nat Rev Cancer 3(10): 756-67 (2003).

Radtke, F., Schweisguth, F. and Pear, W.: "The Notch 'gospel'." EMBO Rep. 6(12): 1120-5 (2005).

Radtke, F., Wilson, A., Stark, G., Bauer, M., van Meerwijk, J., MacDonald, H. R. and Aguet, M.: "Deficient T cell fate specification in mice with an induced inactivation of Notch1." Immunity 10(5): 547-58 (1999).

Rebay, I., Fleming, R. J., Fehon, R. G., Cherbas, L., Cherbas, P. and Artavanis-Tsakonas, S.: "Specific EGF repeats of Notch mediate interactions with Delta and Serrate: implications for Notch as a multifunctional receptor." Cell 67(4): 687-99 (1991).

Reid, L. E. and Walker, N. I.: "Acinar cell apoptosis and the origin of tubular complexes in caerulein-induced pancreatitis." International journal of experimental pathology 80(4): 205-15 (1999).

Rooman, I., Heremans, Y., Heimberg, H. and Bouwens, L.: "Modulation of rat pancreatic acinoductal transdifferentiation and expression of PDX-1 in vitro." Diabetologia 43(7): 907-14 (2000).

Rose, S. D., Swift, G. H., Peyton, M. J., Hammer, R. E. and MacDonald, R. J.: "The role of PTF1-P48 in pancreatic acinar gene expression." J. Biol. Chem. 276(47): 44018-26 (2001).

Roux, E., Strubin, M., Hagenbüchle, O. and Wellauer, P. K.: "The cell-specific transcription factor PTF1 contains two different subunits that interact with the DNA." Genes Dev 3(10): 1613-24 (1989).

Sanders, T. G. and Rutter, W. J.: "The developmental regulation of amylolytic and proteolytic enzymes in the embryonic rat pancreas." J. Biol. Chem. 249(11): 3500-9 (1974).

Schroeter, E. H., Kisslinger, J. A. and Kopan, R.: "Notch-1 signalling requires ligand-induced proteolytic release of intracellular domain." Nature 393(6683): 382-6 (1998).

Schwitzgebel, V. M.: "Programming of the pancreas." Mol Cell Endocrinol 185(1-2): 99-108 (2001).

Shen, C. N., Slack, J. M. and Tosh, D.: "Molecular basis of transdifferentiation of pancreas to liver." Nat Cell Biol 2(12): 879-87 (2000).

Siveke, J. T., Lubeseder-Martellato, C., Lee, M., Mazur, P. K., Nakhai, H., Radtke, F. and Schmid, R. M.: "Notch signaling is required for exocrine regeneration after acute pancreatitis." Gastroenterology 134(2): 544-55 (2008).

Skipper, M. and Lewis, J.: "Getting to the guts of enteroendocrine differentiation." Nat Genet 24(1): 3-4 (2000).

Slack, J. M.: "Developmental biology of the pancreas." Development 121(6): 1569-80 (1995).

Soriano, P.: "Generalized lacZ expression with the ROSA26 Cre reporter strain." Nat. Genet. 21(1): 70-1 (1999).

Spagnoli, F. M.: "From endoderm to pancreas: a multistep journey." Cell Mol Life Sci 64(18): 2378-90 (2007).

Spooner, B. S., Walther, B. T. and Rutter, W. J.: "The development of the dorsal and ventral mammalian pancreas in vivo and in vitro." J Cell Biol 47(1): 235-46 (1970).

Steidl, C., Leimeister, C., Klamt, B., Maier, M., Nanda, I., Dixon, M., Clarke, R., Schmid, M. and Gessler, M.: "Characterization of the human and mouse HEY1, HEY2, and HEYL genes: cloning, mapping, and mutation screening of a new bHLH gene family." Genomics 66(2): 195-203 (2000).

Sternberg, N. and Hamilton, D.: "Bacteriophage P1 site-specific recombination. I. Recombination between loxP sites." J Mol Biol 150(4): 467-86 (1981).

Strobel, O., Dor, Y., Alsina, J., Stirman, A., Lauwers, G., Trainor, A., Castillo, C. F., Warshaw, A. L. and Thayer, S. P.: "In vivo lineage tracing defines the role of acinar-to-ductal transdifferentiation in inflammatory ductal metaplasia." Gastroenterology 133(6): 1999-2009 (2007).

Swiatek, P. J., Lindsell, C. E., del Amo, F. F., Weinmaster, G. and Gridley, T.: "Notch1 is essential for postimplantation development in mice." Genes Dev. 8(6): 707-19 (1994).

Tamura, K., Taniguchi, Y., Minoguchi, S., Sakai, T., Tun, T., Furukawa, T. and Honjo, T.: "Physical interaction between a novel domain of the receptor Notch and the transcription factor RBP-J kappa/Su(H)." Curr Biol 5(12): 1416-23 (1995).

Tani, S., Kurooka, H., Aoki, T., Hashimoto, N. and Honjo, T.: "The N- and C-terminal regions of RBP-J interact with the ankyrin repeats of Notch1 RAMIC to activate transcription." Nucleic Acids Res 29(6): 1373-80 (2001).

Thellin, O., Zorzi, W., Lakaye, B., De Borman, B., Coumans, B., Hennen, G., Grisar, T., Igout, A. and Heinen, E.: "Housekeeping genes as internal standards: use and limits." J Biotechnol 75(2-3): 291-5 (1999).

Tun, T., Hamaguchi, Y., Matsunami, N., Furukawa, T., Honjo, T. and Kawaichi, M.: "Recognition sequence of a highly conserved DNA binding protein RBP-J kappa." Nucleic Acids Res 22(6): 965-71 (1994).

Uyttendaele, H., Marazzi, G., Wu, G., Yan, Q., Sassoon, D. and Kitajewski, J.: "Notch4/int-3, a mammary proto-oncogene, is an endothelial cell-specific mammalian Notch gene." Development 122(7): 2251-9 (1996).

van Es, J. H., van Gijn, M. E., Riccio, O., van den Born, M., Vooijs, M., Begthel, H., Cozijnsen, M., Robine, S., Winton, D. J., Radtke, F. and Clevers, H.: "Notch/gamma-secretase inhibition turns proliferative cells in intestinal crypts and adenomas into goblet cells." Nature 435(7044): 959-63 (2005).

Wada, M., Doi, R., Hosotani, R., Lee, J. U., Fujimoto, K., Koshiba, T., Miyamoto, Y., Fukuoka, S. and Imamura, M.: "Expression of Bcl-2 and PCNA in duct cells after pancreatic duct ligation in rats." Pancreas 15(2): 176-82 (1997).

Weinmaster, G., Roberts, V. J. and Lemke, G.: "Notch2: a second mammalian Notch gene." Development 116(4): 931-41 (1992).

Wessells, N. K. and Cohen, J. H.: "Early Pancreas Organogenesis: Morphogenesis, Tissue Interactions, and Mass Effects " Developmental Biology 15: 237-270 (1967).

Wharton, K. A., Johansen, K. M., Xu, T. and Artavanis-Tsakonas, S.: "Nucleotide sequence from the neurogenic locus notch implies a gene product that shares homology with proteins containing EGF-like repeats." Cell 43(3 Pt 2): 567-81 (1985).

Wierup, N., Svensson, H., Mulder, H. and Sundler, F.: "The ghrelin cell: a novel developmentally regulated islet cell in the human pancreas." Regul Pept 107(1-3): 63-9 (2002).

Wilson, A. and Radtke, F.: "Multiple functions of Notch signaling in self-renewing organs and cancer." FEBS Lett. 580(12): 2860-8 (2006).

Wu, L., Aster, J. C., Blacklow, S. C., Lake, R., Artavanis-Tsakonas, S. and Griffin, J. D.: "MAML1, a human homologue of Drosophila mastermind, is a transcriptional co-activator for NOTCH receptors." Nat Genet 26(4): 484-9 (2000).

Zecchin, E., Filippi, A., Biemar, F., Tiso, N., Pauls, S., Ellertsdottir, E., Gnügge, L., Bortolussi, M., Driever, W. and Argenton, F.: "Distinct delta and jagged genes control sequential segregation of pancreatic cell types from precursor pools in zebrafish." Dev. Biol. 301(1): 192-204 (2007).